NOT TO BE CITED WITHOUT PRIOR
REFERENCE TO THE AUTHOR(S)

Northwest Atlantic Fisheries Organization

Serial No. N7293 **NAFO SCR Doc. 22/020**

SCIENTIFIC COUNCIL MEETING – JUNE 2022

Environmental and Physical Oceanographic Conditions on the Eastern Canadian shelves (NAFO Sub-areas 2, 3 and 4) during 2021.

by

F. Cyr[1], P. S. Galbraith[2], C. Layton[3] D. Hebert[3], N. Chen[1], G. Han[4]

[1]Northwest Atlantic Fisheries Centre, Fisheries and Oceans Canada, St. John's (NL)
[2]Maurice-Lamontagne Institute, Fisheries and Oceans Canada, Mont-Joli (QC)
[3]Bedford Institute of Oceanography, Fisheries and Oceans Canada, Dartmouth (NS)
[4]Institude of Ocean Sciences, Fisheries and Oceans Canada, Sydney (BC)

Abstract

Oceanographic and meteorological observations in NAFO Sub-areas 2, 3 and 4 during 2021 are presented and referenced to their long-term averages. The winter North Atlantic Oscillation (NAO) index, a key indicator of the direction and intensity of the winter wind field patterns over the Northwest Atlantic was negative for the first time in 8 years. The large majority of the environmental parameters presented in this report were above normal (defined as the average over the 1991-2020 climatological period). The air temperatures across the NW Atlantic were above normal in all regions. The sea-ice season volume and area across the Newfoundland and Labrador shelf was at its third lowest level (after 2010 and 2011) since the beginning of the time series in 1969. Sea surface temperatures averaged over the ice-free months were normal to above normal across the different divisions, and above-normal on average across the zone for the second consecutive year, at +0.9 SD. Observations from the summer AZMP oceanographic survey indicate that the cold intermediate layer area along Seal Island, Bonavista Bay and Flemish Cap section was at its third lowest since 1950. Spatially-averaged bottom temperatures in NAFO divisions 3Ps (spring) and 2J3K (fall) were at their second warmest since 1980, including a record in 3Ps. There were no spring or fall measurements in 3LNO due to limited ship availability. The transport on the Scotian Slope in 2021 remained below normal for eight consecutive years at -1.4 sd.

Introduction

This report presents an overview of the 2021 environmental and physical oceanographic conditions in NAFO sub-areas 2, 3 and 4 on eastern Canadian shelves (see Figure 1). It complements similar reviews of environmental conditions on the Northeast US Shelf, the Labrador Sea and West Greenland Waters as part of the Scientific Council's annual review of environmental conditions in the NAFO Convention Area.

The information presented for 2021 is derived from various sources:

1. Observations made throughout the year at historical monitoring stations 27 (near St. John's, NL), Prince-5 (Bay of Fundy) and Halifax-2 (Scotian Shelf);
2. Measurements made during the summer along standard NAFO and Atlantic Zone Monitoring Program (AZMP) (Therriault et al. 1998) cross-shelf sections (see Figure 1);
3. Oceanographic observations made during multi-species and ground fish resource assessment surveys (NAFO sub-areas 2 to 4);
4. SST data based on infrared satellite imagery (Advance Very High Resolution Radiometer, or AVHRR) of the Northwest Atlantic
5. Other multi-source historical data (ships of opportunity, international campaign, other DFO regions surveys, Argo program, etc.);
6. Ice data are from the Canadian Ice Service and meteorological data are from Environment Canada and other sources cited in the text.

Unless otherwise specified, these data are available from MEDS archives and maintained in a regional data archive at the Northwest Atlantic Fisheries Centre (NAFC) in St. John's, NL and at the Bedford Institute of Oceanography (BIO) in Dartmouth, NS.

Time series of temperature and salinity anomalies and other derived climate indices were constructed by removing the annual cycle computed over a standard climatological. According to the World Meteorological Organization (2017), this period was set last year to 1991-2020 (Cyr et al., 2021). The "*Normal*" is defined here as the average over this period. Annual or seasonal anomalies were sometimes normalized by dividing the values by the standard deviation (SD) of the data time series over the climatological period. A value of 2, for example, indicates that the index was 2 SD higher than its long-term average. As a general guide, anomalies within ±0.5 SD are considered to be normal.

The normalized values of water properties and derived climate indices presented in this document are color-coded in "scorecards" with gradations of 0.5 SD (Figure 2). Shades of blue represent cold-fresh environmental conditions and reds warm-salty conditions. In some instances (NAO, ice and cold water areas or volumes, for example) negative anomalies may indicate warm conditions and hence are colored red. Most of the colormaps used in this report are taken from the *cmocean* colormaps package for oceanography (Thyng et al., 2016).

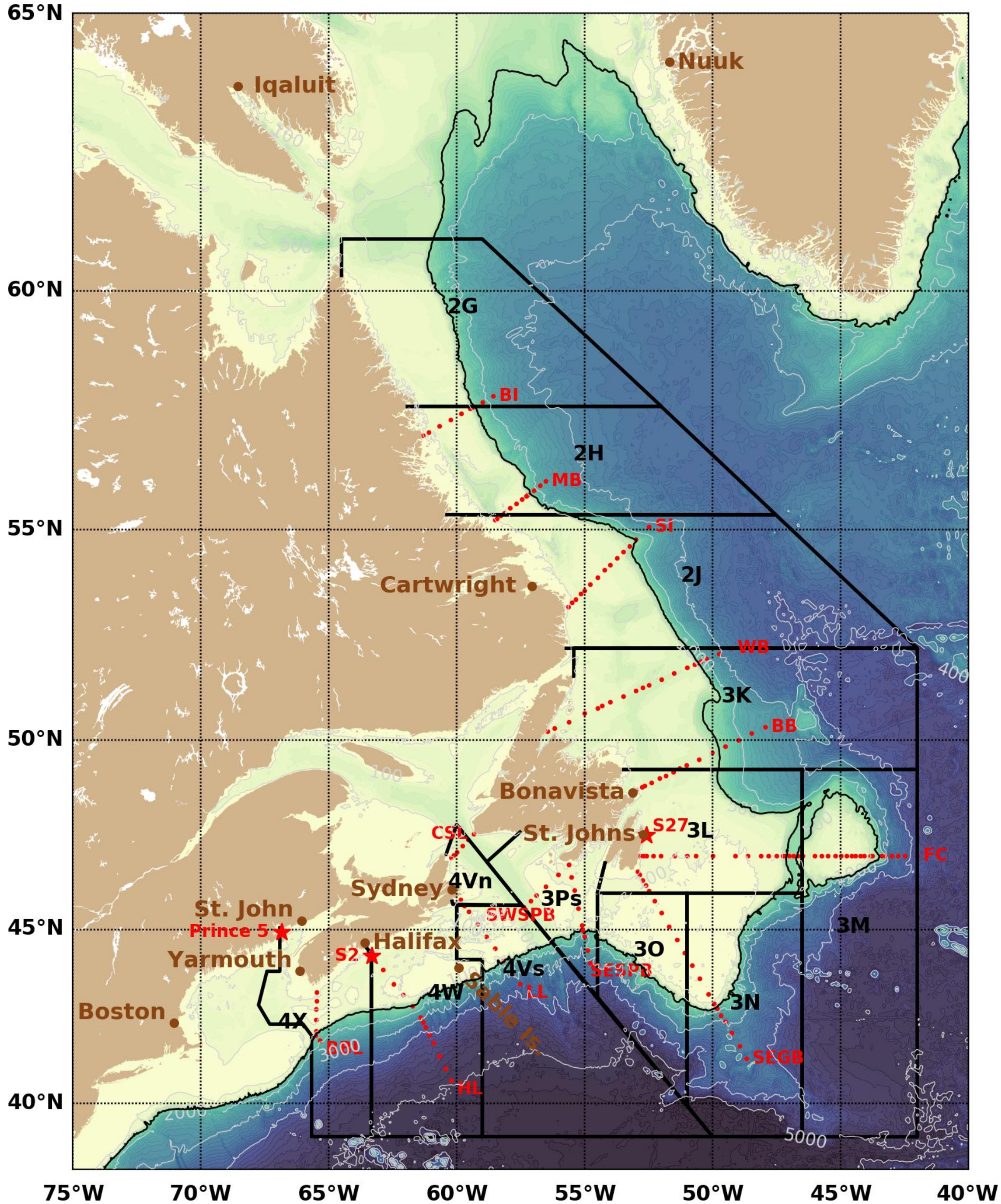

Figure 1. Map showing NAFO Divisions and main bathymetric features of the Northwest Atlantic. The hydrographic sections reported here are shown with red dots and the fixed stations by red stars. The stations used for air temperature time series and in brown. The black contour is the isobath 1000m that is used here to delimit the continental shelf.

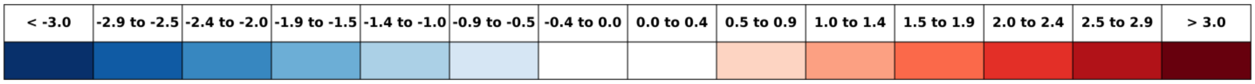

Figure 2. Colorscale used for the presentation of normalized anomalies. Color levels are incremented by 0.5 standard deviations (SD), where blue is below normal and red above normal. Values between 0 and ±0.5 SD remain white indicating normal conditions.

Meteorological Conditions

The winter North Atlantic Oscillation (NAO) is defined as anomaly in the sea-level pressure (SLP) difference between the sub-tropical high (average location near the Azores) and the sub-polar low (average location near Iceland). Several definitions of the NAO exists and the definition used here is the one from the National Center for Environmental Information of the National Oceanic and Atmospheric Administration (NOAA) and available online. The winter NAO (defined here as the average of monthly values from December to March) is considered a measure of the strength of the winter westerly and north westerly winds over the Northwest Atlantic. A high NAO index (positive phase) occurs during an intensification of the Icelandic Low and Azores High. Except for some years for which the SLP patterns are spatially shifted (e.g. 1999, 2000 and 2018 where the location of high and low SLP were reversed in March), positive winter NAO years favor strong northwesterly winds, cold air and sea surface temperatures, and heavy ice conditions on the NL shelves (Colbourne et al., 1994; Drinkwater 1996; Petrie et al., 2007). In 2021, the winter NAO was negative for the first time in 8 years (although only very slightly at -0.1; first row in Figure 3). While the lowest winter NAO index value was reached in 2010, all years between 2012 and 2020 (except 2013) were positive, including the record high of +1.6 in 2015. As we will see during this report, the return to a negative winter NAO index in 2021 was accompanied by a warmer than usual winter, which had important consequences for the region as a large number of variables analyzed here were warmer than normal.

The Arctic Oscillation (AO) is a larger scale index intimately linked with the NAO. During a positive phase, the arctic air outflow to the Northwest Atlantic increases, resulting in colder winter air temperatures over much of the NL and adjacent shelf regions. Similar to the NAO, the AO was slightly negative in 2021 at -0.1 (Figure 3), indicative of warmer than usual air temperatures above the region. In 2015, the AO was at its highest value since 1990 at +1.6. A record low was reached in 2010 when it was below normal at -1.5 (warm air temperatures).

The Atlantic Multidecadal Oscillation (AMO) is also provided in Figure 3. This index, based on the Sea Surface Temperature of the Atlantic Ocean, evolves as part of a 65-80 year cycle that influences the regional climate and has consequences on the ocean circulation in the North Atlantic (e.g., Kerr 2000). The AMO has been in a positive phase since the late 1990s.

Air temperature anomalies (winter and annual values) from five coastal communities around the Northwest Atlantic (Nuuk Greenland, Iqaluit Baffin Island, Cartwright Labrador, Bonavista and St. John's Newfoundland) are shown in Figure 3 as normalized anomalies (referenced to the 1991-2020 period) between 1980 and 2021, and in Figure 4 and Figure 5 as cumulative annual and monthly anomalies, respectively. Except for Nuuk for which data are obtained from the Danish Meteorological Institute, the air temperature data from Canadian sites are from the second generation of Adjusted and Homogenized Canadian Climate Data (AHCCD), which accounts for shifts in station location and changes in observation methods (Vincent et al. 2012). Because the AHCCD product was not ready for the year 2021, historical data from the Government of Canada Monthly Climate Summaries have been used for that year.

Overall, the air temperature was above normal for all sites in 2021 (Figure 3). Temperatures were especially warm during the winter at the northern Canadian sites, being, for example, 7.8°C and 7.2°C above normal in Iqaluit, respectively for January and February, and 6.4°C and 5.0°C above normal for the same months in Cartwright (Figure 5). Over the winter season, Nuuk temperature was 0.9 SD above normal and the four Canadian sites were 2.0 to 2.4 SD above normal (Figure 3). Note that this set new records for Iqaluit, Bonavista and St. John's (tied with 2011). For Cartwright, 2021 was the second warmest winter after 2010. For the rest of the year, temperatures were still mostly on the warm side, but closer to the normal, except for July in St. John's that was cold at -1.0 SD (Figure 5). Averaged over the year the air temperatures were above normal at all sites (Figure 4), making 2021 the second warmest year since 1950 at +1.3 SD (see bottom scorecard). 2010 was the warmest year at +2.1 SD.

Annual air temperature anomalies for six sites in the Scotian Shelf-Gulf of Maine region (location in Figure 1) are shown in Figure 6 and in Table 1. In 2021, the mean annual air temperature anomalies were well above normal at all sites with anomalies ranging from +1.3 to +2.0 SD. The time series of annual anomalies indicates that all sites have increasing temperatures over the long term with decadal scale variability superimposed. Over shorter periods, there are times when there is no trend or a decreasing trend in the temperature. Linear trends from 1900 to present for Sydney, Sable Island, Halifax, Yarmouth, Saint John and Boston correspond to changes (and 95% confidence limits) per century of +1.2°C (+0.8°C, +1.6°C), +1.4°C (+1.1°C, +1.8°C), +2.0°C (+1.6°C, +2.3°C), +1.2°C (+0.9°C, +1.6°C), +1.2°C (+0.9°C, +1.6°C) and +2.8°C (+2.4°C, +3.0°C), respectively.

The anomalies for all 6 sites are displayed in Figure 7 as a composite sum. For most years the anomalies have the same sign. Since 1900, 98 of the 121 years had five or more stations with the annual anomalies having the same signs; for 69 years, all six stations had anomalies with the same sign. This indicates that the spatial scale of the air temperature patterns is greater than the largest spacing among sites.

	80	81	82	83	84	85	86	87	88	89	90	91	92	93	94	95	96	97	98	99	00
-- Climate indices --																					
NAO_{winter}	0.0	0.2	0.3	0.9	0.6	-0.5	0.5	-0.2	0.5	1.4	0.7	0.5	0.6	0.8	1.1	1.3	-0.5	0.3	0.0	0.5	1.2
AO	-0.6	-0.4	0.3	0.0	-0.2	-0.5	0.1	-0.5	0.0	1.0	1.0	0.2	0.4	0.1	0.5	-0.3	-0.5	0.0	-0.3	0.1	0.0
AMO	0.0	-0.1	-0.2	-0.1	-0.2	-0.3	-0.3	0.0	0.0	-0.1	-0.1	-0.2	-0.2	-0.2	-0.2	0.1	-0.1	0.0	0.3	0.1	0.0
-- Winter Air Temperature --																					
Nuuk	0.8	0.2	0.0	-3.0	-3.6	0.4	2.2	-0.4	0.4	-1.4	-0.6	-1.1	-1.4	-2.5	-0.7	-1.3	0.4	0.1	-0.1	-0.3	0.1
Iqaluit	0.4	0.8	0.9	-2.3	-2.0	0.6	1.7	-1.3	-0.4	-1.7	-1.1	-1.7	-0.9	-2.1	-0.8	-0.2	0.2	0.1	-1.9	-0.3	0.2
Cartwright	0.4	0.8	0.1	-1.3	-1.0	-0.2	0.0	-0.2	-0.1	-1.3	-1.3	-1.4	-1.6	-1.5	-1.1	-0.8	0.4	0.1	0.7	0.3	0.2
Bonavista	-0.3	0.6	-0.2	-0.3	-0.4	-1.0	-0.5	-0.9	-0.2	-1.5	-2.4	-1.5	-1.8	-2.1	-1.7	-1.0	0.4	-0.2	0.1	0.8	1.0
StJohns	-0.6	0.6	-0.4	0.6	0.4	-0.8	-0.3	-1.3	-0.4	-1.7	-2.4	-1.3	-1.9	-1.9	-1.5	-1.0	0.1	-0.1	-0.1	1.1	1.2
-- Annual Air Temperature --																					
Nuuk	0.4	-0.2	-1.6	-2.4	-2.7	1.0	-0.2	-0.4	0.0	-1.7	-1.2	-0.7	-2.0	-2.2	-1.1	-0.6	0.1	-0.2	0.0	-0.3	0.1
Iqaluit	0.4	1.2	-1.3	-2.1	-1.6	0.9	-1.1	-1.2	-0.4	-1.6	-1.7	-0.9	-2.3	-2.3	-0.7	0.3	0.3	0.6	-0.2	-0.5	0.2
Cartwright	-0.2	0.9	-1.3	-0.6	-1.1	-0.7	-1.0	0.3	-0.4	-0.6	-1.2	-1.5	-1.3	-1.3	-0.6	-0.5	0.3	-0.4	0.5	0.8	0.4
Bonavista	-1.1	0.6	-1.0	0.1	-0.4	-1.3	-0.9	-0.3	0.2	-0.2	-0.7	-1.7	-1.7	-1.6	-0.6	-0.7	0.5	-0.9	0.6	0.5	0.9
StJohns	-1.6	0.8	-1.3	0.3	0.1	-2.0	-1.3	-0.9	-0.1	-0.9	-0.8	-1.8	-2.2	-1.8	-0.7	-1.0	0.1	-1.4	0.4	1.8	0.8

	01	02	03	04	05	06	07	08	09	10	11	12	13	14	15	16	17	18	19	20	21	$\bar{x}$	sd
-- Climate indices --																							
NAO_{winter}	-0.3	0.4	0.0	0.3	0.2	-0.2	0.6	0.5	0.1	-1.5	-0.4	1.3	-0.4	0.8	1.6	1.2	0.7	0.7	0.7	1.2	-0.1		
AO	-0.2	0.1	0.2	-0.2	-0.4	0.1	0.3	0.2	-0.3	-1.0	0.5	-0.2	0.0	-0.1	0.6	-0.1	0.3	0.2	-0.1	0.8	-0.1		
AMO	0.1	0.0	0.2	0.2	0.3	0.2	0.1	0.1	0.0	0.3	0.1	0.2	0.1	0.1	0.1	0.3	0.3	0.0	0.1	0.3	0.2		
-- Winter Air Temperature --																							
Nuuk	0.2	0.1	0.9	1.3	0.3	0.6	1.0	-1.5	0.6	2.3	1.3	-0.1	0.5	0.1	-1.0	0.1	0.1	-0.5	1.1	-0.5	0.9	-7.2	2.2
Iqaluit	0.4	-0.2	0.3	0.8	-0.6	0.4	1.1	-1.0	-0.1	2.2	2.1	0.6	0.6	0.5	-1.2	0.2	0.4	0.1	0.6	0.3	2.4	-23.9	3.0
Cartwright	-0.1	0.3	0.1	1.6	-0.1	0.6	0.8	-0.9	0.1	2.7	2.0	0.0	0.8	-0.8	-1.2	0.3	-0.2	0.2	-0.3	-0.9	2.2	-12.0	2.6
Bonavista	-0.3	0.1	-0.9	0.9	0.4	1.5	0.2	-0.5	0.4	1.0	1.9	0.8	0.6	-1.2	0.1	0.6	0.0	1.1	-0.7	0.0	2.0	-3.2	1.3
StJohns	-0.8	0.0	-1.0	0.7	0.5	1.4	-0.1	-0.4	0.9	0.9	2.0	0.7	0.4	-1.0	0.5	0.6	-0.1	1.2	-0.8	0.0	2.0	-3.0	1.2
-- Annual Air Temperature --																							
Nuuk	0.5	-0.1	1.1	0.4	1.0	0.6	0.4	-0.1	0.3	2.8	-0.6	0.9	0.5	0.1	-1.5	1.0	0.2	-0.9	1.0	-0.6	0.8	-1.0	1.3
Iqaluit	0.4	-0.5	0.6	-0.2	0.7	1.3	-0.1	-0.4	0.2	2.9	0.3	0.4	0.0	0.2	-1.7	0.1	0.5	-0.6	0.9	0.5	1.5	-8.3	1.5
Cartwright	0.5	-0.4	0.3	0.9	0.7	1.5	0.0	0.0	0.3	2.2	0.5	1.1	0.4	-0.1	-3.0	-0.4	0.1	-0.2	-1.1	0.4	1.5	0.2	1.4
Bonavista	0.5	-0.2	0.2	0.7	0.8	1.2	0.6	0.4	0.2	1.3	-1.6	1.4	0.7	-0.1	-0.7	0.3	0.9	-2.1	-0.5	0.9	1.6	5.0	1.0
StJohns	0.1	-0.7	0.1	0.3	0.5	1.4	-0.4	0.6	0.7	1.3	0.1	1.5	0.7	0.1	-1.0	0.2	0.1	0.2	-0.7	0.8	1.1	5.5	0.8

Figure 3. Scorecard of large-scale indices (winter NAO, AO and AMO) and normalized air temperature anomalies (winter and annual) for five cities between 1980 and 2021. Means and standard deviations for the air temperatures during the 1991-2020 period are provided in the last column (in °C). No means or standard deviations are provided for the large-scale indices (grayed boxes).

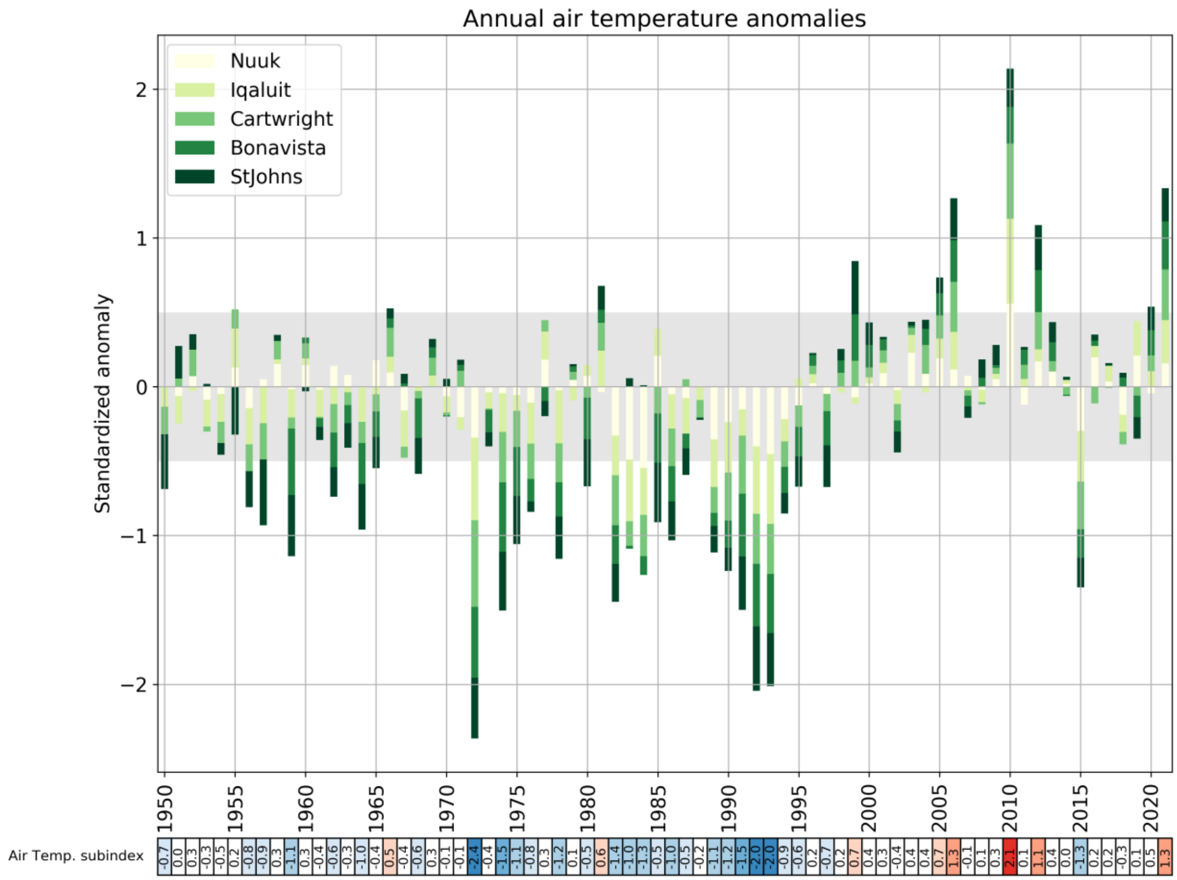

Figure 4. Normalized annual air temperature anomalies for Nuuk, Iqaluit, Cartwright, Bonavista and St. John's. This figure shows the average of the five stations, in which the length of each bar corresponds to the relative contribution of the individual station to the average. The shaded area corresponds to the 1991–2020 average ±0.5 SD, a range considered normal. The numerical values of this time series are reported in a colour-coded scorecard at the bottom of the figure.

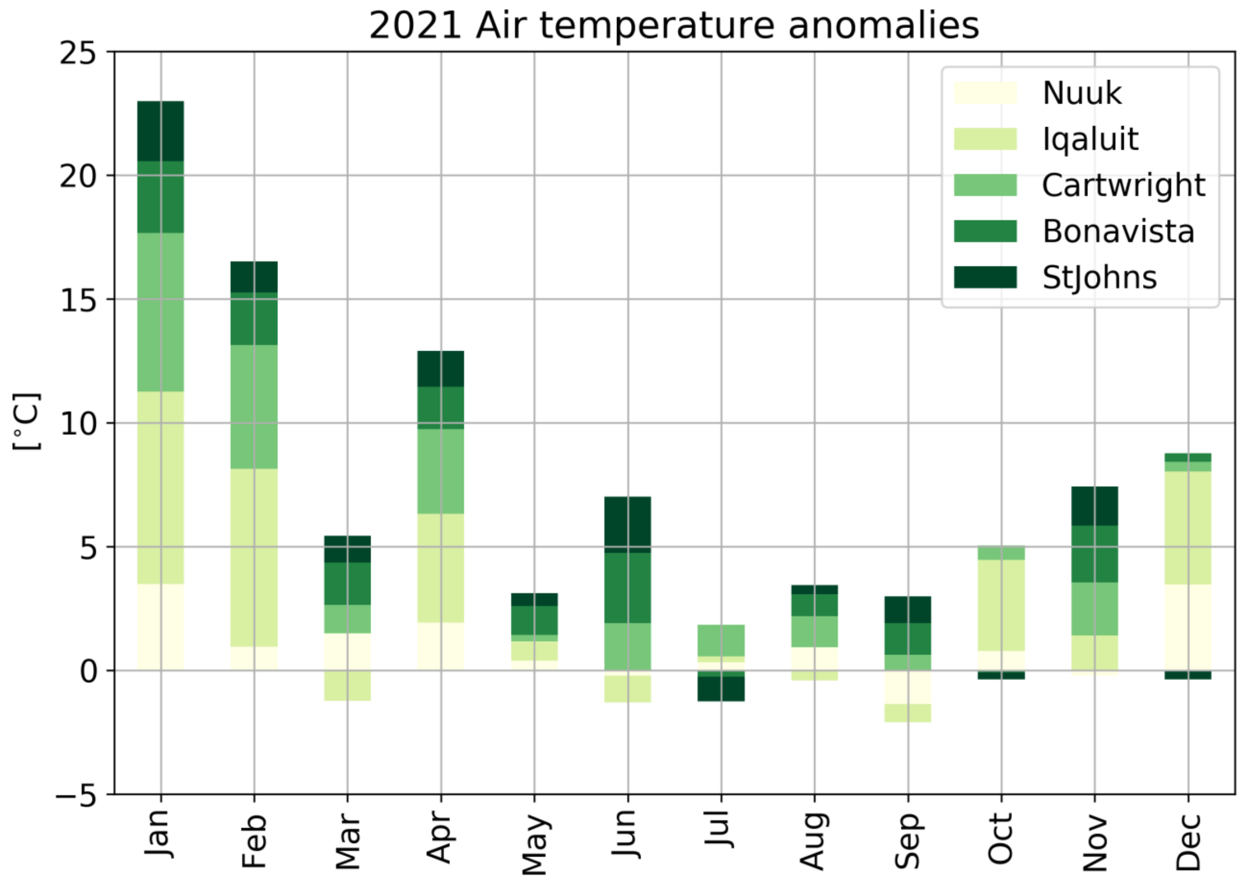

Figure 5. Cumulative monthly air temperature anomalies at Nuuk, Iqaluit, Cartwright, Bonavista and St. John's for 2021.

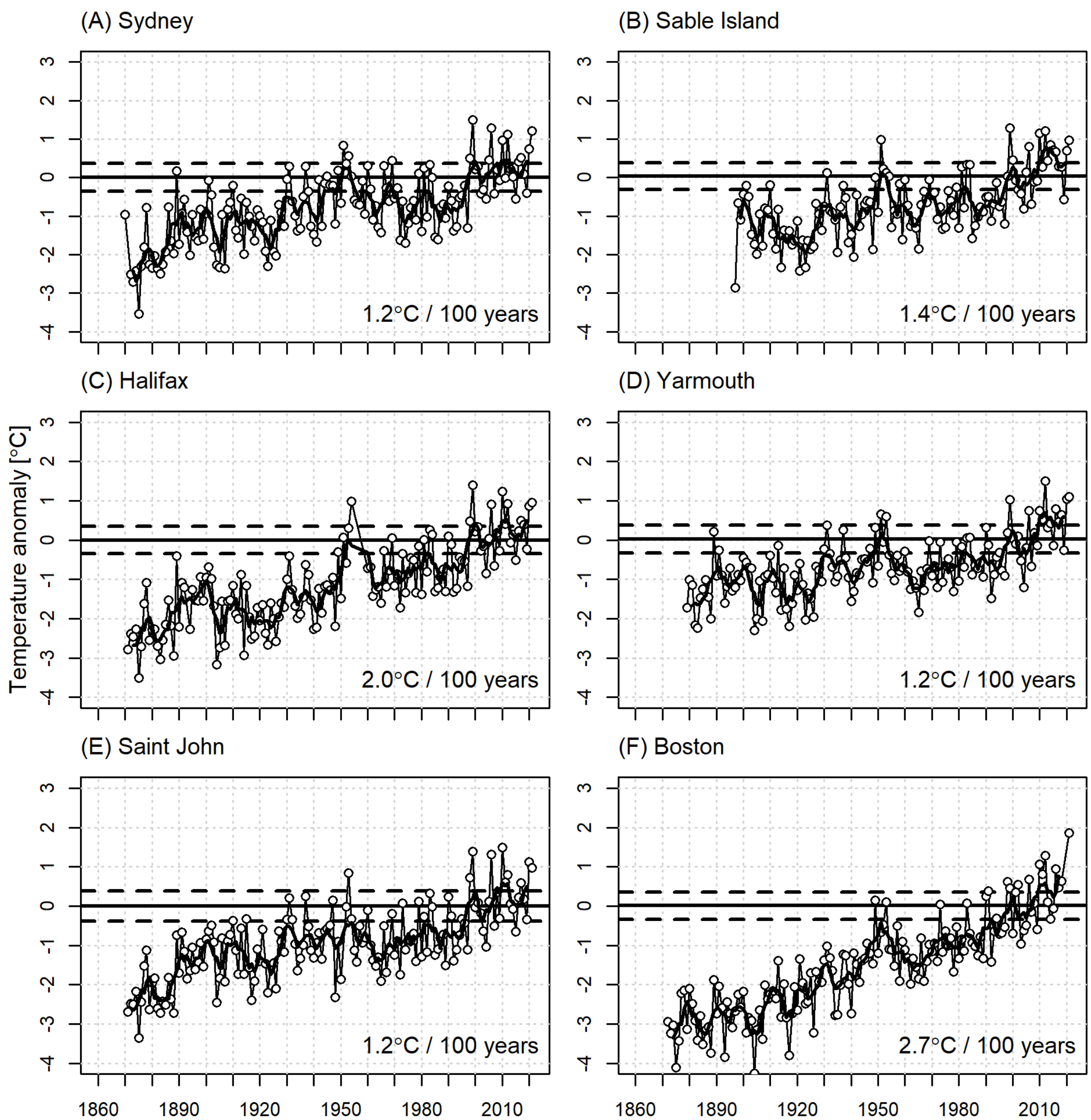

Figure 6. Annual air temperature anomalies in °C (dashed line) and five year running means (solid line) at selected sites (Sydney, Sable Island, Shearwater, Yarmouth, Saint John and Boston) in Scotian Shelf-Gulf of Maine region (years 1860 to 2021). Horizontal dashed lines represent the 1991-2020 climatological average ±0.5 SD.

Table 1. The 2021 annual mean air temperature anomaly in degrees and standardize anomaly (relative to the 1991-2020 climatology) for Scotian Shelf and Gulf of Maine.

Site	Annual Anomaly		1991-2020 Climatology	
	Observed (°C)	Normalized	Mean (°C)	SD (°C)
Sydney	+1.2	+1.7	6.45	0.72
Sable Island	+1.0	+1.4	8.35	0.69
Shearwater (Halifax)	+1.0	+1.4	7.16	0.70
Yarmouth	+1.1	+1.6	7.69	0.71
Saint John	+1.0	+1.3	5.71	0.77
Boston	+1.4	+2.0	10.99	0.72

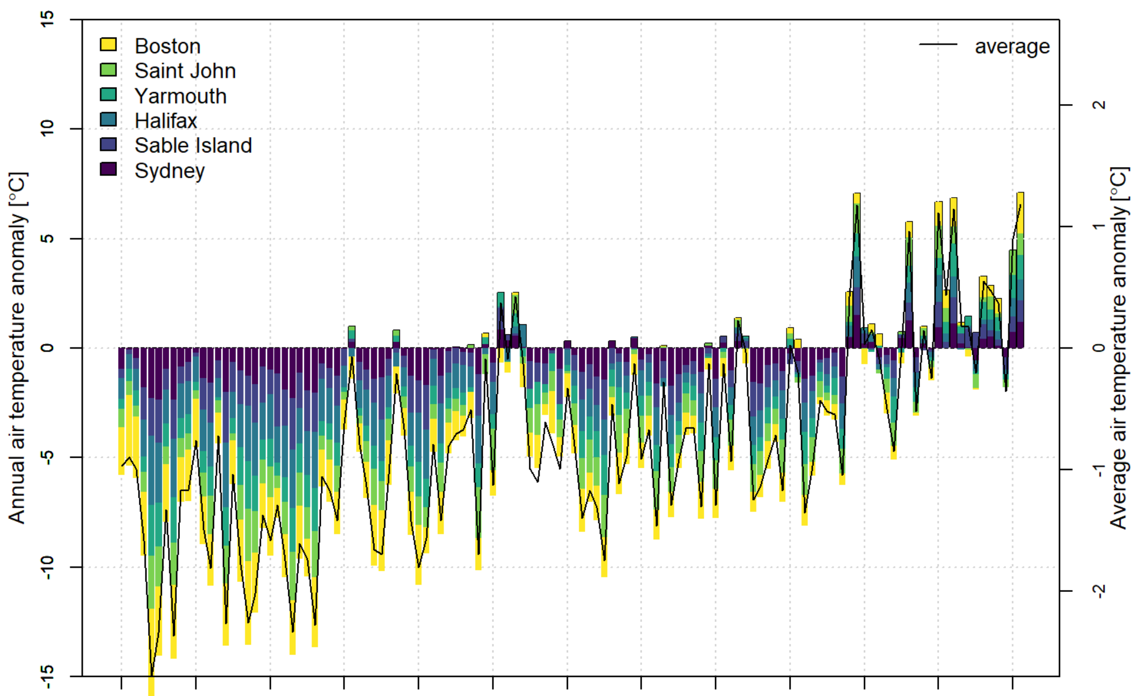

Figure 7. The contributions of each of the annual temperature anomalies for 6 Scotian Shelf-Gulf of Maine sites (Boston, Saint John, Yarmouth, Shearwater, Sable Island and Sydney) are shown as a stacked bar. Anomalies are referenced to the 1991-2020 period.

Sea-Ice Conditions

Ice cover area, volume and seasonal duration are estimated from ice cover products obtained from the Canadian Ice Service (CIS). These products consist of Geographic Information System (GIS) charts covering the East Coast, with weekly charts available for 1969-2021 and daily charts for 2009-2021, and 1980-2021 weekly charts for the Hudson Bay system that cover the Northern Labrador Shelf. All charts were further converted into regular 0.01° latitude by 0.015° longitude grids (approximately 1 km resolution), with ice concentrations and growth stages attributed to each grid point. Average thicknesses (and therefore regional volumes) are estimated from standard thicknesses attributed to each stage of ice growth from new ice and nilas (5 cm), grey ice (12.5 cm), grey-white ice (22.5 cm), thin first year ice (50 cm), medium first year ice (95 cm) and thick first year ice (160 cm). Prior to 1983, the CIS reported ice categories with fewer classifications, where a single category of first year ice (≥ 30 cm) was used with a suggested average thickness of 65 cm. We have found this value to lead to underestimates of the seasonal maximum thickness and volume based on high interannual correlations between the estimated volume of the weekly seasonal maximums and its area or sea-ice season duration. The comparisons of these correlations pre- and post-1983 provided estimates of first-year ice thickness of 85 cm in the Gulf of St. Lawrence and 95 cm on the Newfoundland and Labrador Shelf for this single first year ice category, which were used instead of the suggested 65 cm.

Several products were computed to describe the sea-ice cover inter-annual variability. The day of first and last occurrence, ice season duration (Figure 8) and distribution of ice thickness during the week of maximum volume (Figure 9) are presented as maps. These two figures combine information from the East Coast sea ice charts and Hudson Bay system charts, leading to a slight jump in the climatology maps of first occurrence and duration. The reason this occurs is because there are often missing weeks in the Hudson Bay charts around the period of first occurrence on the northern Labrador Shelf. Therefore anomalies of these two parameters are not as good quality as the rest. Regional scorecards of anomalies in the first and last day of ice, duration of the sea ice season and maximum ice volume are presented in Figure 10 for the Labrador and Newfoundland shelves. Here, the areas defined as Northern and Southern Labrador shelves and Newfoundland Shelf are shown in Figure 9, with the Newfoundland Shelf and Gulf of St. Lawrence delimited at the Eastern end of the Strait of Belle Isle. Evolution of the ice volume during the 2021 ice season is presented in Figure 11 for the three regions in relation to the climatology and historical extremes. The Northern Labrador Shelf progression is shown using weekly data extracted from Hudson Bay charts and the others are shown using daily data extracted from East Coast charts. Time series of seasonal maximum ice volume, area (excluding thin new ice) and ice season duration are presented for the Northern (top left) and Southern (top right) Labrador Shelf and for the Newfoundland Shelf (bottom) in Figure 12. December-to-April air temperature anomaly at Cartwright is included with reversed scale in the Newfoundland Shelf panel. The durations shown in Figure 10 and Figure 12 are different products. The first corresponds to the number of weeks where the volume of ice anywhere within the region exceeded 5% of the climatological maximum, while the second is the average duration at every pixel of Figure 8, which is much shorter than the first.

Ice typically starts forming in December along the Labrador coast and only by late February at the southern extent of sea-ice presence (Figure 8). Last occurrence is typically in late June to early July on the Labrador coast, leading to sea-ice season durations of 23 weeks or more. There has been a declining trend in ice cover severity since the early 1990s reaching the lowest values in 2011 and 2010, with a rebound in 2014 (Figure 10 and Figure 12). On the Newfoundland Shelf, the sea ice metrics of annual maximum ice area, volume, and ice cover duration are well correlated with each other ($R2 = 0.70$ to 0.74; Figure 12). The best correlation with air temperature was found between the December-April air temperature anomaly at Cartwright and the sea-ice metrics of the Newfoundland Shelf ($R2 = 0.64$-0.80), indicative of the advective nature of sea ice on the

Newfoundland Shelf; i.e. strong ice cover is associated with cold air temperatures in the source area. Sensitivity of the Newfoundland Shelf ice cover to air temperature increase (e.g. through anthropogenic climate change) can thus be estimated using 1969-2021 co-variations between winter air temperature and sea-ice parameters, which indicate losses of 14 km3, 26 000 km^2 and 8 days of sea-ice season for each 1°C increase in winter air temperature.

In 2021 the sea-ice cover first appeared at a near normal period on the Northern Labrador Shelf and inshore on the Southern Labrador Shelf, but later than normal by many weeks offshore and on northern parts of the Newfoundland Shelf and never appeared at all on southern parts (Figure 8), leading to regional numbers that were also later than normal (Figure 10). Last occurrence was much earlier than normal everywhere (Figure 8 and Figure 10). Sea ice volume progressed below normal throughout the season in the three regions (Figure 11), reaching daily record lows in May to early June, late April to mid-May and mid to late April respectively in the three north to south regions. The seasonal maximum combined ice volume were below normal in the three regions, at 75 km^3 (-1.0 SD), 59 km^3 (-1.5 SD) and 18 km^3 (-1.3 SD) (Figure 10), while the December-to-June seasonal averages were second lowest of the time series (after 2011 for the two Labrador Shelf regions and 2010 for the Newfoundland Shelf). The bulk durations (Figure 10) on the Northern and Southern Labrador and Newfoundland Shelves were below normal, respectively of 165 (-1.1 SD), 129 (-1.8 SD) and 47 days (-2.0 SD), while the spatial average durations were of 91 (-1.9 SD), 57 (-1.8 SD) and 9 days (-1.8 SD) (Figure 8 and Figure 12). An overview of sea ice conditions (volume and season duration) for NL since 1969 is presented in Figure 13 as the average of normalized anomalies. In 2021, this index was below normal at -1.5 SD and third lowest of the time series after 2010 and 2011.

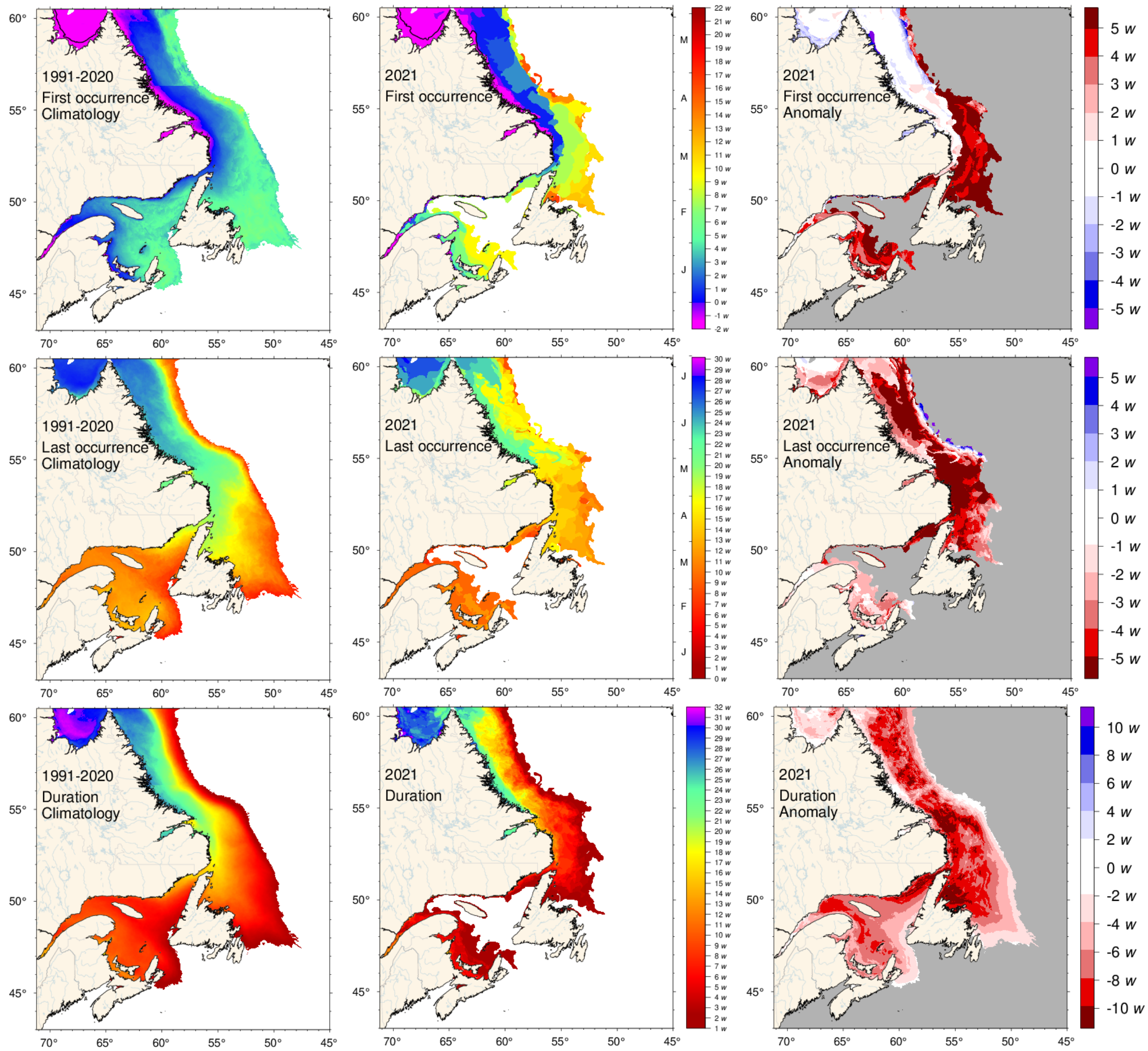

Figure 8. First (top) and last (middle) occurrence of ice and ice season duration (bottom) based on weekly data. The 1991-2020 climatologies are shown (left) as well as the 2021 values (middle) and anomalies (right). First and last occurrences are defined here as the first and last weekly chart in which any amount of ice is recorded for each pixel and are illustrated as day-of-year. Ice duration sums the number of weeks with ice cover for each pixel. Climatologies are shown for pixels that had at least 15 years out of 30 with occurrence of sea-ice, and therefore also show the area with 50% likelihood of having some sea-ice at any time during any given year. The duration anomaly map includes pixels with no ice cover where some was expected based on the climatology.

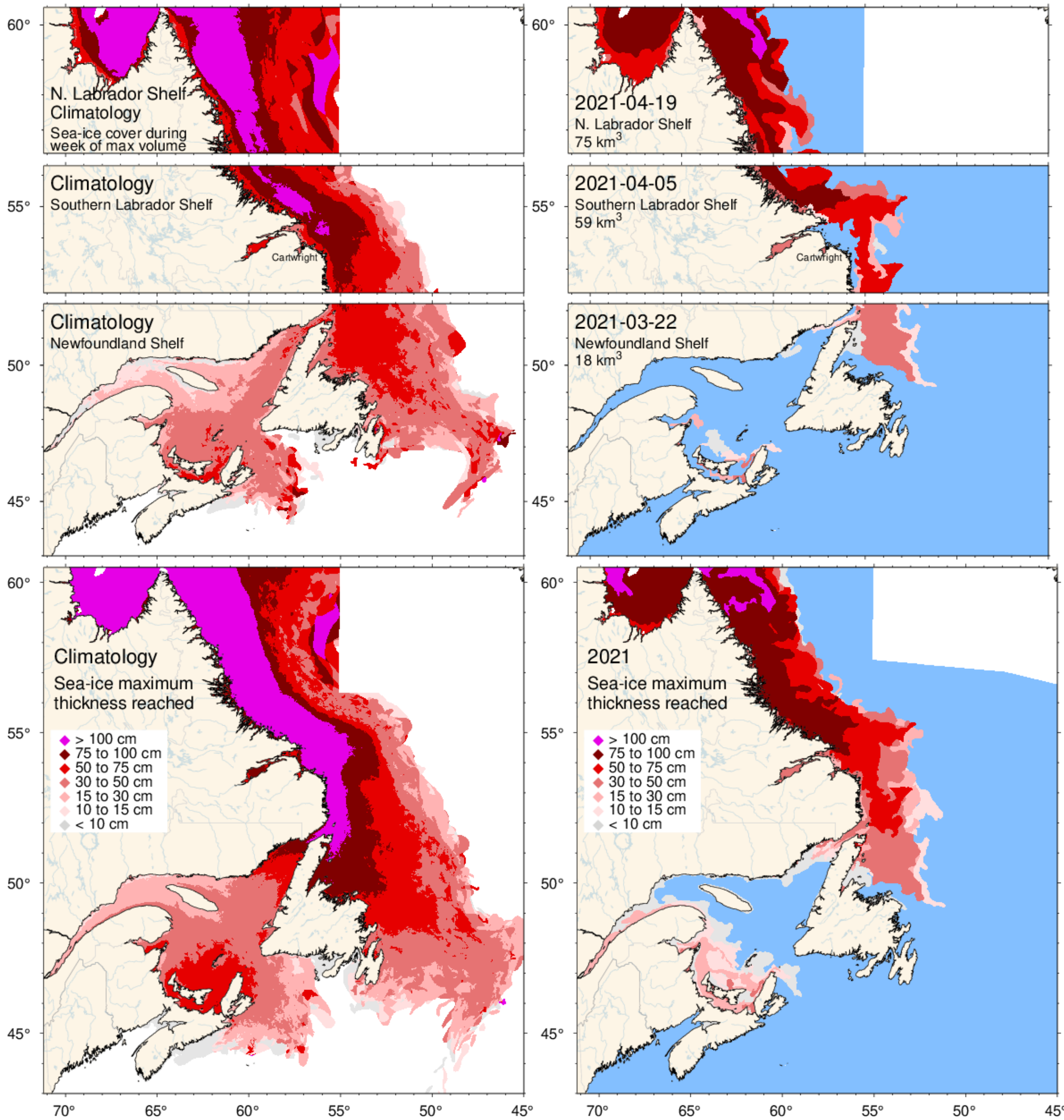

Figure 9. Ice thickness map for 2021 for the week with the maximum annual volume on the Newfoundland and Labrador Shelf (three upper right panel) and similarly for the 1991-2020 climatology of the weekly maximum (three upper left panel). Note that these maps reflect the ice thickness distribution on that week. The maximum ice thickness observed at any given location during the year is presented in the lower panels, showing the 1991-2020 climatology and 2021 distribution of the thickest ice recorded during the season at any location.

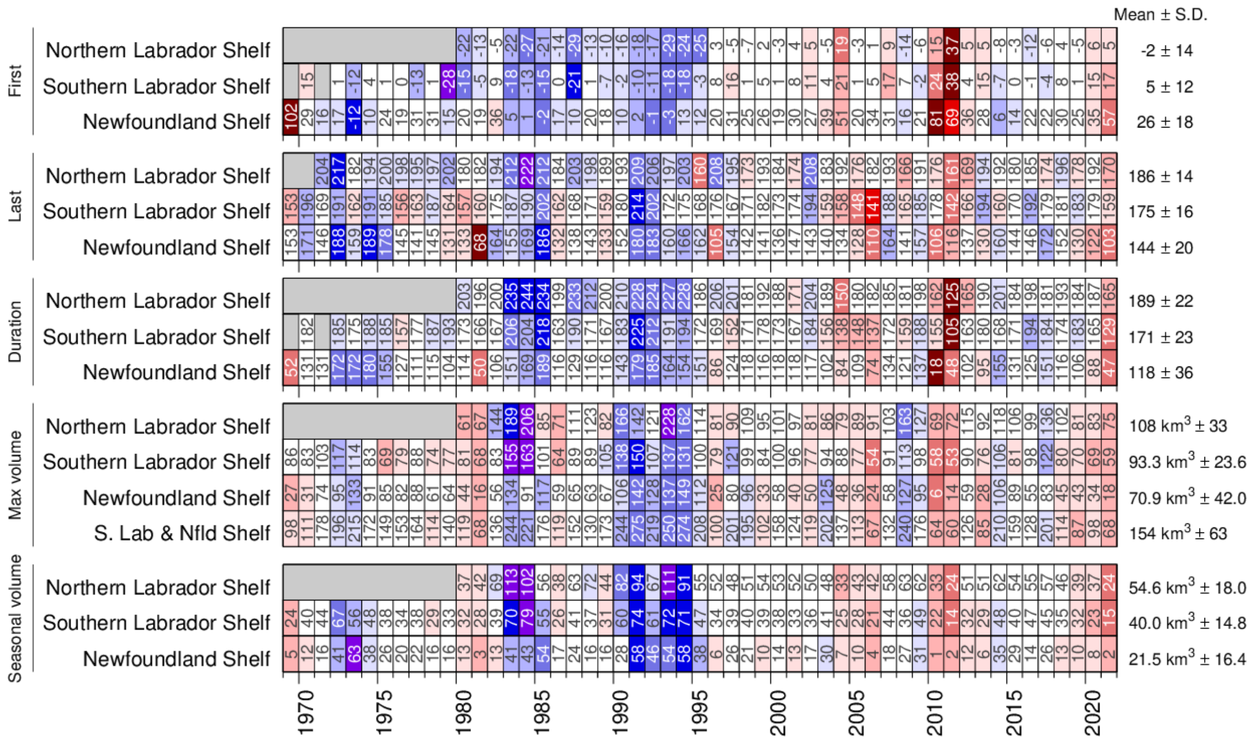

Figure 10. First and last day of ice occurrence, ice duration, maximum seasonal ice volume and average seasonal (DJFMAMJ) ice volume by region. The moment when ice was first and last observed in days from the beginning of each year is indicated for each region, and the color code expresses the anomaly based on the 1991–2020 climatology, with blue (cold) representing earlier first occurrence and later last occurrence. The threshold is 5% of the climatological average of the seasonal maximum ice volume. Numbers in the table are the actual day of the year or volume, but the color coding is according to normalized anomalies based on the climatology of each region. Duration is the numbers of days that the threshold was exceeded. Seasonal average volumes (last block of lines) are reported in the ICES Report on Ocean Climate (e.g. Cyr and Galbraith 2020)

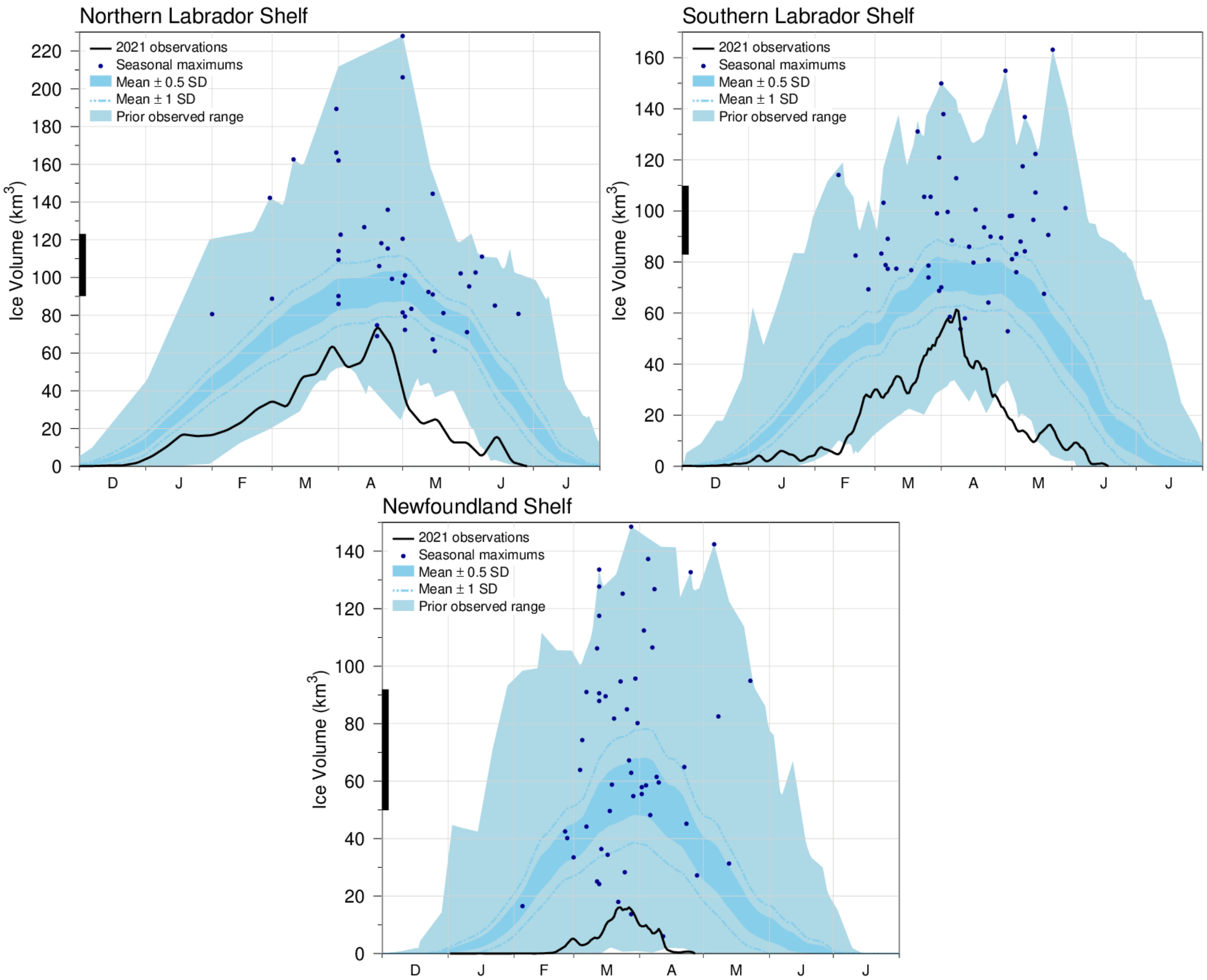

Figure 11. Time series of the 2020-2021 mean ice volume (black lines) for the Northern Labrador Shelf (top left), Southern Labrador Shelf (top right), and Newfoundland Shelf (bottom), the 1991-2020 climatological mean volume ±0.5 and ±1 SD (dark blue area and dashed line respectively), the minimum and maximum span of 1969-2020 observations (light blue), and the date and volumes of 1969-2020 seasonal maximums (blue dots). The black thick line on the left indicates the mean volume ±0.5 SD of the annual maximum ice volume, which is higher than the peak of the mean daily ice volume distribution.

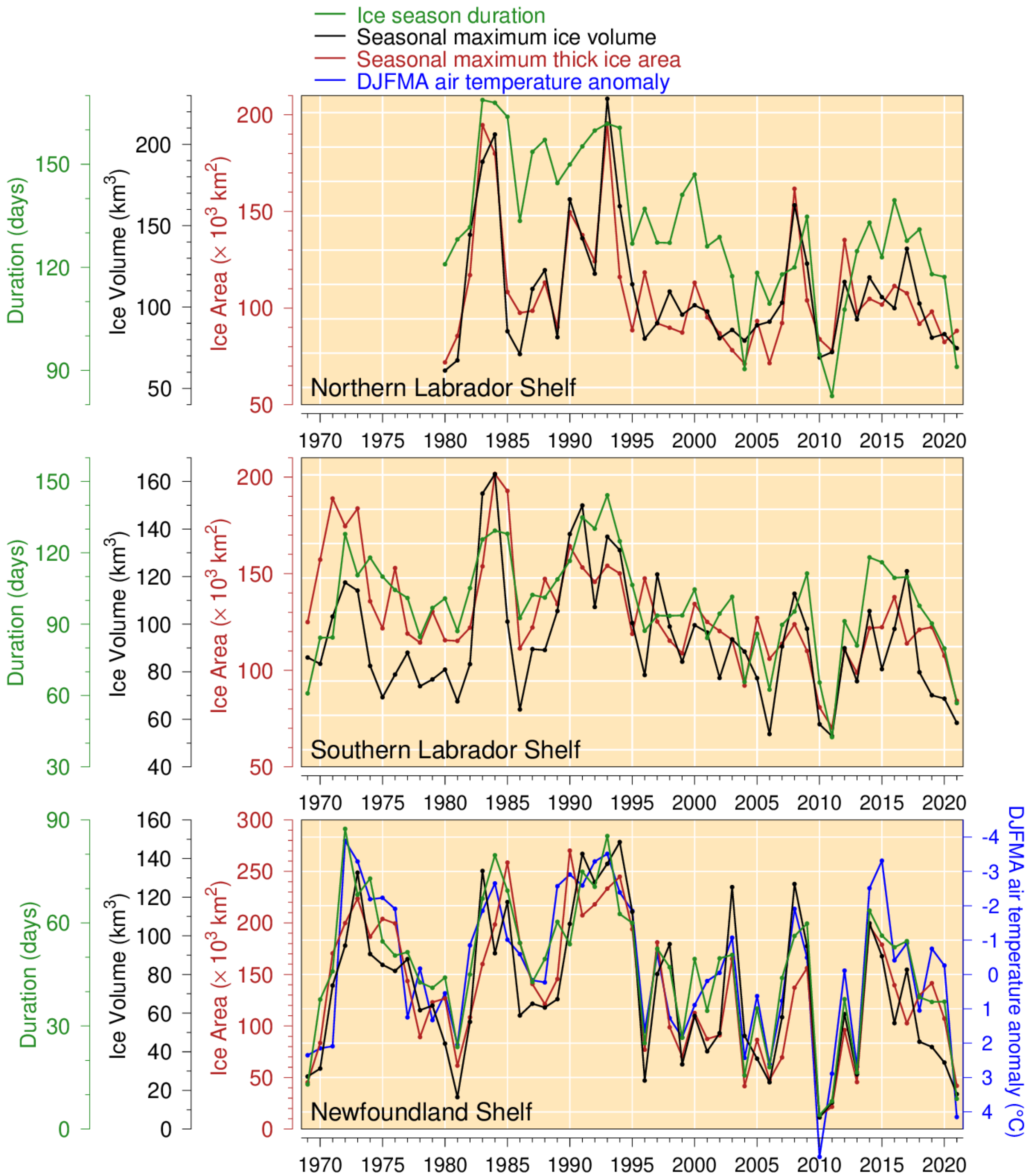

Figure 12. Seasonal maximum ice volume and area (excluding ice less than 15 cm thick), and ice season duration for the Northern and Southern Labrador Shelf (top and middle) and Newfoundland Shelf (bottom), and December-to-April air temperature anomaly at Cartwright.

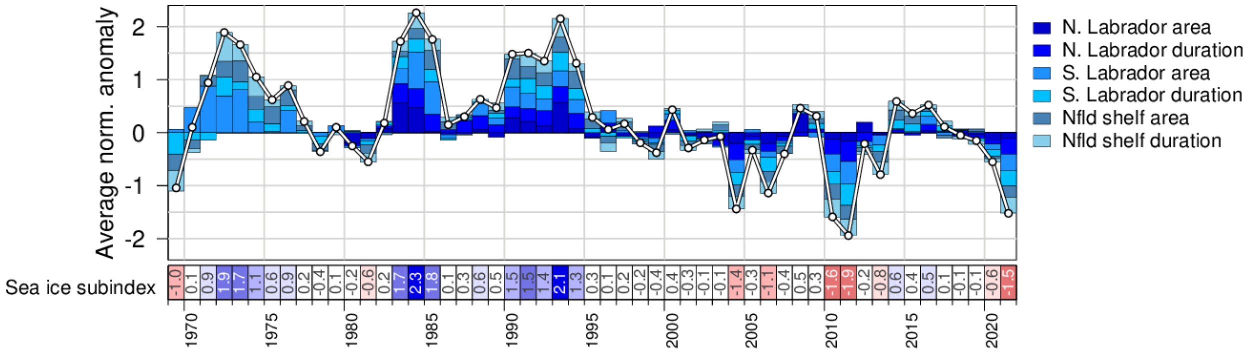

Figure 13. Newfoundland and Labrador sea ice index established by averaging the normalized anomalies of volume and duration of sea ice for Newfoundland and Labrador shelves (black and green time series in Figure 12).

Satellite Sea-Surface Temperature Conditions

Sea Surface Temperatures (SSTs) used here is a blend of data from Pathfinder version 5.3 (1982-2014), Maurice Lamontagne Institute (1985-2013) and Bedford Institute of Oceanography (1997-2019) and monthly temperature composites are based on averaged daily anomalies to which monthly climatological average temperatures are added (see Galbraith et al. 2021 for details).

Averaged over ice-free periods of the year as short as June to November on the Labrador Shelf, May to November in the Gulf, to the entire year on the Scotian Shelf, air temperature has been found to be a good proxy of sea surface temperature. The warming trend observed in air temperature since the 1870s of about 1°C per century is also expected to have occurred in surface water temperatures across Atlantic Canada (Galbraith et al. 2021). The Zone experienced its warmest surface temperatures in 2012 when all regions had positive anomalies over ice-free months, with records reached in the Bay of Fundy-Gulf of Maine (4X eGoM+BoF), Scotian Shelf (4X SS, 4W, 4Vn, 4Vs), St. Pierre Bank (3P) and Flemish pass (3M).

In 2021, monthly average sea surface temperatures were generally normal to above normal in ice-free areas with only 4 of the regional monthly averages showing below normal values (Figure 14 to Figure 16). Multiple monthly series records were recorded, including in January in all 3 shown regions, June in eastern Gulf of Maine and Bay of Fundy, and October, November and December in many regions of the Scotian Shelf and into the Bay of Fundy.

Sea surface temperatures averaged over the ice-free months were normal to above normal across the zone and on average above-normal for the second consecutive year, at +0.9 SD (Figure 17, scorecard at the bottom).

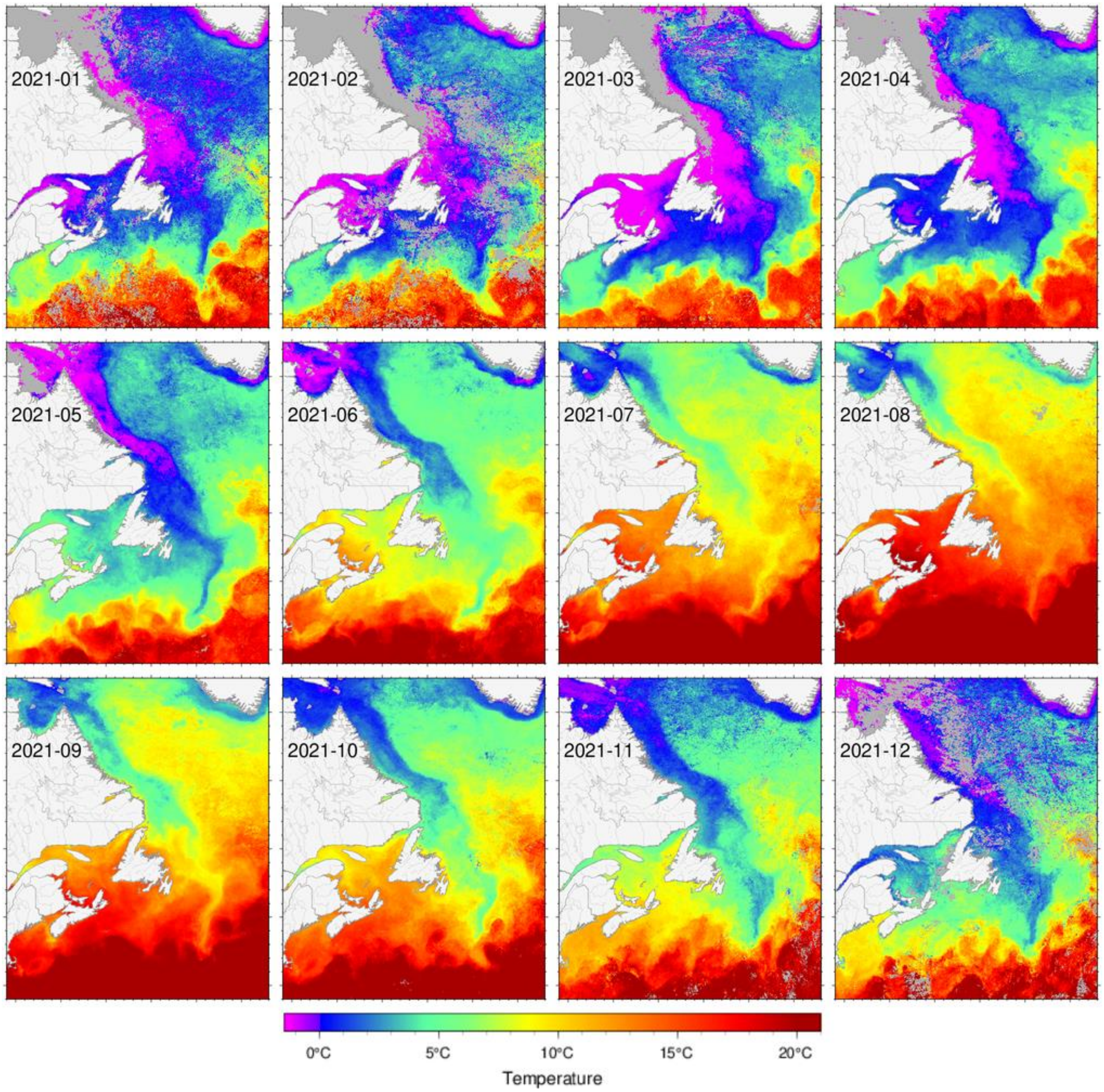

Figure 14. Sea-surface temperature monthly averages for 2021 in the Atlantic zone.

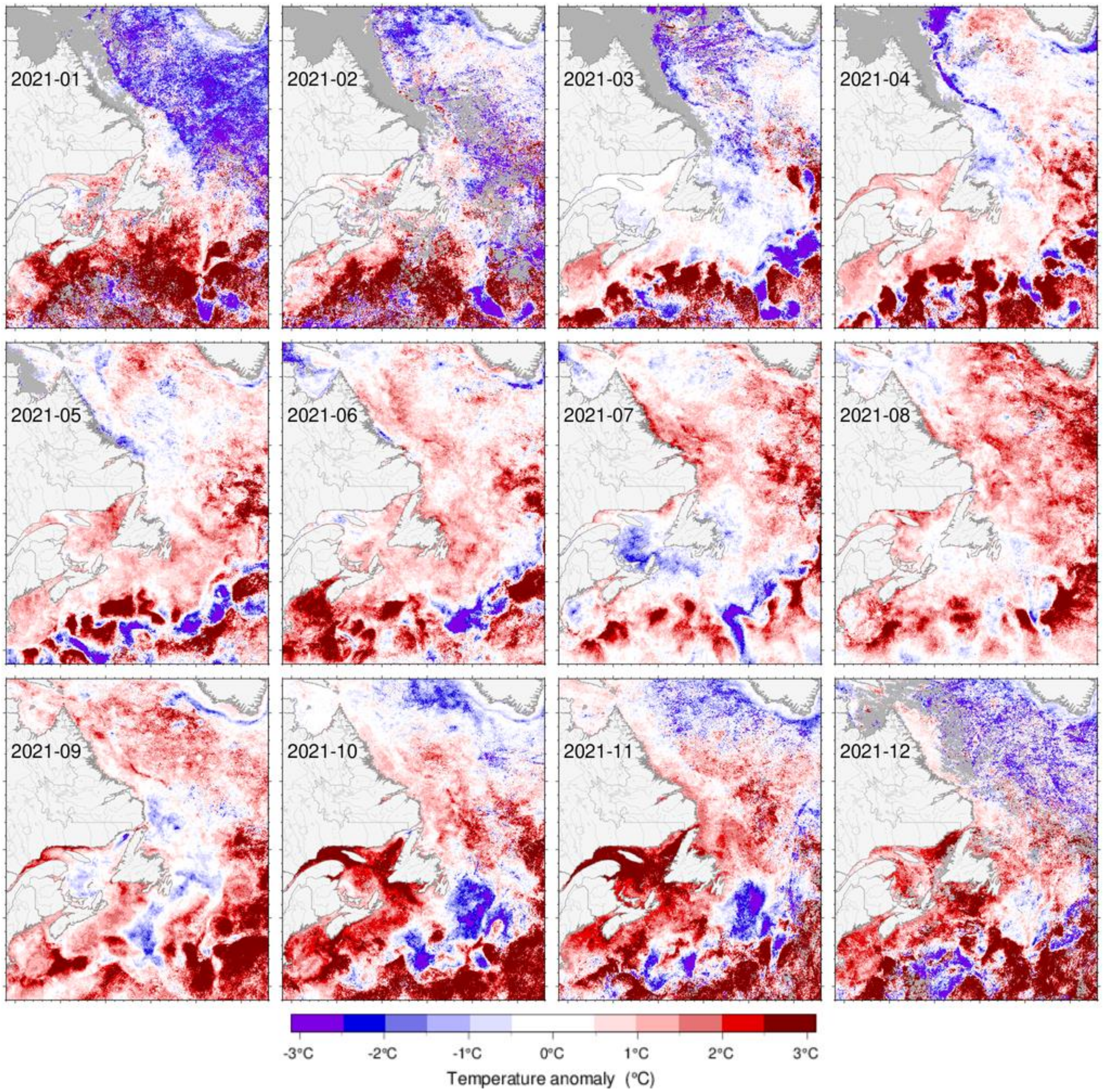

Figure 15. Sea-surface temperature monthly anomalies for 2021 in the Atlantic zone. Temperature anomalies are based on a 1985-2010 climatology.

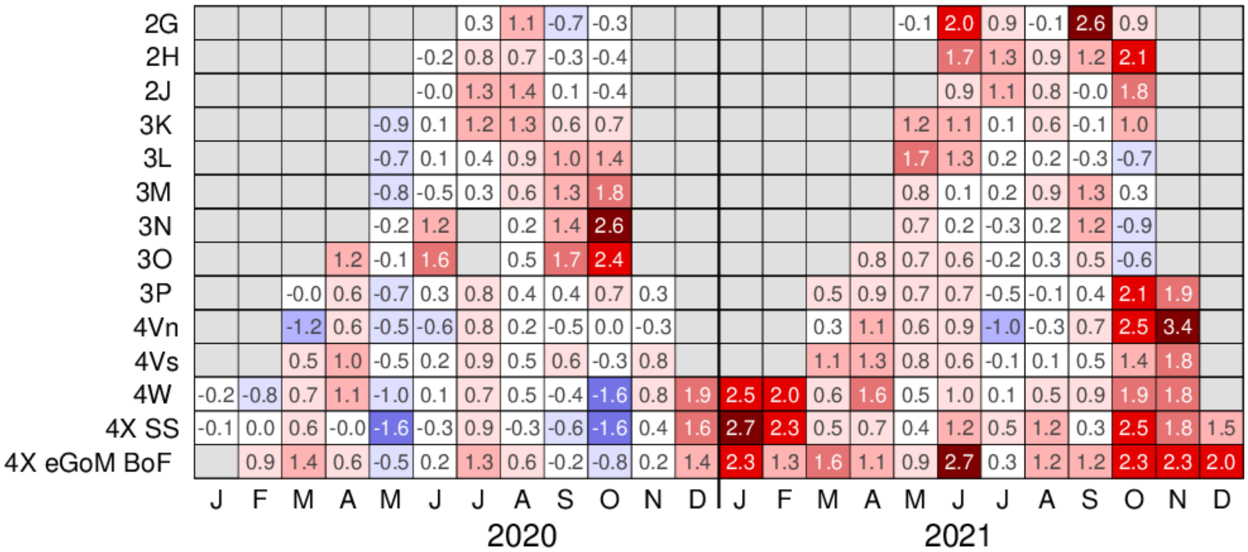

Figure 16. Monthly standardized anomalies of SST for NAFO subareas 2, 3 and 4 during 2020 and 2021 based on 1991-2020 climatologies. The area used for each division is limited to the continental shelf (see black contour in Figure 1). Grayed boxes represent months ignored either because of missing climatology due to ice cover or because coverage was less than 7%.

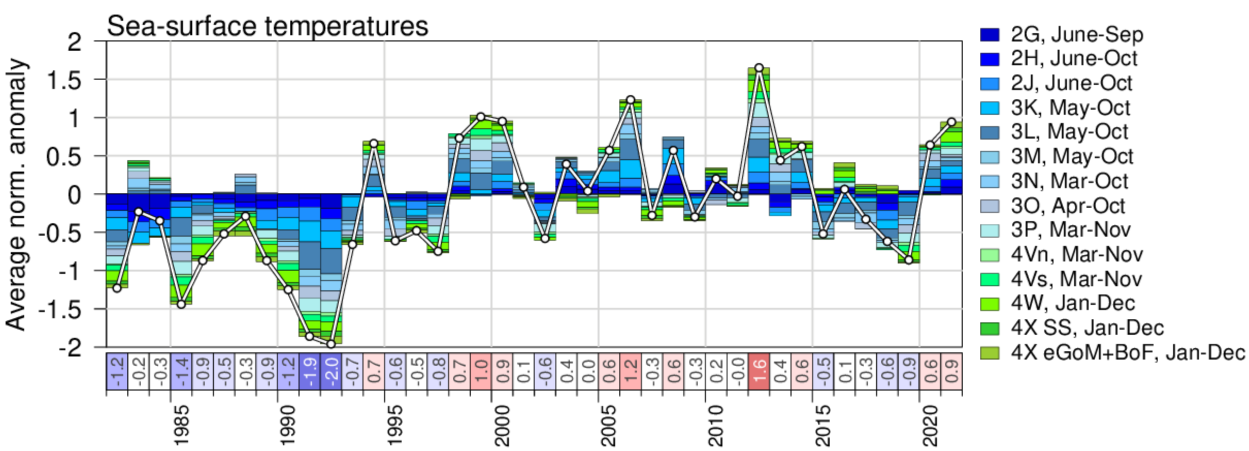

Figure 17. Sea Surface Temperature (SST) composite index in NAFO sub-areas 2 (dark blue), 3 (light blue) and 4 (green) since 1982. This index is built by performing a weighted-area average of the seasonal SST normalized anomaly for each NAFO division (divisions and months used are provided on the right-hand side of the figure).The scorecard at the bottom of the figure represents the index.

Ocean Conditions on the Newfoundland and Labrador Shelf (NAFO Sub-areas 2 and 3)

Long-term observations at Station 27

Station 27 (47° 32.8’ N, 52° 35.2’ W), is located in the Avalon Channel off Cape Spear, NL (Figure 1). It is one of longest hydrographic time series in Canada with frequent, near-monthly, occupations since 1948. In 2021, the station was however only occupied 9 times (April 23, June 29, July 19, August 21, September 25, October 6, October 13, November 22, and December 20), including 5 Conductivity-Temperature-Depth (CTD)-only casts, 4 full AZMP physical-biogeochemical sampling and 0 Expandable Bathythermograph (XBT). Since the first observation was only made late April, 2021 is perpetuating a recurrent problem since 2016 of late first occupation of the year. These late starts miss the re-stratification of the water column that occur early April, which can be used to predict the timing of the phytoplankton bloom in the area.

Since 2017, an automatic profiling system installed on a surface buoy (type Viking) usually provides extended temporal coverage of temperature (T) and salinity (S) at Station 27. Unfortunately, in 2021, the system was deployed in late April and stopped functioning early June. The buoy was recovered and re-deployed late in the summer, but the CTD data suffered electronic spikes that have not been corrected at the time this report was written.

Station occupation and April-June Viking buoy automatic casts were combined to obtain the annual evolution of temperature and salinity at Station 27, as well as the anomaly compared to the 1991-2020 climatology, shown in Figure 18 and Figure 19. These figures demonstrate the seasonal warming of the top layer (~20 m), with temperature peaking in August before being mixed during the fall. The cold intermediate layer (CIL; Petrie et al. 1988), a remnant of the previous winter cold layer and defined as temperature below 0°C (thick black line in Figure 18) is also evident below 100 m throughout the summer. Interestingly, the coldest water body within the CIL (darkest shades of blue in the middle panel of Figure 18) is generally found in the summer between mid-June and mid-August, suggesting advection of cold waters from the Labrador shelf and the Arctic to the Newfoundland shelf. The surface layer is generally freshest between early-September and mid-October, with salinities below 31 (Figure 19). These low near-surface salinities, generally from early summer to late fall, are a prominent feature of the salinity cycle on the Newfoundland Shelf and is largely due to the melting of coastal sea-ice. This presence of large volume of freshwater late in the summer season also points out towards advection from northern areas (Labrador and the Arctic).

The rapid cooling observed above the CIL in October 2021 (which looks like near-vertical contours in Figure 18, top panel) is the result of a storm that hit St. John’s on October 8th-9th, in between the two occupations of October 6th and October 13th. The storm caused a rapid mixing of the water column and a deepening of the CIL. This led to cooling of the upper part of the water column and a warming at depth (see the rapid vertical displacement down of the September-October warm anomaly in Figure 18, bottom panel). This is also accompanied by a similar displacement of the fresh anomaly (Figure 19, bottom panel)

Overall, however, most of the water column was warmer and fresher than normal in 2021 (Figure 18 and Figure 19, top and bottom panels). Over 2021, the annual temperature anomaly (defined as the average of monthly anomalies) for the vertically averaged (0-176 m) temperature was at a record-high since 1951 (Figure 20, top panel). Note that while the fact that Station 27 was les sampled in 2021 compared to historical data adds an extra source of uncertainty on this record, the fact that the warm anomaly is consistent across the year (Figure 19) adds confidence to this result. In addition, warm temperatures at Station 27 are also expected during mild winters such as the one observed in 2021 (see sections on air temperature and sea ice).

The annual anomaly for the vertically-averaged salinity was its second-freshest since 1971 (the freshest was 2018). The fresh anomaly of the early 1970s (Figure 20, bottom panel) is commonly referred to as the Great Salinity Anomaly in the North Atlantic (Dickson et al. 1988). Normalized anomalies of temperature and salinity for all years since 1980 and for different depth ranges (0-176 m, 0-50 m and 150-176 m) are reported in scorecards in Figure 21.

The summer (May-July) CIL statistics at Station 27 since 1951 are presented in Figure 22. Here the CIL mean temperature corresponds to the average of all temperature below 0°C. The CIL thickness as well as the CIL core temperature (the minimum temperature of the CIL) and its depth are also presented in Figure 22. The striking feature in this figure is the exceptionally warm anomaly from the early 1960s to the mid-1970s for the CIL mean and core temperatures (coldest temperature within the CIL), top and middle panels, respectively. These warm anomalies are accentuated by the fact that the climatological reference period (1991-2020) includes a relatively cold period that spanned the mid-1980s to the mid-1990s (see Figure 20). After the prevalence of a warm CIL in the early 2010s (with some of the warmest years since the mid-1970s), there has been a cooler period between about 2014 and 2017. In recent years, the CIL was warmer than normal in 2018, 2019 and 2021, while 2020 was in the normal range. The standard deviations of these metrics are reported in a scorecard in Figure 21.

The monthly mean mixed layer depth (MLD) at Station 27 was also estimated from the density profiles as the depth of maximum buoyancy frequency (*N*) calculated from the monthly averaged density profiles (ρ(z)):

$$N^2 = -\frac{g}{\rho_0}\frac{\Delta\rho(z)}{\Delta z};$$

with g = 9.8 ms^{-2} as the gravitational acceleration, z the depth and ρ_0 as a reference density.

Climatological monthly MLD values, as well as for 2020, are presented in Figure 23. The climatological annual cycle shows a gradual decrease of the MLD between late fall and summer (mixed layer thickest in December-January and shallowest in July-August). Because of the relatively low number of occupation realized in 2021 (most of the time just one profile per month), it is difficult to confidently draw conclusions related to the MLD. Overall, the MLD was close to normal, except slightly shallow in April, slightly thicker in the summer and much thicker than normal in December. Figure 24 shows a time series of the annual mean values of the MLD (solid gray line) and its 5-year moving average (dashed-black line). In general, there is a strong interannual and decadal oscillation in MLD, with a recent increase since the mid-2000s. A scorecard of annual and seasonal MLD anomalies since 1980 can be found in Figure 21.

Stratification is an important characteristic of the water column since it influences, for example, the transfer of solar heat to lower layers and the vertical exchange of biogeochemical tracers between the deeper layers and the surface. The seasonal development of stratification is also an important process influencing the formation and evolution of the CIL on the shelf regions of Atlantic Canada. It essentially insulates the lower water column from the upper layers, thus slowing vertical heat flux from the seasonally heated surface layer.

The stratification index at Station 27 is computed from the density (ρ) difference between 8 and 50 m for each monthly average density profiles (i.e. Δρ/Δz). The annual anomalies are then calculated as the average of monthly anomalies. The 2021 and climatological evolution of the stratification throughout the year are shown in Figure 25. The stratification is generally weakest between December and April, before rapidly increasing at the onset of spring until it peaks in August. While the stratification was close to normal or slightly below/above normal for most of 2021, a notable observation is the high stratification in August, followed by a rapid reduction of the stratification in September (Figure 25). This rapid de-stratification is likely a consequence of Hurricane

Larry that hit Newfoundland between September 10 and 11 with wind gusts observed at 145 km/h at St. John's airport.

The interannual evolution of the stratification anomaly since 1950 is shown in Figure 26. While strong decadal variations exists, the main observation is an increase in stratification from the 1950s to about 2000, followed by a slight decrease since. In 2021, the annual stratification was weaker than normal. A scorecard of annual and seasonal stratification anomalies since 1980 can be found in Figure 21.

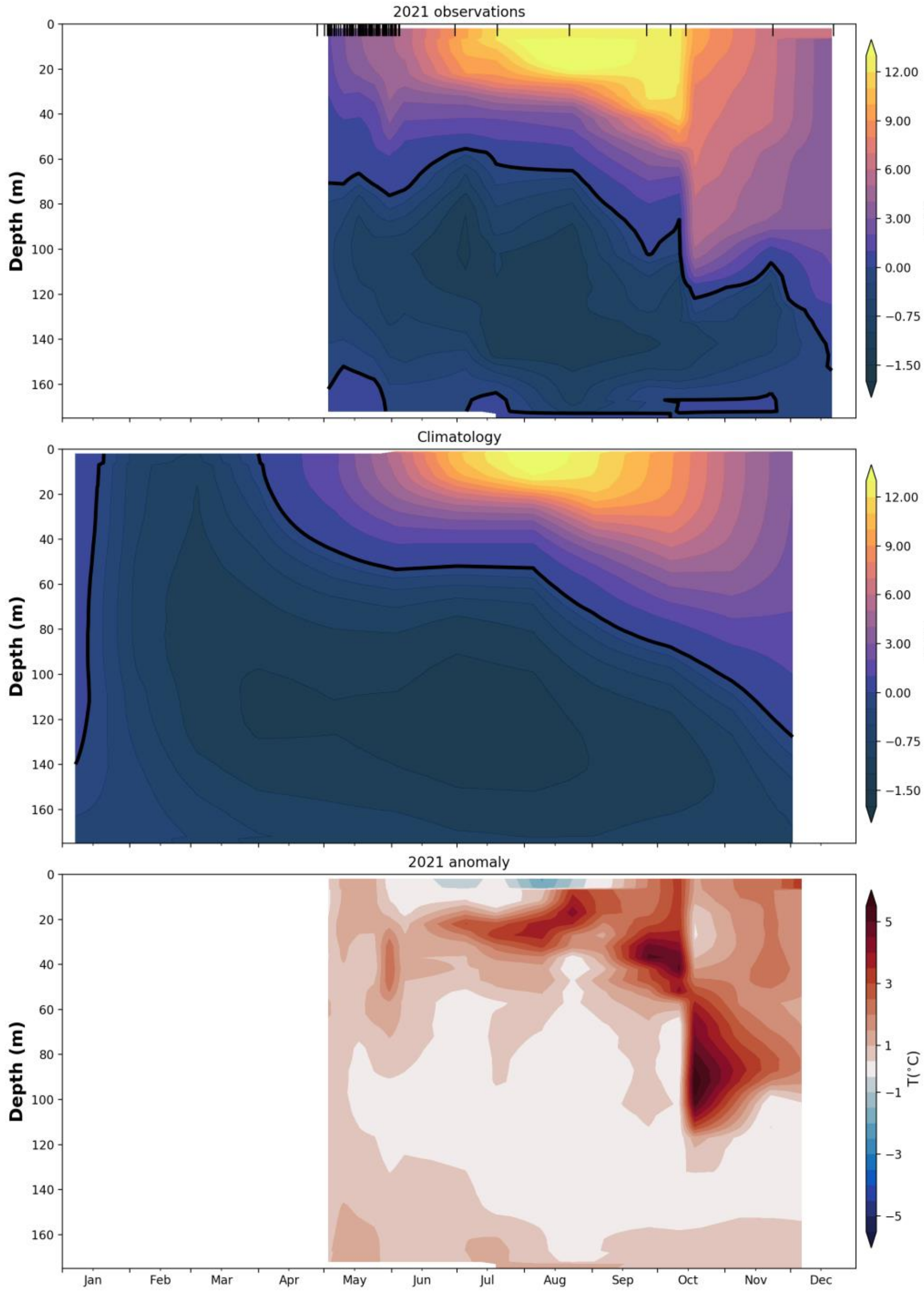

Figure 18. Annual evolution of temperature at Station 27. The 2021 contour plot (top panel) is generated from weekly averaged profiles from all available data, including station occupations and Viking buoy casts (indicated by black tick marks on top of panel). The solid black contour delineates the cold intermediate layer (CIL), defined as water below 0°C. The 1991–2020 weekly climatology is plotted in the middle panel. Note the uneven colorbar used in the two first panels: below 0°C, 0.25°C increments are used, while 1°C increments are used above 0°C. The anomaly (bottom panel) is the difference between the 2021 field and the climatology.

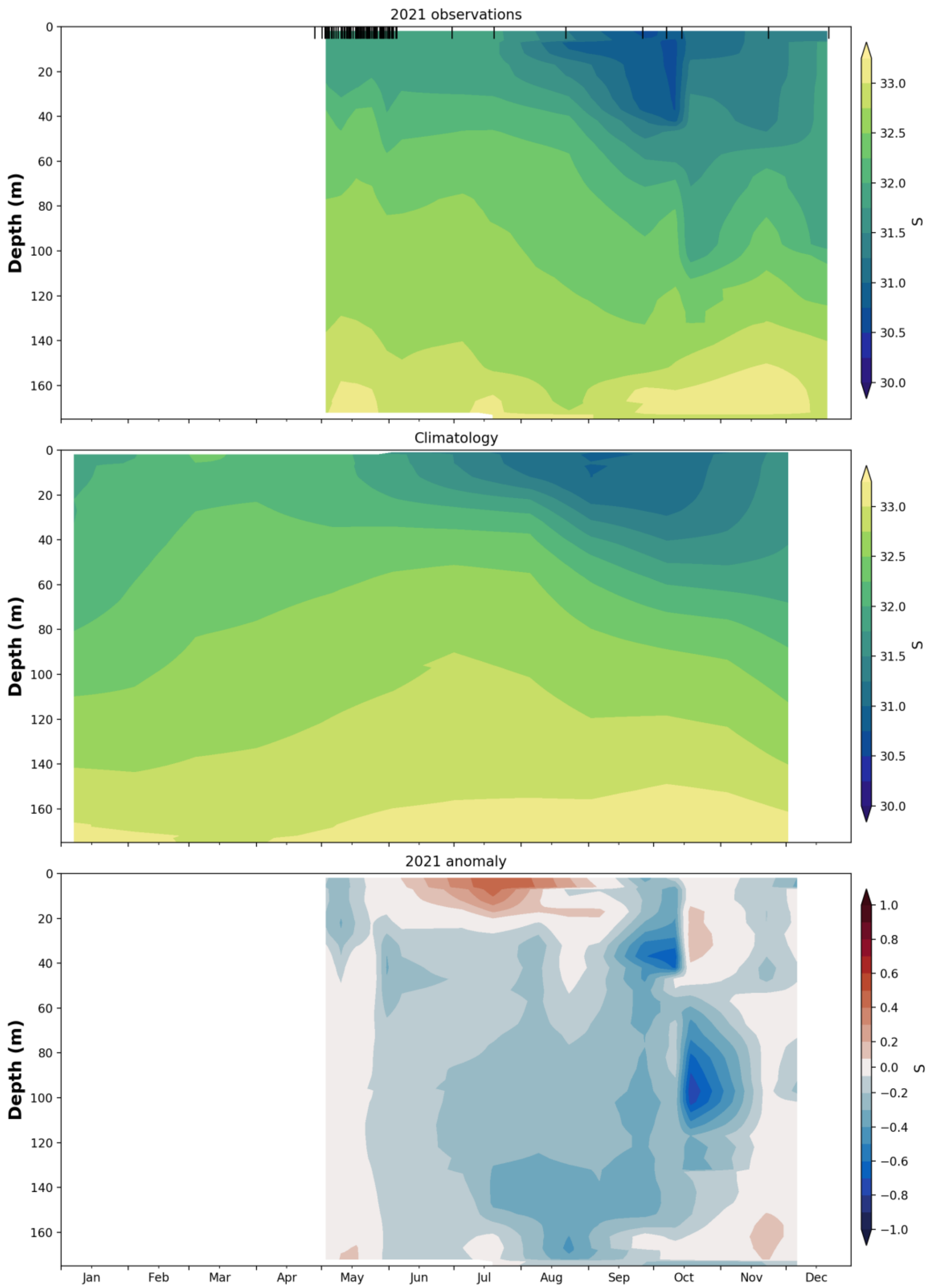

Figure 19. Same as in Figure 18, but for salinity.

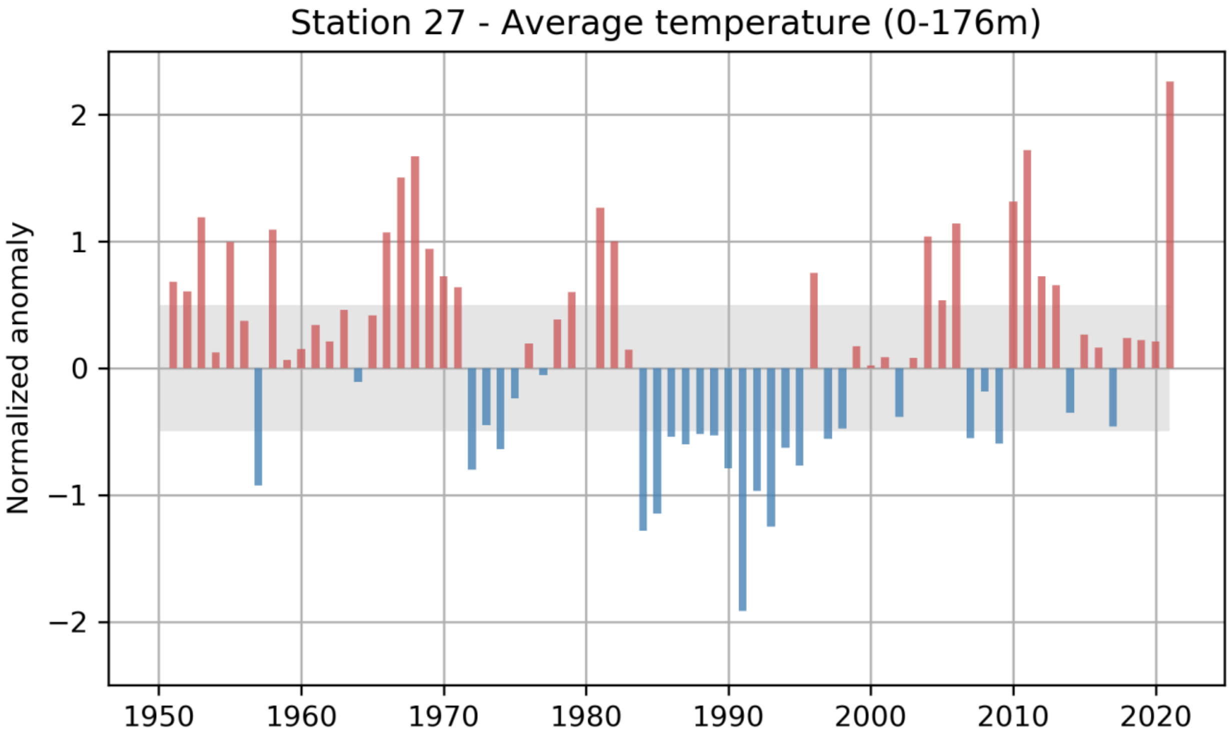

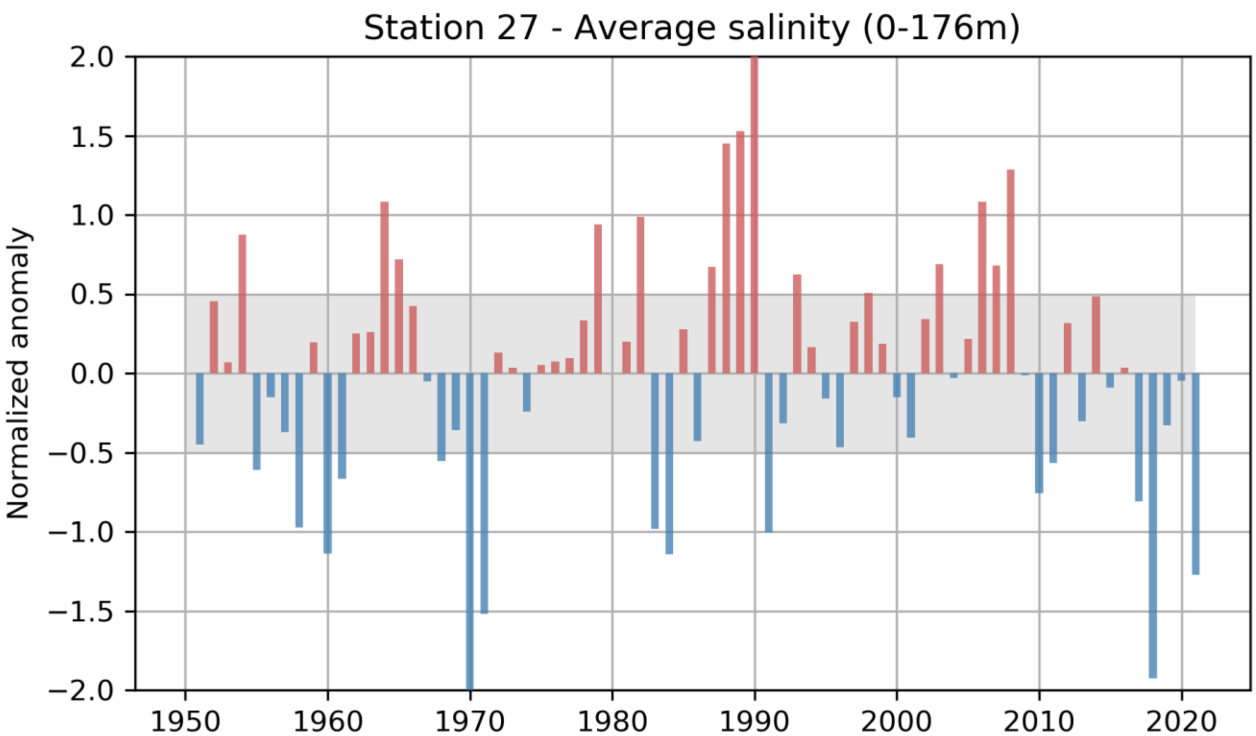

Figure 20. Annual normalized anomaly of vertically averaged (0–176 m) temperature (top) and salinity (bottom) at Station 27 calculated from all occupations since 1951. Only years where at least 8 months of the year are sampled are presented. Shaded gray areas represent the climatological (1991–2020) average ±0.5 SD range considered "normal".

	81	82	83	84	85	86	87	88	89	90	91	92	93	94	95	96	97	98	99	00	01	02	03	04	05	06	07	08	09	10	11	12	13	14	15	16	17	18	19	20	21	x̄	sd
-- Vertically averaged temperature --																																											
Temp 0-176m	1.3	1.0	0.1	-1.3	-1.1	-0.5	-0.6	-0.5	-0.5	-0.8	-1.9	-1.0	-1.2	-0.6	-0.8	0.8	-0.6	-0.5	0.2	0.0	0.1	-0.4	0.1	1.0	0.5	1.1	-0.6	-0.2	-0.6	1.3	1.7	0.7	0.7	-0.4	0.3	0.2	-0.5	0.2	0.2	0.2	2.3	0.6	0.5
Temp 0-50m	0.8	0.0	0.0	-1.3	-1.1	-0.5	-0.6	-0.6	-0.7	-0.7	-1.6	-0.8	-1.0	-0.3	-0.6	0.4	-0.6	-0.1	0.3	0.1	0.2	-0.6	0.1	0.6	0.5	1.2	-0.6	0.5	-0.9	0.9	1.1	0.9	0.7	-0.1	0.1	0.5	-0.4	-0.2	-0.4	0.1	1.7	3.5	0.8
Temp 150-176m	0.0	-0.6	-0.5	-1.0	-1.5	-0.6	-0.6	-0.5	-0.7	-1.1	-1.4	-1.1	-1.4	-1.2	-0.8	0.2	-0.2	0.1	0.3	0.1	0.3	-0.2	-0.3	1.3	0.9	1.0	0.1	-0.2	-0.6	1.1	2.5	0.4	0.6	-0.7	-0.7	-0.6	-0.7	0.5	0.2	1.0	1.9	-0.8	0.4
-- Vertically averaged salinity --																																											
Sal 0-176m	0.2	1.0	-1.0	-1.1	0.3	-0.4	0.7	1.4	1.5	2.4	-1.0	-0.3	0.6	0.2	-0.2	-0.5	0.3	0.5	0.2	-0.2	-0.4	0.3	0.7	0.0	0.2	1.1	0.7	1.3	0.0	-0.8	-0.6	0.3	-0.3	0.5	-0.1	0.0	-0.8	-1.9	-0.3	0.0	-1.3	32.4	0.1
Sal 0-50m	0.4	1.7	-0.9	-1.4	0.6	0.6	1.0	1.3	1.9	1.9	-1.3	-0.2	0.2	0.0	-0.9	-0.1	0.0	-0.1	0.0	-0.5	-0.6	1.0	1.2	0.4	0.4	0.6	0.4	0.7	0.4	-0.9	-0.4	0.3	0.0	0.1	0.0	0.2	-1.0	-0.8	0.7	0.0	-0.5	31.8	0.1
Sal 150-176m	0.5	1.2	0.2	0.5	0.0	-0.6	0.9	2.0	1.0	2.7	-0.6	-0.5	0.8	0.0	0.2	-0.6	0.3	0.7	0.2	0.3	0.0	0.0	-0.5	0.1	0.3	1.3	0.7	0.9	-0.4	0.1	0.0	0.4	-0.6	0.4	-0.3	-0.6	-0.6	-1.7	-1.1	0.5	-1.1	33.0	0.1
-- Cold intermediate layer (CIL) properties --																																											
CIL temp	1.0	0.4	-0.8	-0.8	-1.4	-0.8	-0.5	-0.2	-0.3	0.0	-1.5	-1.1	-1.5	-1.0	-1.0	1.1	-0.6	-0.8	0.2	0.6	0.5	-0.5	-0.3	1.1	0.1	1.1	-0.6	-0.4	-1.1	2.2	2.1	-0.1	1.0	-0.3	-0.5	-0.1	-0.8	1.3	0.9	-0.1	1.5	-1.0	0.2
CIL core T	0.9	0.0	-0.8	-0.8	-1.4	-1.1	-0.8	0.0	-0.3	-0.3	-1.5	-0.8	-1.2	-1.4	-1.1	1.2	-0.4	-0.7	0.0	0.6	0.5	-0.4	-0.4	1.0	-0.1	1.5	-0.5	-0.5	-1.3	2.5	2.0	-0.3	1.3	-0.1	-0.2	-0.3	-0.3	0.7	0.6	-0.2	1.7	-1.4	0.2
CIL core depth	-3.0	-1.4	1.9	-1.1	1.9	-0.7	0.6	0.0	1.2	2.9	-1.4	0.6	0.9	-0.1	-0.1	1.5	-1.4	-0.7	0.9	1.2	-0.7	1.2	-0.1	-0.1	-0.7	-0.7	-1.4	-1.4	0.9	0.6	-1.4	-1.1	-0.7	2.2	0.6	0.9	0.0	0.2	0.9	-0.7	-1.4	123.2	15.4
CIL thickness	-1.1	-4.5	-0.1	0.7	0.6	0.1	-0.4	0.3	-1.2	-0.8	2.0	-0.2	0.0	1.0	0.3	-1.3	0.7	0.9	0.1	-0.1	0.2	0.4	-1.3	0.0	0.8	-0.2	1.1	0.9	0.9	-2.4	-1.7	-1.4	0.1	0.5	-0.1	-0.4	1.0	-1.6	-0.6	0.3	-1.5	124.3	11.3
-- Mixed layer depth (MLD) --																																											
MLD winter	-0.8	-0.3		0.1	-1.1	-0.6	-0.2		-0.4	0.7	1.2		-0.6	0.6	-1.0	0.3	0.0	0.5	-0.3	0.0	-0.8	0.2	-0.3	0.7	0.3	1.1	0.1	-0.6	-1.8	-1.2	0.1	-0.3	1.9	0.3	0.8	-0.4			-1.1			59.5	7.8
MLD spring	0.4	-0.9	-0.8	-1.7	-1.4	-0.7	-1.0	-0.7	-0.8	-0.1	0.1	-0.5	-0.3	0.6	-0.8	-0.4	-0.6	-0.6	-0.9	0.2	0.1	0.1	-0.4	-0.2	-0.4	-0.1	0.4	0.0	-0.4	0.1	-0.4	1.3	0.3	0.5	0.0	-0.5	0.2	0.7	1.8		-0.2	37.1	9.0
MLD summer	0.7	0.4	-0.3	-0.7	0.1	0.1	-0.6	-0.9	-1.3	-0.4	-0.6	1.4	1.2	0.6	0.7	1.0	0.4	-0.4	-0.3	-0.5	0.4	-0.5	-0.2	-0.7	-0.6	0.3	-0.7	-0.7	-0.3	-0.4	1.6	-1.0	-0.1	-0.9	0.5	0.9	-0.5	0.3	-0.5	-0.6	1.3	21.8	6.1
MLD fall			-0.2	-1.2	0.2	0.6	-0.7	-1.0	-0.4	-1.5	-0.2	0.8	-0.7	-0.6	-0.2	-0.7	-0.2	0.3	0.4	0.0	-0.6	0.2	-0.6	0.6	0.5	-0.6	0.3	-0.4	1.0	-0.5	0.5	1.1	-0.5	0.4	0.7	-0.9	-0.7	0.3	0.5	0.0	0.8	57.1	7.3
MLD annual	0.2	-0.4	-0.4	-1.1	-0.6	-0.2	-0.7	-0.8	-0.7	-0.4	-0.1	0.6	-0.1	0.3	-0.2	0.1	-0.1	-0.1	-0.3	-0.1	-0.2	0.0	-0.4	0.1	-0.1	0.1	0.0	-0.4	-0.2	-0.4	0.4	0.3	0.1	0.0	0.5	-0.2	-0.3	0.4	0.4	-0.3	0.6	43.9	17.4
-- Stratification --																																											
strat winter		-0.3		-0.1	0.7	-0.3	-0.6		-0.3	-1.0	-1.2		1.5	-1.4	1.5	-0.2	0.5	-0.8	0.4	0.2	0.2	0.5	0.4	-0.3	-0.5	0.0	-0.5	1.0	0.7	0.2	0.1	-0.8	-1.1	-1.0	0.0	-0.6			-0.1			0.008	0.001
strat spring	0.8	-0.1	2.6	1.6	-0.9	-0.2	2.4	0.5	-0.3	-1.1	0.4	-0.4	0.4	-0.5	2.2	-0.5	0.2	0.9	1.1	-0.1	0.2	-0.8	-0.7	0.1	0.2	0.6	0.1	-0.2	1.1	-0.3	-0.1	0.0	-0.3	-0.8	0.0	-0.4	0.3	-1.1	-1.1		0.8	0.017	0.009
strat summer	1.4	-1.4	-0.1	1.1	-0.1	-0.8	-1.2	0.0	-0.8	-0.4	-0.5	-0.5	-0.7	1.1	0.5	-1.4	-0.1	0.8	1.0	-0.1	0.4	0.1	-0.6	-0.2	0.3	0.0	0.9	0.1	0.3	-0.5	-1.9	0.0	0.9	1.9	-1.2	-0.5	1.5	-1.2	-1.0	0.5	-0.4	0.059	0.01
strat fall			-1.0	0.2	-0.9	-1.3	-0.5	0.3	-0.1	0.3	1.8	-0.5	-0.6	0.0	0.6	-0.1	0.1	0.4	-0.2	0.6	1.1	-0.9	0.3	0.0	-0.5	0.8	-0.2	0.8	-1.1	0.6	-0.8	-0.8	0.0	-0.4	-1.0	1.3	0.3	-0.6	-0.9	0.3	-1.0	0.018	0.011
strat annual	0.9	-0.6	0.3	0.9	-0.2	-0.6	0.2	0.3	-0.3	-0.6	0.5	-0.4	0.2	-0.1	1.1	-0.6	0.1	0.4	0.6	0.2	0.4	-0.4	-0.2	-0.1	-0.1	0.4	0.1	0.4	0.1	0.0	-0.7	-0.4	0.0	0.1	-0.6	0.0	0.7	-1.0	-0.9	0.4	-0.1	0.025	0.022

Figure 21. Annual normalized anomalies of hydrographic parameters for Station 27. The different boxes from top to bottom are: vertically averaged temperature and salinity for different depth ranges, cold intermediate layer (CIL) properties, mixed layer depth (MLD), and stratification for the 4 seasons and annual average. The cells are color-coded according to Figure 2. Gray cells indicate absence of data.

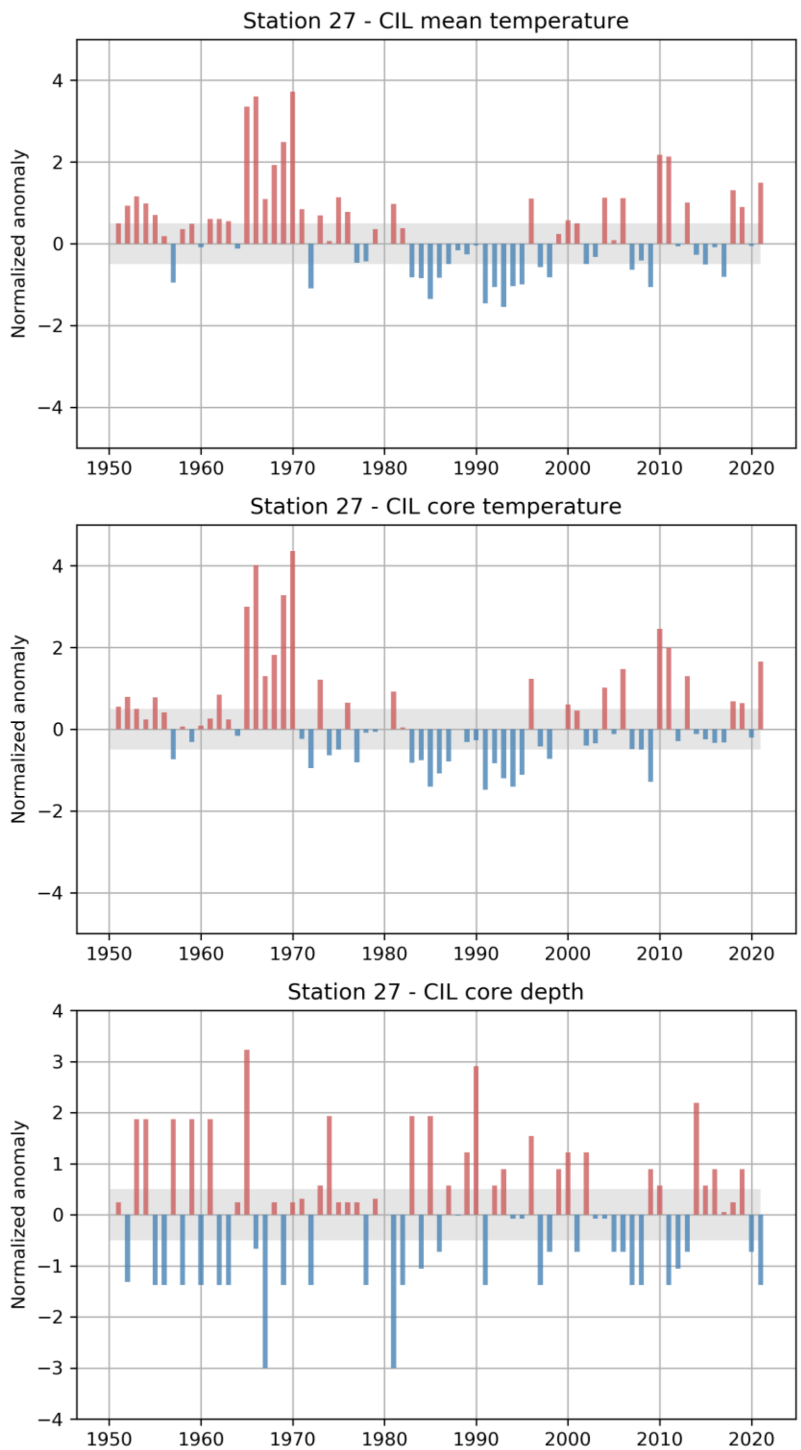

Figure 22. Normalized anomalies of summer (May-July) cold intermediate layer (CIL) statistics at Station 27 since 1951. Only years where at least 8 months of the years are sampled are presented. The top panel shows the CIL mean temperature, the middle the CIL core temperature (minimum temperature of the CIL) and the bottom panel the depth of the CIL core. Shaded gray areas represent the climatological (1991–2020) average ±0.5 SD range considered "normal".

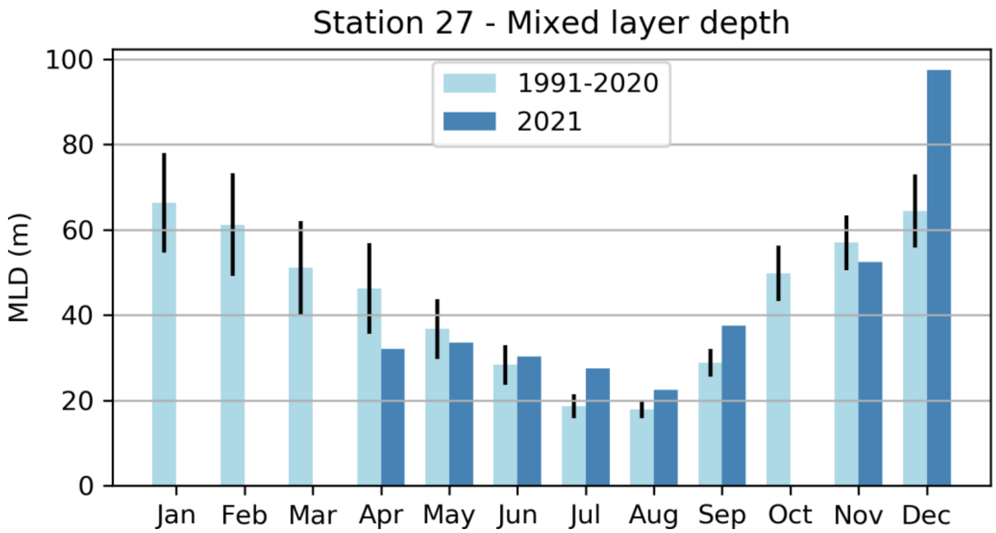

Figure 23. Bar plot of the monthly averaged mixed layer depth (MLD) at Station 27. The 1991–2020 climatology is shown in light blue while the update for 2021 is shown in dark blue. The black lines represent 0.5 SD above and below the climatology. No observations were made between January and March.

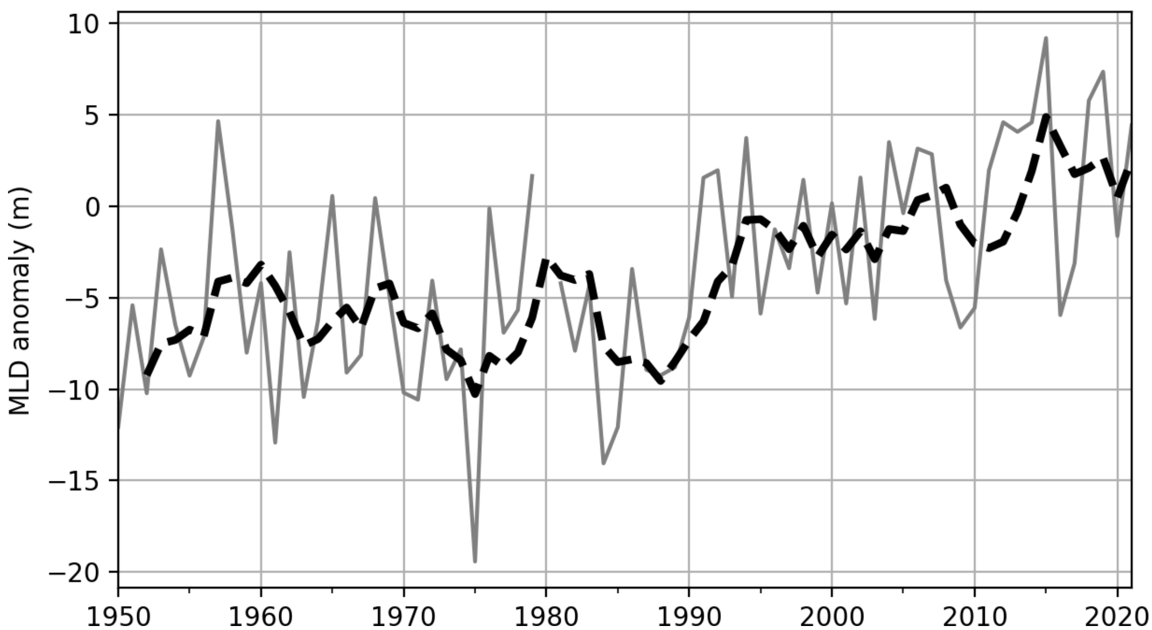

Figure 24. Time series of the annual mixed layer depth (MLD) average at Station 27 since 1950 (gray solid line) and its 5-year running mean (dashed-black line).

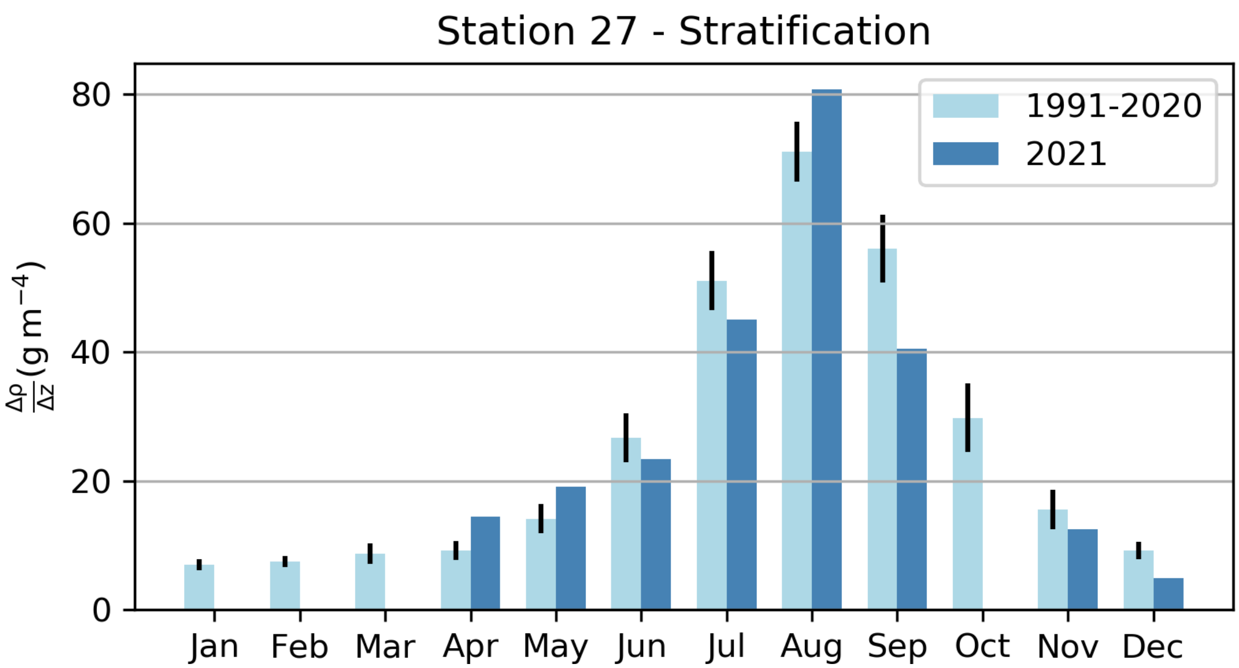

Figure 25. Bar plot of the monthly average stratification (defined as the density difference between 0 and 50 m) at Station 27. The 1991–2020 climatology is shown in light blue while the update for 2021 is shown in dark blue. The black lines represent 0.5 SD above and below the climatology. No observations were made between January and March.

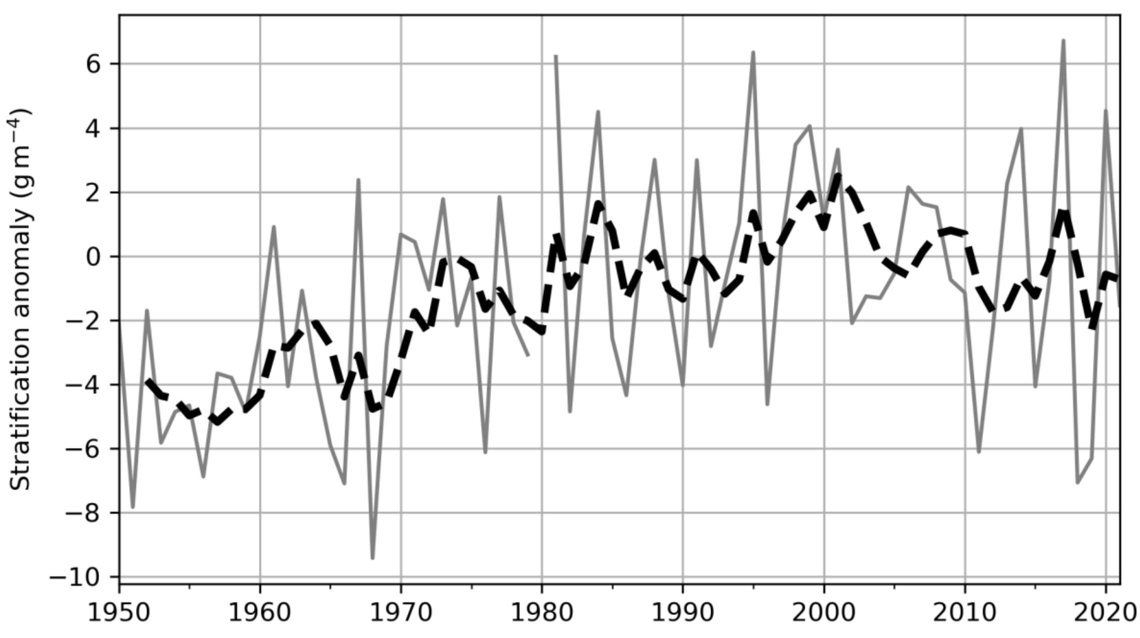

Figure 26. Time series of the annual average stratification at Station 27 since 1950 (gray solid line) and its 5-year running mean (dashed-black line).

Standard Hydrographic Sections

In the early 1950s, several countries under the auspices of the International Commission for the Northwest Atlantic Fisheries (ICNAF) carried out systematic monitoring along hydrographic sections in Newfoundland and Labrador waters. In 1976, ICNAF normalized a suite of oceanographic monitoring stations along sections in the Northwest Atlantic Ocean from Cape Cod (USA) to Egedesminde (West Greenland) (ICNAF 1978). In 1998 under the Atlantic Zone Monitoring Program (AZMP) of Fisheries and Oceans Canada, the Seal Island (SI), Bonavista Bay (BB), Flemish Cap (47°N) (FC) and Southeast Grand Bank (SEGB) historical stations were selected as core monitoring sections. The White Bay section (WB) continued to be sampled during the summer as a long time series ICNAF/NAFO section (see Figure 1).

Two ICNAF sections on the mid-Labrador Shelf, the Beachy Island (BI) and the Makkovik Bank (MB) sections, were selected to be sampled during the summer if survey time permitted. Starting in the spring of 2009, a section crossing south-west over St. Pierre Bank (SWSPB) and one crossing south-east over St. Pierre Bank (SESPB) were added to the AZMP surveys.

In 2021, both the spring and fall survey were canceled. In 2020, the spring survey was also canceled due to the COVID-19 pandemic. During the summer 2021 survey (June 29-July 19), section FC, BB, WB, SI and MB were sampled. In this manuscript we present the summer cross sections of temperature and salinity and their anomalies along the SI, BB and FC sections to represent the vertical temperature and salinity structure across the NL Shelf during 2021.

Temperature and Salinity Variability

The water mass characteristics observed along the standard sections crossing the NL Shelf are typical of subpolar waters with a subsurface temperature range of -1.5°C to 2°C and salinities from 31.5 to 33.5. Labrador Slope water flows southward along the shelf edge and into the Flemish Pass and Flemish Cap regions. This water mass is generally warmer and saltier than the subpolar shelf waters with a temperature range of 3° to 4°C and salinities in the range of 34 to 34.75. Surface temperatures normally warm to between 10° and 12°C during late summer while bottom temperatures remain < 0°C over much of the Grand Banks but increase to between 1° and 3.5°C near the shelf edge below 200 m and in the deep troughs between the banks. In the deeper (> 1000 m) waters of the Flemish Pass and across the Flemish Cap, bottom temperatures generally range from 3° to 4°C. In general, the near-surface water mass characteristics along the standard sections undergo seasonal modification from annual cycles of air-sea heat flux, wind forced mixing, and the formation and melting of sea ice. These mechanisms cause intense vertical and horizontal temperature and salinity gradients, particularly along the frontal boundaries separating the shelf and slope water masses. The seasonal changes in the temperature and salinity fields along the Bonavista section are presented in Colbourne et al. (2015).

The 2021 summer temperature and salinity structures along the SI, BB and FC; (along 47°N) hydrographic sections are presented in Figure 27 to Figure 29. The dominant thermal feature along these sections is associated with the cold and relatively fresh CIL overlying the shelf. This water mass is separated from the warmer and denser water of the continental slope region by strong temperature and salinity fronts. The cross sectional area (or volume) of the CIL is bounded by the 0°C isotherm and highlighted as a thick black contour in the temperature panels. The CIL parameters are generally regarded as robust indicators of ocean climate conditions on the eastern Canadian Continental Shelf. While the CIL area undergoes significant seasonal variability, the changes are highly coherent from the Labrador Shelf to the Grand Banks. The CIL remains present throughout most of the summer until it gradually decays during the fall as increasing winds and storm episodes deepen the surface mixed layer.

During 2021, temperatures were above normal for all sections and most depth ranges (Figure 27 to Figure 29, bottom left). The conditions were also getting warmer from north to south, reaching more than 3.5°C above normal in most of the FC section. Warmer than normal temperatures were also found near the bottom at all sections. The latter information is important to note because, as presented in the next section, the reduced coverage of the multi-species survey in 2021 prevented the calculation of spring and fall bottom temperatures in large areas of the NL shelf, including on the Grand Banks of Newfoundland, an area crossed by section FC. The observations made during AZMP missions show widespread warmer than normal temperatures. This is important and will be discussed further.

The corresponding salinity cross sections show a relatively fresh (<33) upper water layer over the shelf with sources from Arctic outflow on the Labrador Shelf, in contrast to the saltier Labrador Slope water further offshore with values >34 (Figure 27 to Figure 29, right panels). In 2021, salinities corresponding to the CIL were slightly lower than normal for all sections, while the slope waters were above normal. The latter is likely due to an unusual extension of the saltier Labrador Current onto the slope in 2021 compared to the climatology. This is especially evident for sections SI and FC (see the difference in the salinity field between the top two right panels of all three figures). The fresher waters on the shelf (see also the large fresh anomaly at Station 27; Figure 20, bottom), may be related to the warm air temperature anomalies observed in Labrador and the Arctic in 2021.

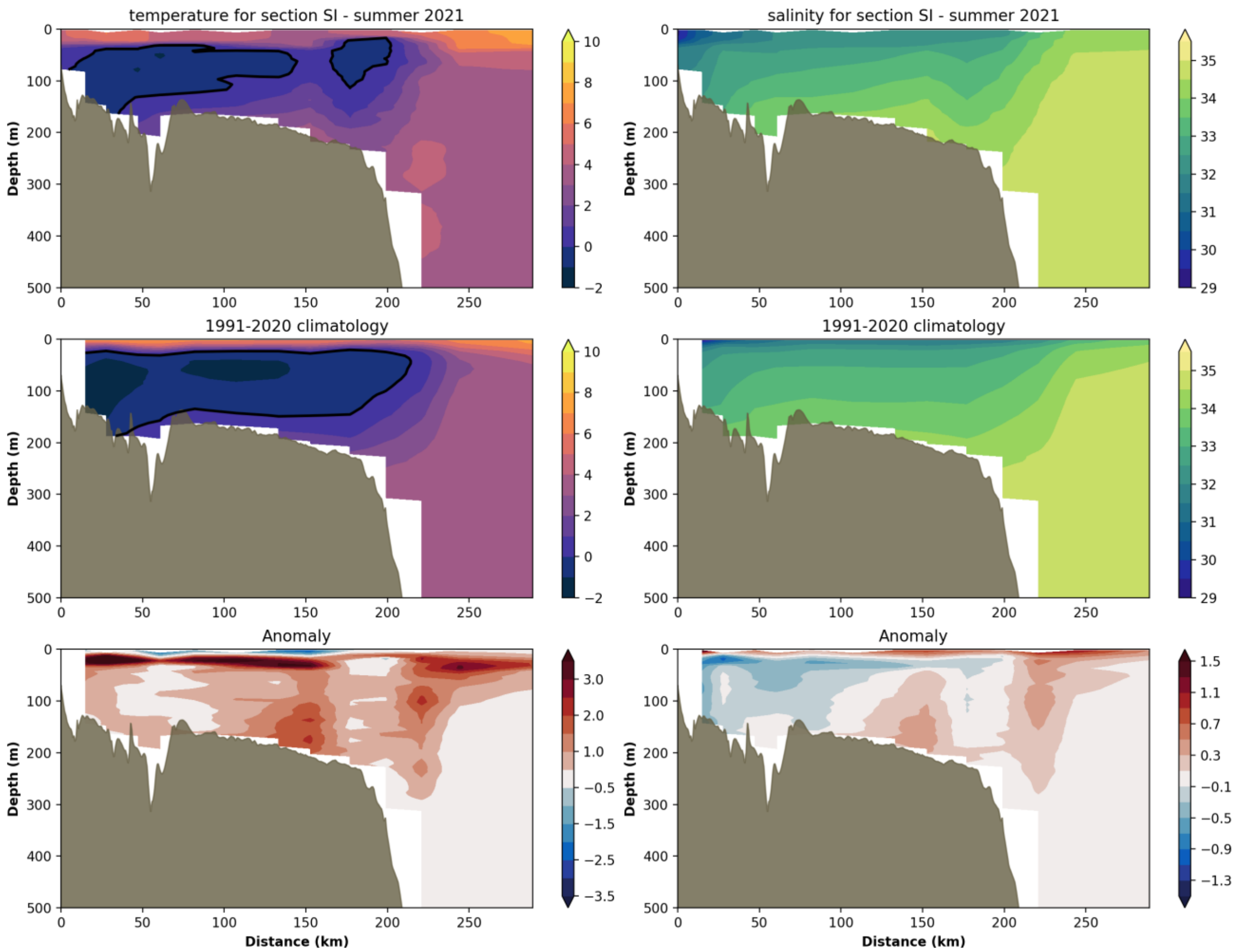

Figure 27. Contours of temperature (°C) and salinity during summer 2020 (top row) and climatological average (middle row) for Seal Island (SI) hydrographic section (see map Figure 1 for location). Their respective anomalies for 2021 are plotted in the bottom panels.

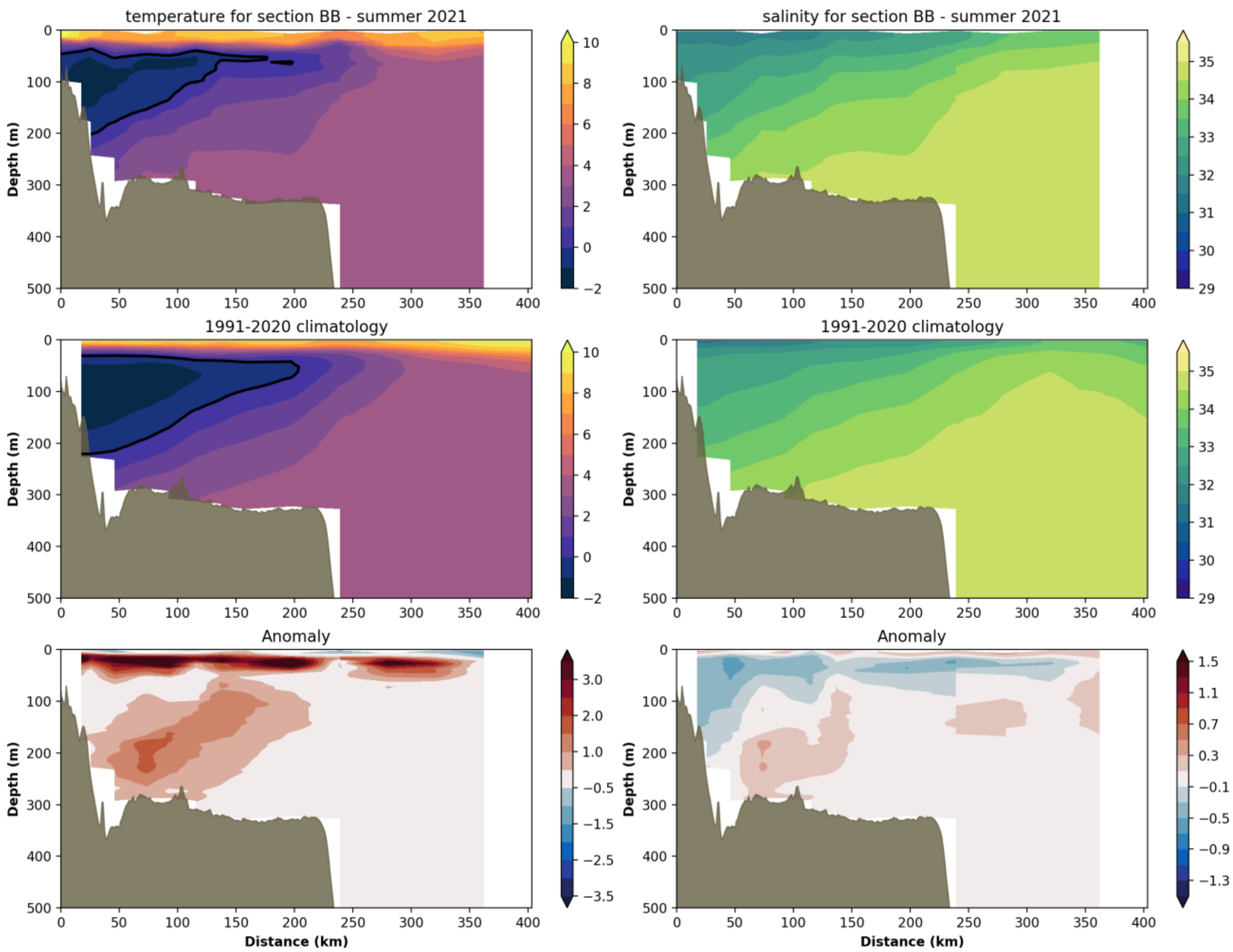

Figure 28. Same as in Figure 27, but for Bonavista (BB) hydrographic section (see map Figure 1 for location).

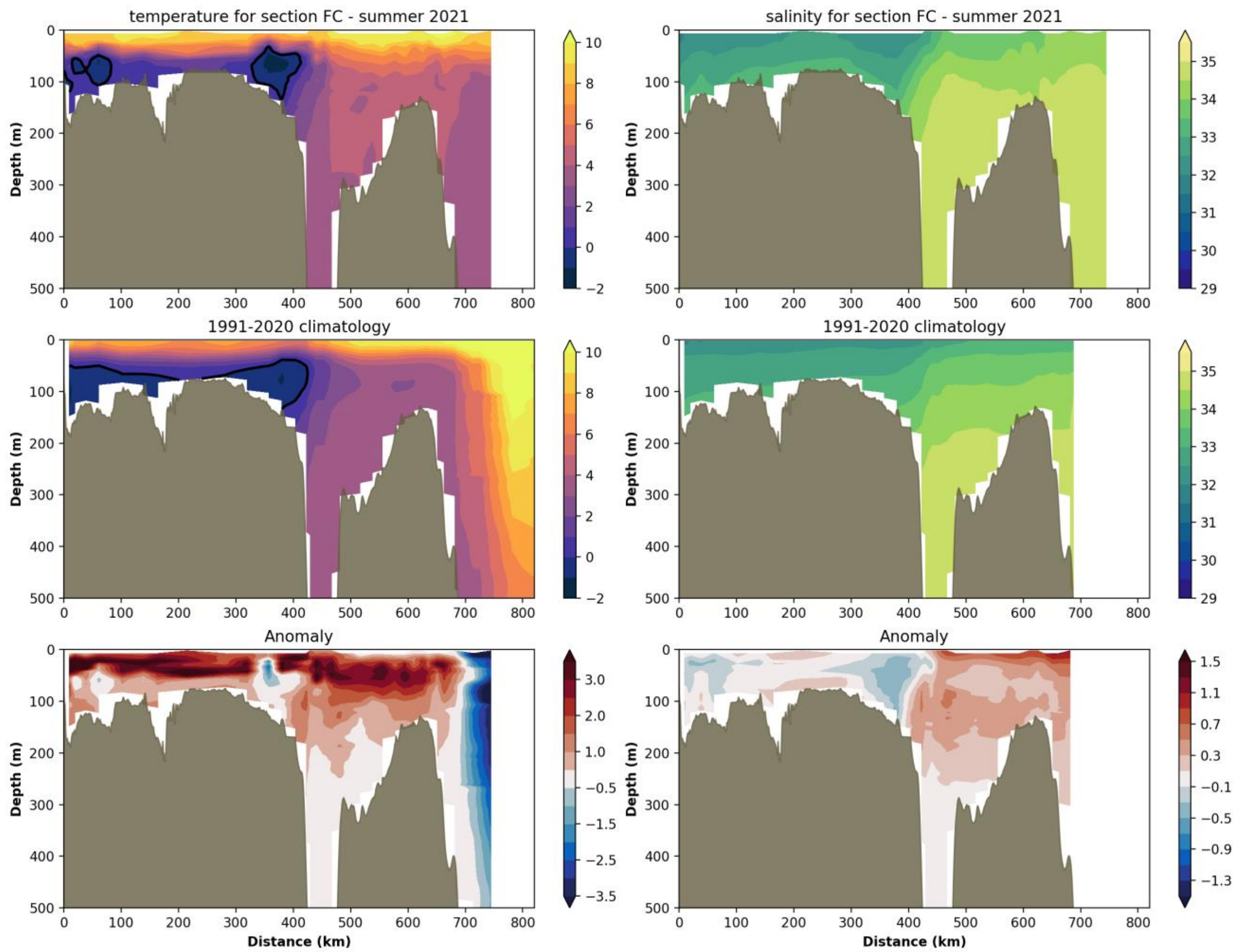

Figure 29. Same as in Figure 27, but for Flemish Cap (FC) hydrographic section (see map Figure 1 for location).

Cold Intermediate Layer Variability

Statistics of summer CIL anomalies (CIL area, CIL core temperature and CIL core depth) for the three sections discussed above (SI, BB and FC) are presented in a scorecard in Figure 30. The climatological average cross sectional area of the summer CIL along these sections are 19.9 ± 4.1 km^2, 22.9 ± 7.6 km^2 and 16.5 ± 6.4 km^2, respectively. The averaged anomalies of the CIL core temperature (minimum temperature of this layer) and volume (defined as the cross sectional area) for these three sections are summarized in Figure 31 as a time series going back to 1950. In general, the summer CIL has been predominantly warmer/smaller than average since the mid 1990's, with a cooling trend emerging since about 2012 or 2014 to 2017. However, the most striking aspect of this long time series is the warm conditions that prevailed in the 1960's (that stands as a unique feature for this nearly 70-year time series, although measurements during this period were largely made from reversing thermometers that might have missed the CIL core), followed by a cold period that lasted from the mid-1980's to the mid-1990's. In 2021, the CIL conditions were much warmer than normal, including and north-south anomaly gradient, with warmest CIL condition on the northernmost section SI. On average over these three sections, 2021 is the year with the smallest CIL area since 1966 at -1.7 SD (Figure 31).

	80	81	82	83	84	85	86	87	88	89	90	91	92	93	94	95	96	97	98	99	00
-- Seal Island section --																					
CIL area (km²)	0.0		0.2	-0.3	2.0	0.7	-0.4	-0.1	-0.7		1.2	1.4	-0.1	1.7	0.0	-0.3	0.2	-0.7	0.5	-1.6	-0.1
CIL core (°C)	0.9		1.2	-0.4	-0.8	-0.1	2.2	1.7	1.3		-0.5	-0.5	0.0	-0.6	-0.5	-0.5	0.7	-0.5	-0.5	-0.5	-0.5
core depth (m)	1.1		1.3	0.0	1.3	-1.4	1.1	1.3	-0.3		0.4	0.4	0.0	-1.2	0.4	0.4	-1.8	0.4	0.4	0.4	0.4
-- Bonavista section --																					
CIL area (km²)	-0.4	-0.2	1.5	1.7	3.2	2.0	-0.4	-0.7	0.9	0.7	1.8	2.4	1.2	1.4	1.0	-0.2	0.2	-0.4	0.3	-0.4	0.7
CIL core (°C)	1.2	0.6	-0.3	-1.7	-1.2	-1.0	0.3	-0.7	0.5	-1.0	-0.9	-1.3	-1.1	-1.1	-1.2	-0.6	0.8	-0.6	-0.6	0.0	-0.2
core depth (m)	0.5	-0.8	0.4	1.4	-1.5	-1.3	-0.1	1.4	-0.1	0.2	1.9	-1.3	0.4	1.1	0.4	-0.1	-0.3	-0.5	-1.3	0.7	0.9
-- Flemish Cap section --																					
CIL area (km²)	-1.6	-0.3	-1.5	2.0	2.3	0.8	0.2	-1.2	-0.8	1.0	0.8	2.0	-0.5	1.7	0.0	-0.5	0.0	0.4	0.8	0.5	-1.1
CIL core (°C)	0.0	1.1	-0.3	-0.9	-0.9	-0.9	-0.7	-0.9	0.4	-1.2	-0.5	-1.1	-0.8	-1.1	-0.6	-1.4	1.2	0.1	-0.5	0.4	0.2
core depth (m)	1.4	2.9	1.4	-0.4	-1.0	0.1	0.6	0.9	3.0	-0.2	0.3	-1.0	-1.7	-0.4	0.6	1.4	-1.0	-1.0	0.3	1.1	-0.2

	01	02	03	04	05	06	07	08	09	10	11	12	13	14	15	16	17	18	19	20	21	$\bar{x}$	sd
-- Seal Island section --																							
CIL area (km²)	0.5	0.0	0.9	-0.9	0.0	-0.5	0.1	0.2	0.6	-0.6	-1.2	0.6	-0.5	0.4	2.0	-0.1	1.9	-2.1	-0.4	-1.9	-2.1	19.9	4.1
CIL core (°C)	2.6	-0.5	1.8	-0.5	-0.5	-0.5	-0.5	-0.5	-0.5	2.6	-0.5	-0.5	2.6	-0.1	-0.5	-0.5	-0.5	-0.5	0.5	-0.5	3.7	-1.7	0.1
core depth (m)	-2.3	0.4	0.6	0.4	0.4	1.3	0.4	0.4	0.4	-2.7	0.4	1.1	-0.7	-1.2	1.1	0.4	0.4	0.4	-1.6	0.4	-1.6	87.4	22.5
-- Bonavista section --																							
CIL area (km²)	-0.4	-0.4	0.1	-1.4	-0.8	-1.2	-0.3	-0.9	0.5	-0.3	-2.1	-0.2	-0.6	1.8	1.0	0.8	0.5	-0.4	-0.9	-1.2	-1.4	22.9	7.6
CIL core (°C)	0.5	-0.1	-0.3	1.8	0.9	2.0	0.0	-0.3	-0.7	0.8	2.5	-0.8	0.4	-0.9	-1.0	-0.6	-0.8	0.8	0.4	1.2	1.5	-1.6	0.1
core depth (m)	-1.3	1.1	0.2	-0.5	-1.7	0.7	0.7	-0.1	-1.7	-1.7	0.2	1.1	-0.8	0.7	2.1	0.4	-0.5	-0.3	1.4	-0.1	-0.1	92.7	20.8
-- Flemish Cap section --																							
CIL area (km²)	-0.6	0.2	-0.5	-0.4	0.2	-1.5	-0.1	-1.1	0.4	-1.9	-0.9	0.8	-0.7	-0.2	-0.2	2.6	-0.9	0.1	1.3	0.2	-1.5	16.5	6.4
CIL core (°C)	1.4	-0.8	-0.2	0.7	0.3	0.6	-0.4	-0.2	-0.9	2.4	1.9	-1.0	2.3	-0.8	-1.0	-0.2	0.2	-0.4	0.3	-0.7	-0.2	-1.5	0.2
core depth (m)	1.1	-0.4	0.9	0.6	-0.4	0.6	-0.2	-1.0	2.2	-1.0	-0.7	-0.2	1.1	-1.0	0.9	0.3	-1.7	1.6	-0.4	-0.4	-0.7	75.0	19.3

Figure 30. Scorecards of the cold intermediate layer (CIL) summer statistics along Seal Island, Bonavista and Flemish Cap hydrographic sections. The CIL area is defined as all water below 0°C (see black contours in Figure 27 to Figure 29), and the CIL core temperature and depth are the minimum temperature of the CIL and the depth at which it is encountered respectively. Color codes for the area and depth have been reversed (positive is blue and negative is red) because they represent cold conditions. Grayed cells indicate absence of data.

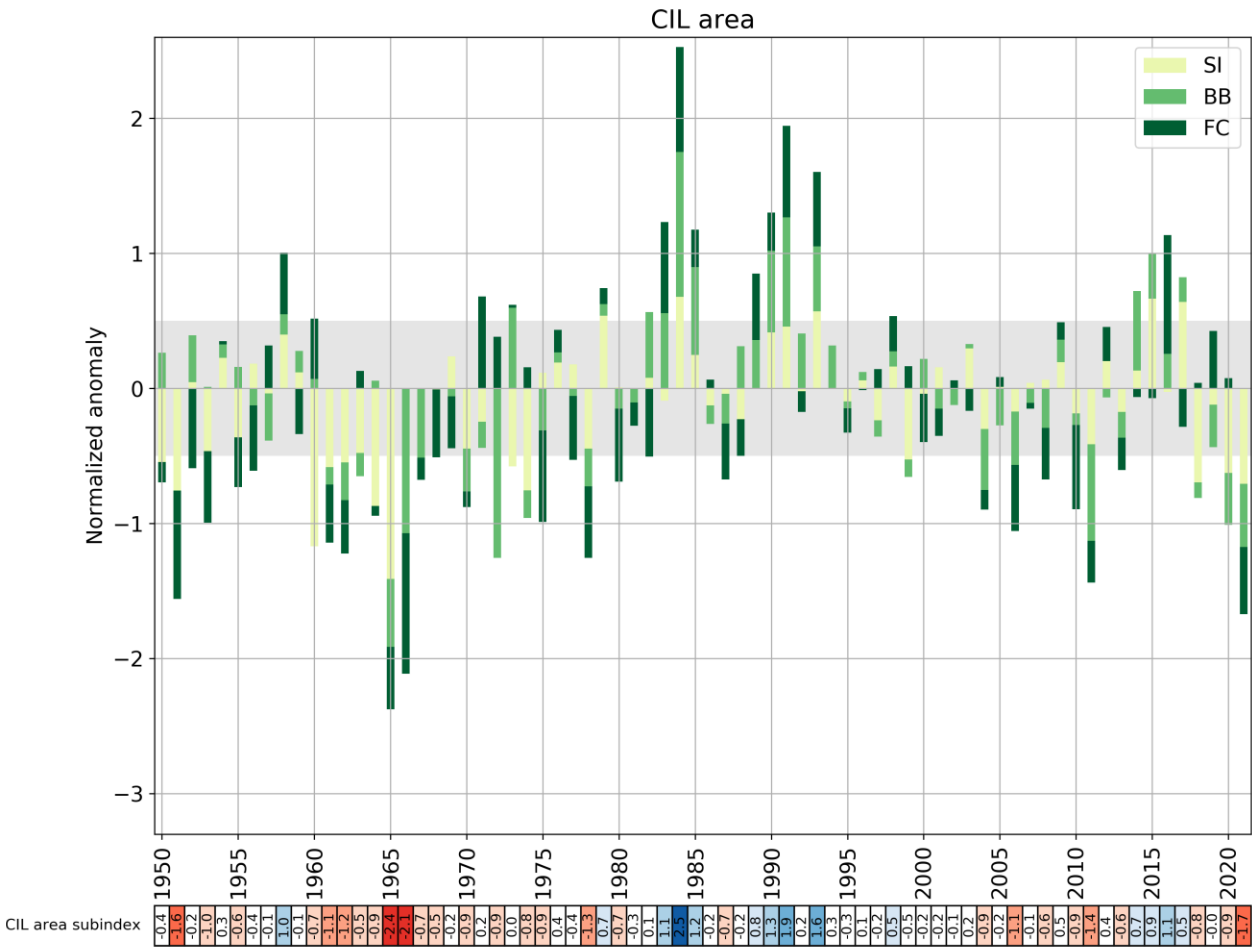

Figure 31. Normalized anomalies of the mean CIL area for hydrographic sections Seal Island (SI), Bonavista Bay (BB) and Flemish Cap (FC). This time series corresponds to the average of the three sections, in which the contribution of each section is represented (values for each separate section since 1980 can be found in Figure 30). The shaded area corresponds to the 1991–2020 average ±0.5 SD, a range considered "normal". The numerical values of this time series are reported in a color-coded scorecard at the bottom of the figure. Here negative anomalies (generally corresponding to warmer conditions) are colored red and positive anomalies blue.

Bottom Observations in NAFO sub-areas

Canada has been conducting stratified random bottom trawl surveys in NAFO Sub-areas 2 and 3 on the NL Shelf since 1971. Areas within each division, with a selected depth range, were divided into strata, and the number of fishing stations in an individual stratum was based on an area-weighted proportional allocation (Doubleday, 1981). Temperature profiles (and salinity profiles since 1990) are available for most fishing sets in each stratum. These surveys provide large spatial-scale oceanographic data sets for the Newfoundland and Labrador Shelf. NAFO Subdivision 3Ps on the Newfoundland south coast and Divisions 3LNO on the Grand Banks are surveyed in the spring, and Divisions 2HJ off Labrador in the north, 3KL off eastern Newfoundland, and 3NO on the southern Grand Bank are surveyed in the fall. The hydrographic data collected on these surveys are routinely used to assess the spatial and temporal variability in the thermal habitat of several fish and invertebrate species. A number of products based on the data are used to characterize the oceanographic bottom habitat. Among these are contour maps of the bottom temperatures and their anomalies, the area of the bottom covered by water in various temperature ranges, etc. In addition, species-specific *thermal habitats* indices are often used in marine resource assessments for snow crab and northern shrimp.

The current method to derive the bottom temperature was introduced by Cyr et al. (2019). First, all available annual profiles of temperature and salinity (from AZMP hydrographic campaigns, multi-species resources assessments, surveys from other DFO regions, international oceanographic campaigns, Argo program, etc.) are vertically averaged in 5 m bins and vertically interpolated to fill missing bins. Then, for each season (April-June for spring and September-December for fall), all data are averaged on a regular 0.1° x 0.1° (latitudinal x longitudinal) grid to obtain one seasonal profile per grid cell. Since this grid has missing data in many cells, each depth level is horizontally linearly interpolated. For each grid point, the bottom observation is considered as the data at the closest depth to the GEBCO_2014 Grid bathymetry (version 20141103), to a maximum 50 m difference. Lastly, bottom observations deeper than 1000 m are clipped. This method is applied for all years between 1980 and 2021 from which the 1991-2020 climatology is derived. Anomalies for 2021 are calculated as the difference between annual observations and the climatology.

Spring Conditions

Maps of spring climatological temperature and salinity, together with 2021 observations and anomalies for NAFO divisions 3LNOPs, are presented in Figure 32 and Figure 33, respectively (with the center panel for station occupation coverage). Due to the COVID-19 pandemic, the area was not surveyed during the spring of 2020, while in 2021 only the division 3Ps was properly sampled. Temperatures were generally above 0°C over the shallower St. Pierre Bank (eastern 3Ps) and above 6°C in the deep Laurentian Channel, leading to widespread warm anomalies over this division, especially in the shallower part where temperatures 1.5 to 2.5°C above the climatological mean (Figure 32, right panel).

Spring bottom salinities in 3LNO generally range from 32 to 33 over the central Grand Bank, and from 33 to 35 closer to the shelf edge (Figure 33, left panel). In 3Ps, salinities were between 32 and 33 over shallower areas and above 34.5 in the Laurentian Channel. In 2021, salinity conditions were close to normal in 3Ps (Figure 33, right panel).

Climate indices based on normalized spring bottom temperature anomalies (mean temperature and temperature in areas shallower than 200 m), as well as the area of the sea floor covered by water above 2°C and below 0°C between 1980 and 2021 are shown in a color-coded scorecard in Figure 34. Overall, the colors visually highlight two contrasting periods of this time series: the cold period of the late 1980s / early 1990s (mostly blue cells) and the warm period of the early 2010s (mostly red cells). This warm period lasted between

2010 and 2013 (2011 being the warmest at 2.1 SD above normal in 3LNO) before returning towards to normal values. Between 2015 and 2017 the bottom area that was covered by <0°C water was normal at -0.2 to 0.4 SD.

Division 3Ps bottom temperatures exhibit some similarities to those from 3LNO, with two periods of warm years, 1999–2000 and 2005–06, separated by a colder period (2003 is the coldest year on record since 1991 at -2.1 SD). With the exception of 2014 and 2017 (normal), all years between 2010 and 2021 were warmer than normal. As mentioned above, very little information is available for 2020 and 2021. In 3Ps, the only division with available data, 2021 was the warmest year on record since 1980 at +2.0 SD. 2021 was also the year with the smallest area of the seafloor covered by water <0°C at -1.5 SD (tied with 2011).

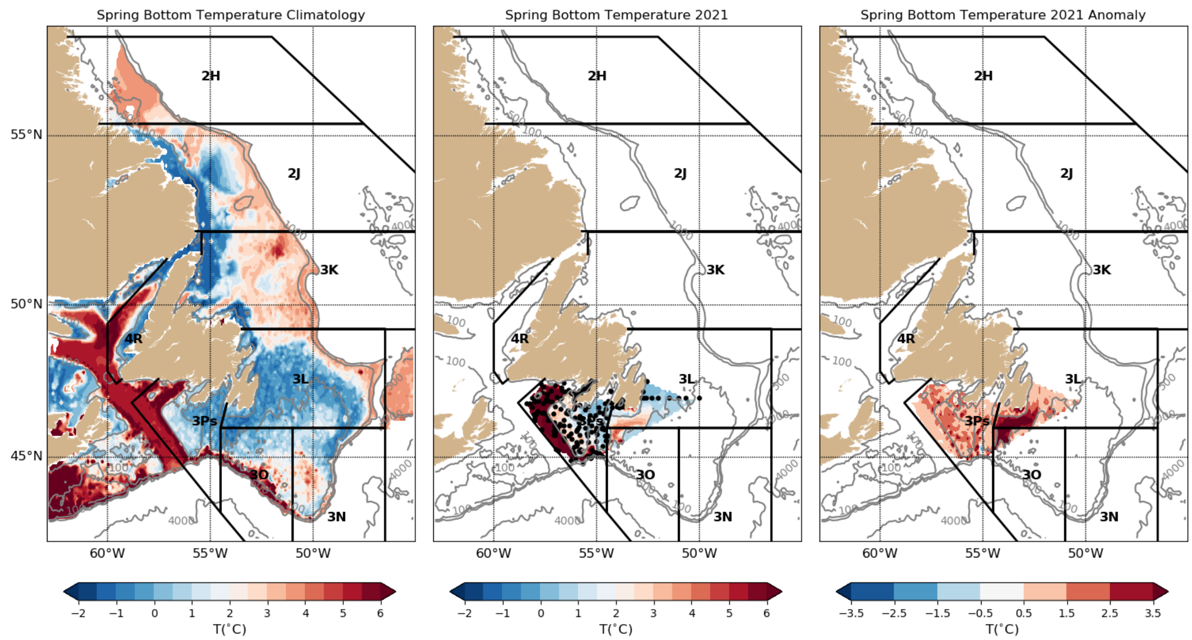

Figure 32. Maps of the mean 1991-2020 spring bottom temperature (left), and spring 2021 bottom temperature (center) and anomalies (right) for NAFO Divisions 3LNOPs only. The location of observations used to derive the temperature field is shown as black dots in the center panel.

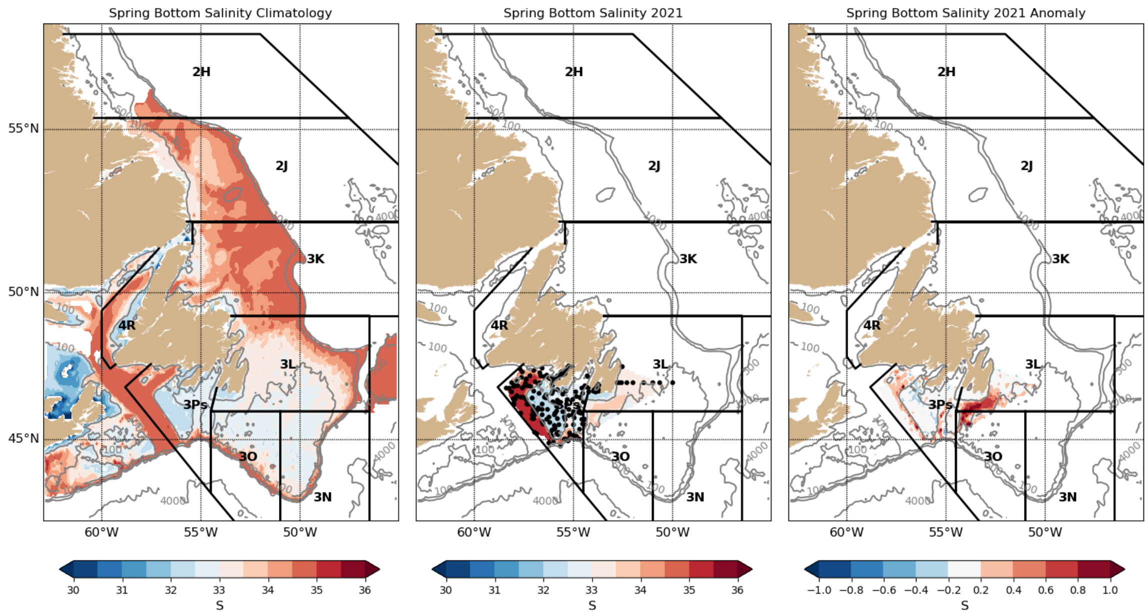

Figure 33. Maps of the mean 1991-2020 spring bottom salinity (left), and spring 2021 bottom salinity (center) and anomalies (right) for NAFO Divisions 2J3KLNO only. The location of observations used to derive the salinity field is shown as black dots in the center panel.

	80	81	82	83	84	85	86	87	88	89	90	91	92	93	94	95	96	97	98	99	00
-- NAFO division 3LNO --																					
T_{bot}	-0.1	1.4	-0.8	0.4	-0.9	-1.5	-1.3	-0.5	0.0	-1.4	-2.1	-2.1	-1.7	-1.3	-1.6	-0.8	-0.1	-0.9	0.6	1.2	0.6
$T_{bot<200m}$	-0.3	1.6	-0.6	0.7	-0.9	-1.5	-1.3	-0.4	0.0	-1.2	-2.0	-2.0	-1.7	-1.2	-1.6	-0.9	0.0	-1.0	0.6	1.4	0.7
$Area_{>2^\circ C}$	-0.2	1.3	-1.5	0.6	-0.7	-1.6	-1.2	-0.4	0.0	-1.4	-2.1	-1.8	-1.8	-1.1	-1.4	-0.4	-0.1	-0.8	0.4	1.2	0.4
$Area_{<0^\circ C}$	-0.3	-1.1	0.2	0.3	1.0	1.4	1.2	0.9	0.5	1.1	1.6	1.9	1.4	1.4	1.3	0.8	0.0	0.9	-0.6	-1.1	-0.1
-- NAFO division 3Ps --																					
T_{bot}			-0.5	0.1	0.2									-1.3	-1.3	-0.8	-0.2	-1.2	-0.2	0.8	1.1
$T_{bot<200m}$			0.2	0.5	0.9									-1.8	-1.5	-0.9	-0.1	-1.3	0.1	1.1	1.3
$Area_{>2^\circ C}$			0.6	1.5	-1.0									-0.2	-0.5	0.5	-0.4	-0.7	0.6	2.4	2.0
$Area_{<0^\circ C}$			-0.2	-0.4	-0.7									1.7	1.3	1.2	-0.3	1.5	0.1	-0.5	-0.9

	01	02	03	04	05	06	07	08	09	10	11	12	13	14	15	16	17	18	19	20	21	$\bar{x}$	sd
-- NAFO division 3LNO --																							
T_{bot}	0.0	-0.2	-1.1	1.3	0.6	0.5	0.2	0.1	0.2	0.9	2.1	1.4	1.1	-0.5	-0.1	-0.6	-0.1	0.2	0.2			1.1	0.5
$T_{bot<200m}$	0.0	-0.2	-1.3	1.3	0.5	0.4	0.1	0.0	0.2	0.8	2.1	1.4	1.1	-0.6	-0.1	-0.3	-0.2	0.2	0.3			0.7	0.6
$Area_{>2^\circ C}$	-0.6	-0.3	-1.0	1.8	0.6	0.3	0.3	0.5	0.7	0.4	2.4	1.5	0.4	-0.4	0.3	-1.0	0.0	-0.3	-0.1			69.3	20.8
$Area_{<0^\circ C}$	0.0	0.2	1.0	-1.7	-0.7	-1.4	0.2	0.2	0.5	-1.6	-1.9	-0.8	-1.0	0.8	0.4	0.3	0.2	-0.2	-0.2			90.0	43.6
-- NAFO division 3Ps --																							
T_{bot}	-1.3	-0.5	-2.1	-0.4	0.6		-1.4	-0.3	0.2	0.5	1.4	1.2	0.7	0.3	0.5	1.6	0.3	1.1	0.7		2.0	2.4	0.5
$T_{bot<200m}$	-1.0	-0.6	-2.0	0.0	1.0		-0.9	0.2	0.5	0.4	1.5	0.9	0.8	0.2	0.4	1.2	-0.4	0.9	0.0		1.8	0.9	0.6
$Area_{>2^\circ C}$	-1.5	-0.7	-1.6	-1.0	0.1		-1.1	0.1	-0.1	0.1	1.8	0.2	0.5	-0.5	-0.2	-0.1	-0.3	1.4	-0.6		1.9	26.5	3.0
$Area_{<0^\circ C}$	0.8	0.4	2.2	-0.8	-1.2		0.7	0.2	-0.1	-0.7	-1.5	-1.2	-1.2	-0.2	-0.6	-0.9	0.4	-0.8	0.4		-1.5	14.2	9.8

Figure 34. Scorecards of normalized spring bottom temperature anomalies for 3LNO and 3Ps.

Fall Conditions

Maps of fall climatological temperature and salinity, together with 2021 observations and anomalies for NAFO Divisions 2HJ3KLNO, are presented in Figure 35 and Figure 36, respectively (see center panel for station occupation coverage). Similar to the spring, Divisions 3LNO (Grand Banks) were not sampled due to ship availability problems. For the divisions where the data are available, a widespread warm anomaly was observed (Figure 35, left panel).

Bottom salinities in divisions 2HJ and 3K generally display an inshore-offshore gradient between <33 close to the coast and 34 to 35 at the shelf edge (Figure 36, left panel). The Grand Banks bottom salinities range from <33 to 35, with the lowest values on the southeast shoal. In 2021 the bottom salinities were slightly above normal in most of 2HJ3K (Figure 36, right panel), suggesting that the fresh anomaly observed at Station 27 (Figure 20, bottom panel) was driven by the upper parts of water column.

Normalized bottom temperature anomalies (mean temperature and temperature in areas shallower than 200 m), as well as area of the sea floor covered by water above 2°C and below 1°C between 1980 and 2021 are shown in a color-coded scorecard in Figure 37. A clear cold period is visible from the early 1980s to the mid-1990s, with the coldest anomalies reached in NAFO Divisions 2J and 3K. This was followed by a warmer period peaking in 2010 and 2011, the warmest years on records for these divisions. After a slight return to normal-to-cold anomalies between 2012 and 2017, bottom temperatures have been generally above normal since. In 2021, they were respectively 0.8 SD, 0.8 SD and 0.7 SD for NAFO Divisions 2H, 2J and 3K, respectively.

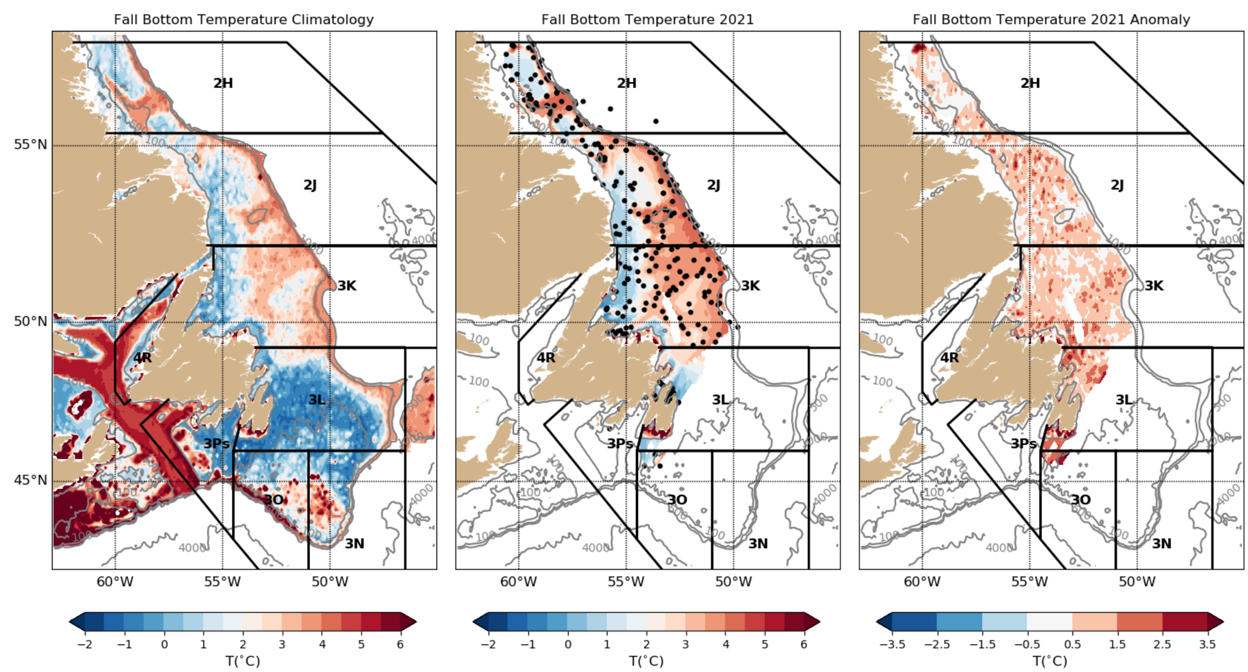

Figure 35. Maps of the mean 1991-2020 fall bottom temperature (left), and fall 2021 bottom temperature (center) and anomalies (right) for NAFO Divisions 2HJ3KLNO only. The location of observations used to derive the temperature field is shown as black dots in the center panel.

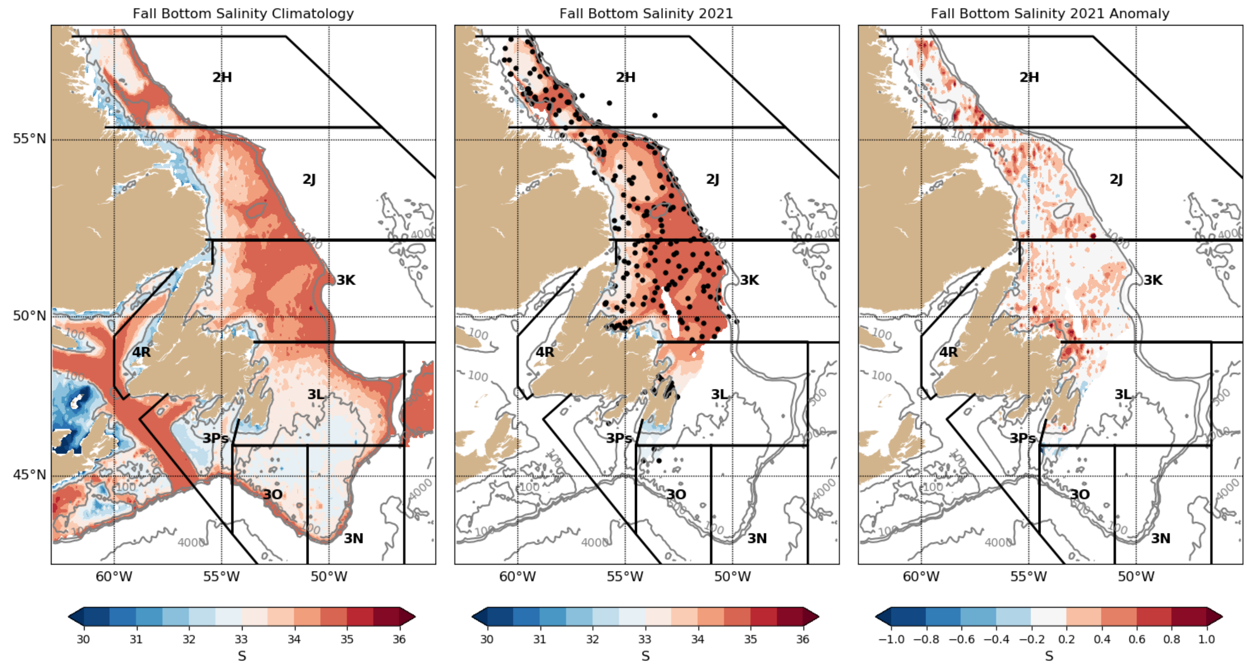

Figure 36. Maps of the mean 1991-2020 fall bottom salinity (left), and fall 2021 bottom salinity (center) and anomalies (right) for NAFO Divisions 2HJ3KLNO only. The location of observations used to derive the salinity field is shown as black dots in the center panel.

	80	81	82	83	84	85	86	87	88	89	90	91	92	93	94	95	96	97	98	99	00	01	02	03	04	05	06	07	08	09	10	11	12	13	14	15	16	17	18	19	20	21	x̄	sd
-- NAFO division 2H --																																												
T_{bot}		-0.5		-3.2								-2.2						-0.2	-0.2	0.2		-0.5			1.2		-0.3		0.1		1.8	2.0	0.3	-0.4	-0.1	-0.6	-0.4	-1.6	0.2	0.2	0.3	0.8	2.3	0.4
$T_{bot_{<200m}}$		0.4		-2.7								-2.0						0.6	0.2	0.4		-1.5			1.0		-0.6		-0.6		1.5	1.9	0.4	-0.8	-0.5	0.1	0.0	-1.4	0.3	0.4	0.7	0.8	1.1	0.5
$Area_{>2^{\circ}C}$		-0.3		-1.4								-1.0						0.7	0.7	0.3		-1.2			1.5		0.0		-0.2		1.6	2.0	-0.2	-0.2	-0.5	-1.6	-0.4	-1.6	0.2	0.0	-0.2	0.1	20.9	4.1
$Area_{<1^{\circ}C}$		-0.9		2.9								2.6						-0.9	0.6	-0.6		0.4			-0.7		0.9		0.9		-1.3	-1.4	-0.2	0.9	0.1	-0.1	-0.1	1.0	-0.5	-0.7	-1.0	-1.0	9.9	7.3
-- NAFO division 2J --																																												
T_{bot}	-0.8	-0.2	-1.7	-1.6	-2.9	-2.4	-0.2	-2.1	-0.4	-0.9	-1.9	-1.4	-2.3	-2.3	-1.6		0.3	0.0	0.0	0.3	-0.5	0.5	0.1	0.6	1.0	1.2	-0.4	1.2	-0.1	0.1	1.7	1.7	-0.1	0.0	-0.7	-0.7	0.2	-0.3	0.8	0.8	0.0	0.8	2.3	0.5
$T_{bot_{<200m}}$	-0.4	0.0	-1.3	-1.8	-2.5	-1.8	0.0	-1.8	-0.3	-0.9	-1.5	-1.5	-2.1	-2.0	-1.3		0.5	-0.2	-0.2	0.4	-0.5	0.7	0.3	0.6	0.7	1.2	-0.7	1.2	-0.2	0.1	1.5	1.7	-0.3	-0.4	-1.0	-0.8	0.8	-0.3	0.6	1.2	0.0	0.6	1.0	0.7
$Area_{>2^{\circ}C}$	-0.5	-0.3	-1.8	-1.1	-2.2	-2.0	-0.1	-1.7	-0.4	-1.0	-1.8	-1.2	-1.6	-1.9	-1.3		0.7	0.1	-0.2	-0.3	-0.5	0.6	-0.6	0.5	0.9	1.4	-0.3	1.5	-0.7	-0.3	1.9	2.2	-0.6	-0.3	-0.7	-0.5	0.2	-0.4	0.6	0.9	0.1	0.4	52.4	13.3
$Area_{<1^{\circ}C}$	0.5	-0.1	1.8	1.7	2.2	2.0	-0.1	2.1	-0.1	1.0	1.8	1.6	1.9	2.0	1.4		-0.4	-0.1	0.3	-0.8	0.5	-0.7	-0.5	-0.7	-0.5	-1.3	0.7	-1.2	0.6	-0.1	-1.3	-1.3	0.5	0.4	1.0	0.8	-1.1	0.4	-0.6	-1.3	-0.2	-0.7	19.5	14.6
-- NAFO division 3K --																																												
T_{bot}	-0.3	-0.4	-0.6	-1.0	-1.7	-2.6	-0.5	-1.5	-0.8	-0.7	-2.2	-1.3	-2.2	-2.2	-1.7	-1.1	-0.4	0.3	0.2	0.6	0.2	-0.2	0.4	0.5	1.3	0.7	0.0	0.8	0.5	0.0	1.4	2.1	0.1	0.3	-0.5	-0.2	-0.5	-0.9	0.6	0.7	0.5	0.7	2.6	0.4
$T_{bot_{<200m}}$	-0.2	-0.5	-2.2	-1.9	-2.1	-2.0	-0.2	-1.8	-1.1	-0.9	-1.8	-1.7	-1.8	-2.0	-1.6	0.0	0.4	-0.3	-0.6	0.3	-0.6	0.2	0.4	0.4	1.1	0.7	-0.3	0.9	-0.3	-0.2	1.8	1.6	-0.1	-0.5	-0.9	-0.3	0.9	-0.5	0.8	1.5	1.0	0.8	0.6	0.7
$Area_{>2^{\circ}C}$	-0.3	-0.1	-0.3	-1.1	-1.4	-2.7	-0.2	-1.5	-0.8	-0.8	-2.1	-1.0	-2.1	-2.1	-1.8	-1.5	-0.4	0.6	0.4	0.6	0.4	-0.2	0.8	0.2	1.0	0.9	0.0	0.8	0.5	-0.5	1.6	1.4	0.0	0.5	-0.7	-0.1	-0.8	-0.9	0.8	0.8	0.9	-0.3	77.7	13.0
$Area_{<1^{\circ}C}$	0.3	0.1	0.6	1.2	1.4	2.6	-0.4	0.8	0.2	0.3	2.8	1.4	2.0	2.5	1.8	0.2	-0.5	0.1	0.2	-0.3	0.4	0.0	-0.6	0.0	-1.2	-0.9	0.4	-1.0	0.2	0.3	-1.3	-1.4	0.3	-0.2	0.6	0.1	-0.7	0.8	-0.9	-1.3	-0.9	-0.6	13.3	9.0
-- NAFO division 3LNO --																																												
T_{bot}	0.3	-0.1	1.0	0.1	-0.5	-1.0	0.0	-0.7	-1.1	0.1	-1.0	-1.4	-1.3	-2.0	-1.4	-0.3	0.1	-0.1	0.7	1.7	-0.3	0.0	0.0	-0.3	0.8	0.2	0.5	-0.1	-0.5	0.5	1.3	2.4	0.4	0.6	-0.8	-0.1	0.2	-2.1	0.2	0.1	1.1		1.2	0.5
$T_{bot_{<200m}}$	0.5	-0.1	1.2	0.2	-0.4	-0.9	0.2	-0.7	-1.0	0.2	-0.7	-1.3	-1.1	-2.0	-1.3	-0.2	0.2	-0.2	0.7	1.8	-0.5	0.1	-0.1	-0.4	0.7	0.2	0.6	-0.3	-0.8	0.6	1.4	2.4	0.3	0.6	-0.9	-0.3	0.3	-2.0	0.1	0.2	1.2		0.8	0.5
$Area_{>2^{\circ}C}$	0.1	-0.3	0.5	0.5	0.1	-1.4	0.1	-0.6	-1.5	0.7	-1.1	-1.0	-1.3	-1.8	-1.3	-0.5	-0.1	-0.1	1.0	2.1	-0.1	-0.1	-0.2	-0.4	0.5	0.1	0.2	-0.1	-0.7	0.5	1.2	2.3	0.7	0.7	-1.0	0.0	0.3	-2.0	-0.1	0.1	1.3		73.5	22.3
$Area_{<0^{\circ}C}$	-0.6	0.8	0.1	0.8	1.1	0.4	0.0	0.5	0.4	0.2	0.6	1.4	1.1	2.0	1.4	-0.2	0.1	0.3	-0.2	-1.2	0.7	0.1	-0.3	0.0	-1.6	-0.5	-0.9	0.1	0.5	-0.1	-1.1	-2.5	0.2	0.0	0.0	0.2	0.3	2.0	-0.4	-0.1	-1.3		91.6	33.2

Figure 37. Scorecards of normalized fall bottom temperature anomalies for 2H, 2J, 3K and 3LNO.

Ocean Conditions on the Scotian Shelf and Gulf of Maine (NAFO Sub-area 4)

Coastal Temperatures and Salinities

Coastal sea surface temperatures have been collected at Halifax (Nova Scotia) and St. Andrews (New Brunswick) since the 1920s (Figure 38). In 2021 the SST anomaly was +1.7°C (+2.0 SD) for Halifax, an increase of 1.1°C from 2020. Unfortunately due to work on the St. Andrews pier, no data was collected for 2021.

Temperature and salinity measurements through the water column, for the most part sampled monthly, have been taken since 1924 at Prince 5, at the entrance to the Bay of Fundy (Figure 38). It is the longest continuously operating hydrographic monitoring site in eastern Canada. Its waters are generally well-mixed from the surface to the bottom (90 m). The depth-averaged (0-90 m) temperature, salinity and density anomaly time series are shown in x (C-E). In 2021, the annual temperature anomaly was +1.4°C (+2.0 SD) and the salinity anomaly was +0.2 (+1.1 SD). These represent changes of +0.6°C and +0.3 from the 2020 values. The below-normal density anomaly is accounted for by the positive temperature anomaly.

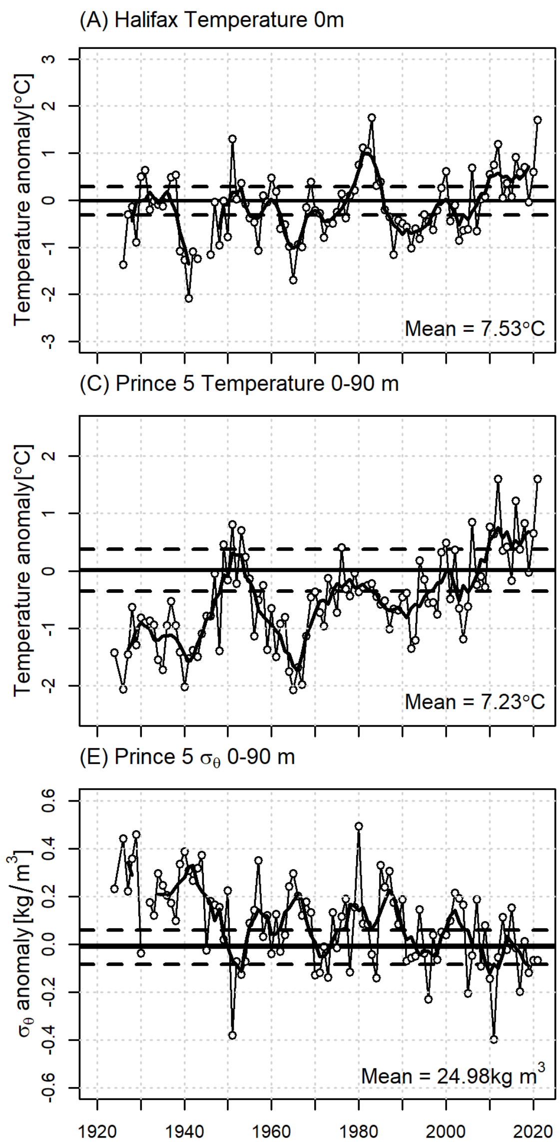

Figure 38. The annual surface temperature anomalies (dotted line with circles) and their 5-year running means (heavy black line) for (A) Halifax Harbour and (B) St. Andrews; annual depth-averaged (0-90 m) (C) Temperature, (D) salinity and (E) density anomalies for the Prince 5 monitoring station at the mouth of the Bay of Fundy. Horizontal dashed lines are the 1991-2020 climatological average ±0.5 SD.

Temperatures from Long-term Stations

Drinkwater and Trites (1987) tabulated monthly mean temperatures and salinities from available bottle data for areas on the Scotian Shelf and in the eastern Gulf of Maine that generally correspond to topographic features such as banks and basins. Petrie et al. (1996) updated their report using these same areas and all available hydrographic data. An updated time series of annual mean and filtered (5 year running means) temperature anomalies at selected depths for six areas (see map Figure 39) is presented in Figure 40. The Cabot Strait temperatures represent a mix of Labrador Current Water and Warm Slope Water (e.g., Gilbert et al., 2005) entering the Gulf of St. Lawrence along Laurentian Channel; the Misaine Bank series characterizes the colder near bottom temperatures on the Eastern Scotian Shelf by either inshore Labrador Current water or cold-intermediate layer water from the Gulf of St. Lawrence (Dever et al., 2016); the deep Emerald Basin anomalies represent the Slope Water intrusions onto the Shelf that are subsequently trapped in the deep inner basins (note the large anomaly “events” in Figure 40C, for example, around 1980 and 2009 indicative of pulse of Labrador Slope Water); the Lurcher Shoals observations define the ocean climate on the southwest Scotian Shelf and the shallow waters entering the Gulf of Maine via the Nova Scotia Current; last, the Georges Basin series indicates the slope waters entering the Gulf of Maine through the Northeast Channel. Annual anomalies are based on the averages of monthly values; however, observations may not be available for each month in each area. For Cabot Strait, Misaine Bank, Emerald Basin, Georges Basin, eastern Georges Bank and Lurcher Shoals, 2021 annual anomalies are based on observations from five, two, five, six, five and one month, respectively.

In 2021, the annual anomaly was +1.2°C (+1.9 SD) for Cabot Strait at 200-300 m (the second largest anomaly; five of the last six years were the warmest). For the shallow Misaine Bank on the eastern Scotian Shelf, the annual anomaly was +1.3°C (+2.2 SD) at 100 m. For the deep basins on the central Scotian Shelf and Gulf of Maine, the 2021 anomalies were +1.6°C (+1.1 SD) for Emerald Basin at 250 m (6th highest value, 2019 was a record high; the last sixyears were the warmest in the record) and +1.1°C (+1.6 SD) for Georges Basin at 200 m (third warmest, 2019 was the second warmest with 2018 the warmest; the last nine years were the warmest in the record). For the shallow banks in western Nova Scotia, the anomalies were +1.0°C (+1.5 SD) for eastern Georges Bank at 50 m and +1.6°C (+1.8 SD) for Lurcher Shoals at 50 m (2021 was the third warmest; 2018 was the second highest with 2012 having the record). These values correspond to changes of -0.4˚C, +0.9˚C, -0.2˚C, +0.4˚C, +0.4˚C, and +0.9˚C, from the 2020 values.

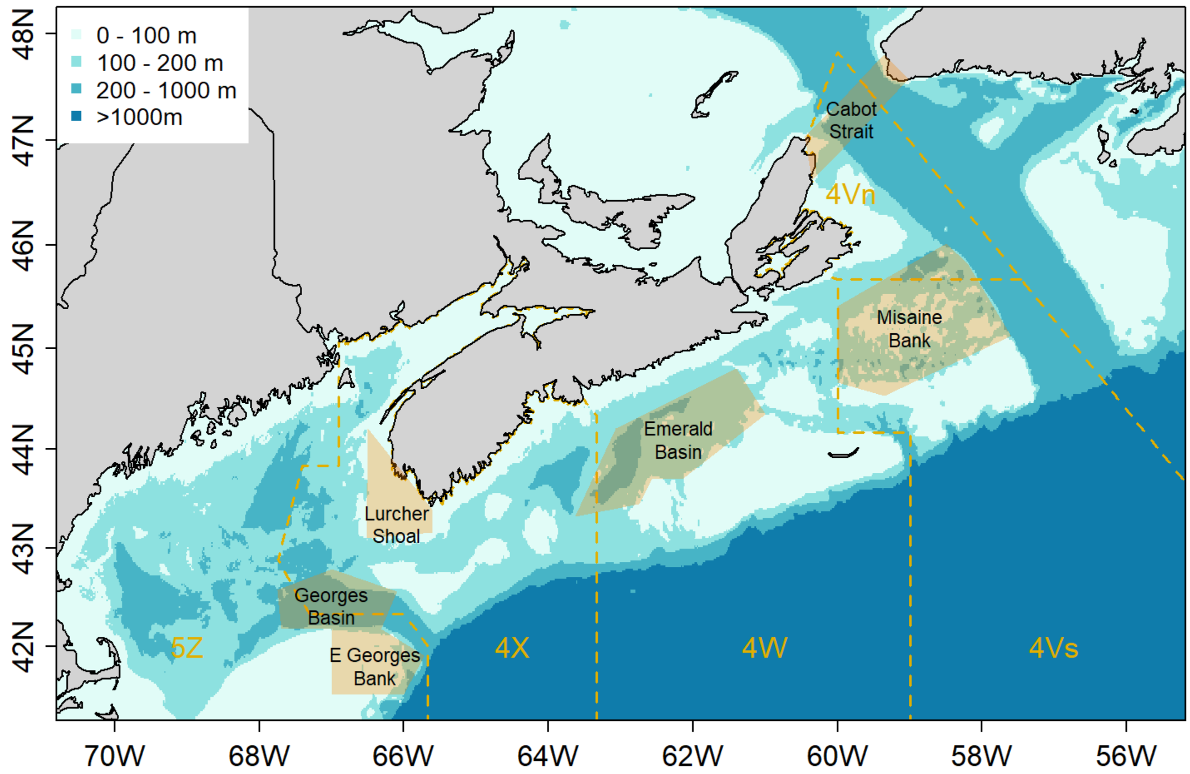

Figure 39. Areas on the Scotian Shelf and eastern Gulf of Maine used to characterize the different water masses.

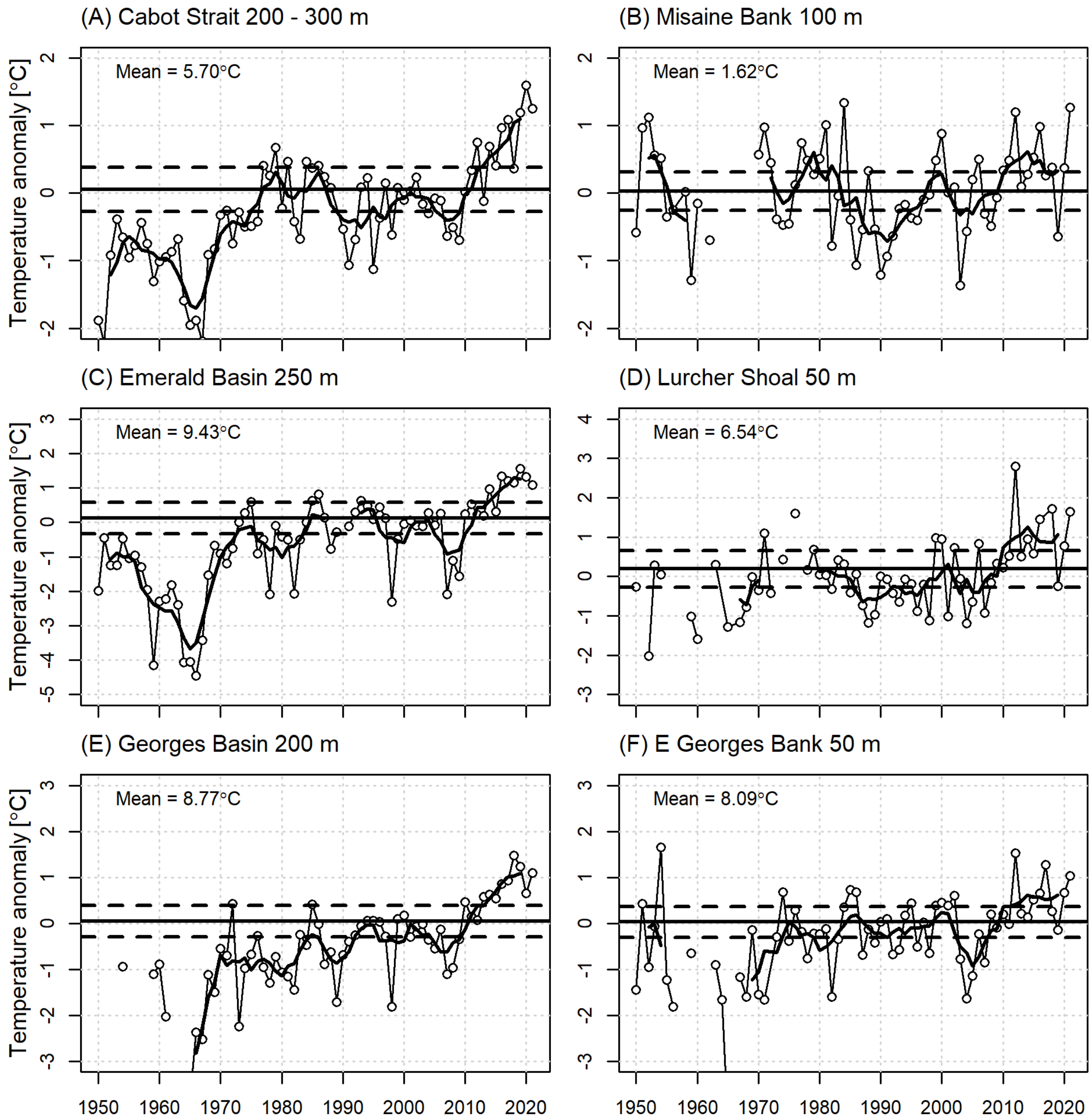

Figure 40. The annual mean temperature anomaly time series (dotted line with circles) and the 5 year running mean filtered anomalies (heavy solid line) on the Scotian Shelf and in the Gulf of Maine at (A) Cabot Strait (200-300 m); (B) Misaine Bank (100 m); (C) Emerald Basin (250 m); (D) Lurcher Shoals (50 m); and Georges Basin (200 m) (see Figure 39). Horizontal dashed lines are the climatological average ±0.5 SD.

Temperatures during the Summer Groundfish Surveys

The broadest spatial temperature and salinity coverage of the Scotian Shelf is obtained during DFO's annual summer groundfish survey which covers the Scotian Shelf from Cabot Strait to the Bay of Fundy. The deep water boundary of the survey is marked roughly by the 200 m isobath along the shelf break at the Laurentian Channel, at the outer Scotian Shelf, and at the Northeast Channel into the Gulf of Maine towards the Bay of Fundy. No survey was done in 2021.

The temperatures from the survey were combined and interpolated onto a 0.2° by 0.2° latitude-longitude grid using an objective analysis procedure known as optimal estimation. The interpolation method uses the 15 "nearest neighbours" with a horizontal length scale of 30 km and a vertical length scale of 15 m in the upper 40 m and 25 m at deeper depths. Data near the interpolation grid point are weighted proportionately more than those farther away. Temperatures were optimally estimated for at the standard depths (e.g. 0 m, 10 m, 20 m, etc.) and for near the bottom. Only the bottom temperatures are presented here using the new 1991-2020 climatology (Figure 41).

The volume of the Cold Intermediate Layer (CIL), defined as waters with temperatures <4°C, was estimated from the full depth CTD profiles for the region from Cabot Strait to Cape Sable (Figure 39). There is considerable variation in the volume of the CIL from 1998 until 2009 (Figure 42). The smallest volume was in 2012. In the last six years, the CIL volume has been trending toward normal. The low-frequency variability of the area-weighted average minimum temperature mirrors the CIL volume.

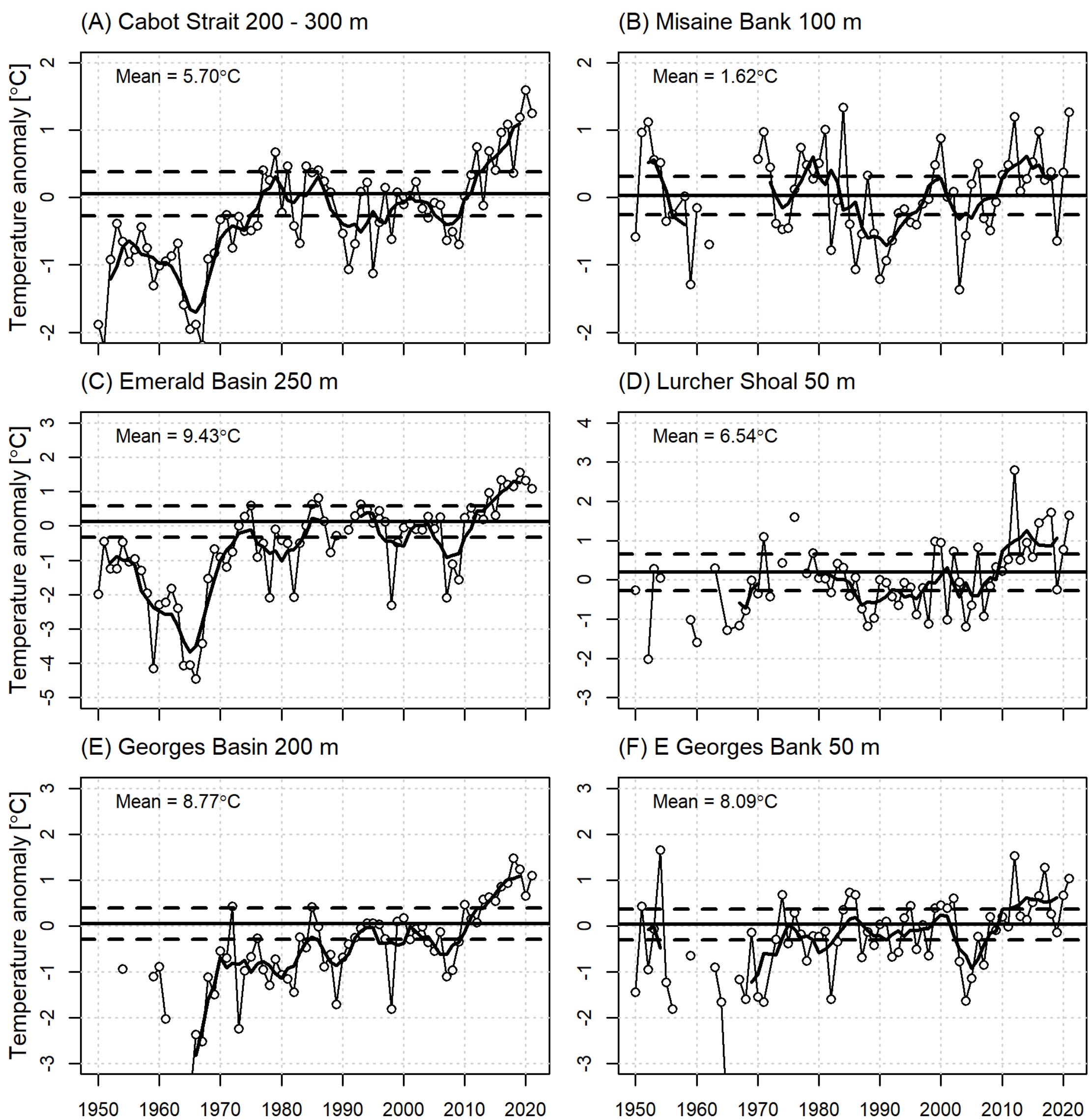

Figure 41. Time series of July bottom temperature anomalies (dashed lines with circles) and 5 year running mean filtered series (heavy line) for areas (A) 4Vn, (B) 4Vs, (C) 4W and (D) 4X. The solid horizontal line is the 1991-2020 mean and dashed lines represent ±0.5 SD.

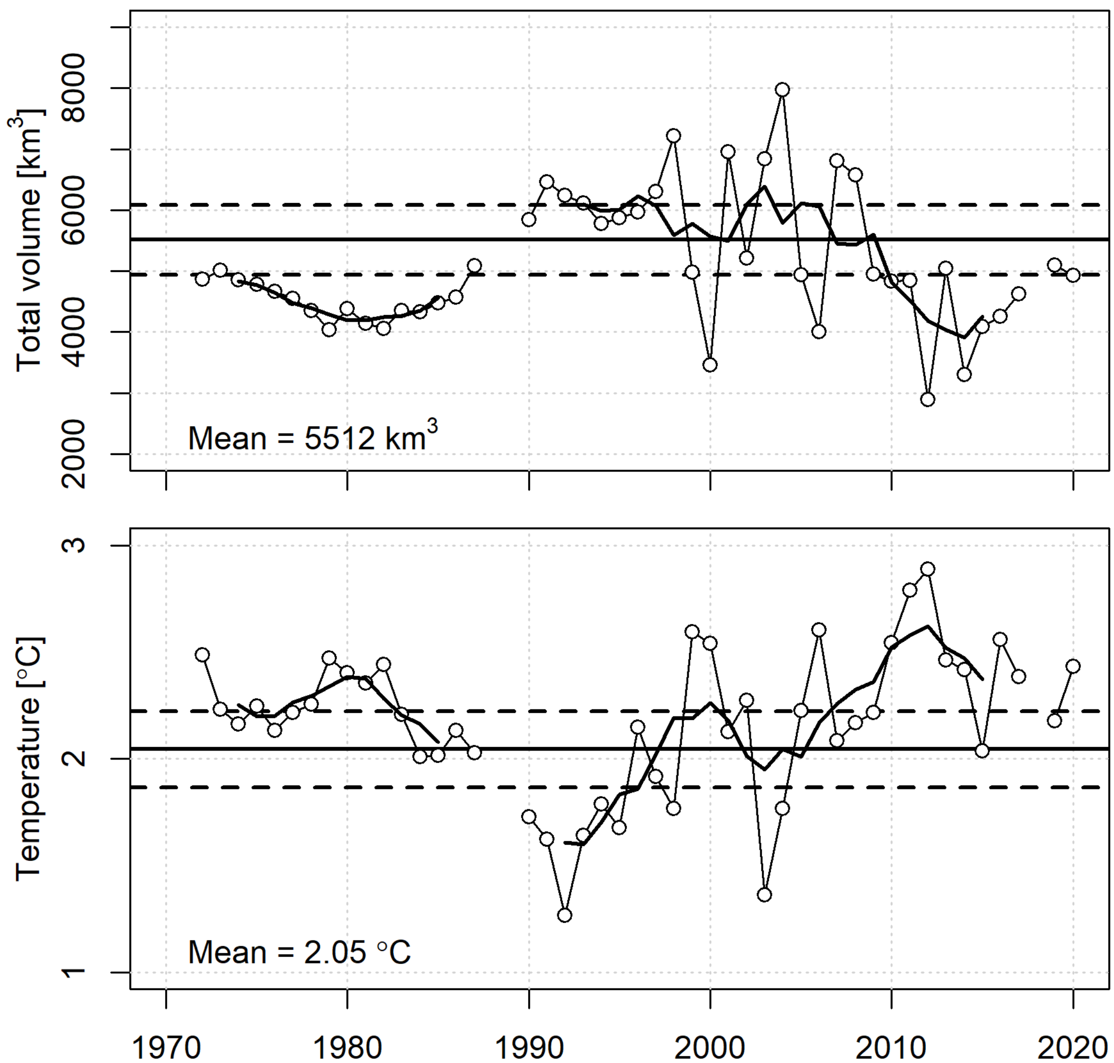

Figure 42. Time series of the Cold Intermediate Layer (CIL, defined as waters with T<4˚C) volume on the Scotian Shelf based on the July ecosystem survey. The solid horizontal line is the 1991-2010 mean CIL volume and dashed lines represent ±0.5 SD.

Density Stratification

Stratification of the near surface layer influences physical and biological processes in the ocean such as vertical mixing, the ocean's response to wind forcing, the timing of the spring bloom, vertical nutrient fluxes and plankton distribution. Under increased stratification, there is a tendency for more primary production to be recycled within the upper mixed layer and hence less available for the deeper layers. The variability in stratification by calculating the density (σ_t) difference between 0 and 50 m was examined based on monthly mean density profiles on the Scotian Shelf. The long-term monthly mean density gradients for 1991-2020 were estimated; these were subtracted from the individual monthly values to obtain monthly anomalies. Annual anomalies were estimated by averaging all available monthly anomalies within a calendar year. This could be misleading if, in a particular year, most data were collected in months when stratification was weak, while in another year, sampling occurred when stratification was strong. However, initial results, using normalized monthly anomalies, were qualitatively similar to the plots presented here. The annual anomalies and their 5-year running means were for the Scotian Shelf. A value of 0.01 kg m^{-3}/m represents a difference of 0.5 kg m^{-3} over 50 m.

The dominant feature is the period from about 1950 to 1990 that featured generally below average stratification in contrast to the past 25 years that is characterized by above normal values (Figure 43). Since 1948, there has been an increase in stratification on the Scotian Shelf, resulting in a change in the 0-50 m density difference of 0.38 kg m^{-3} over 50 years. This change in mean stratification is due mainly to a decrease in the surface density, composed of equally of warming and freshening.

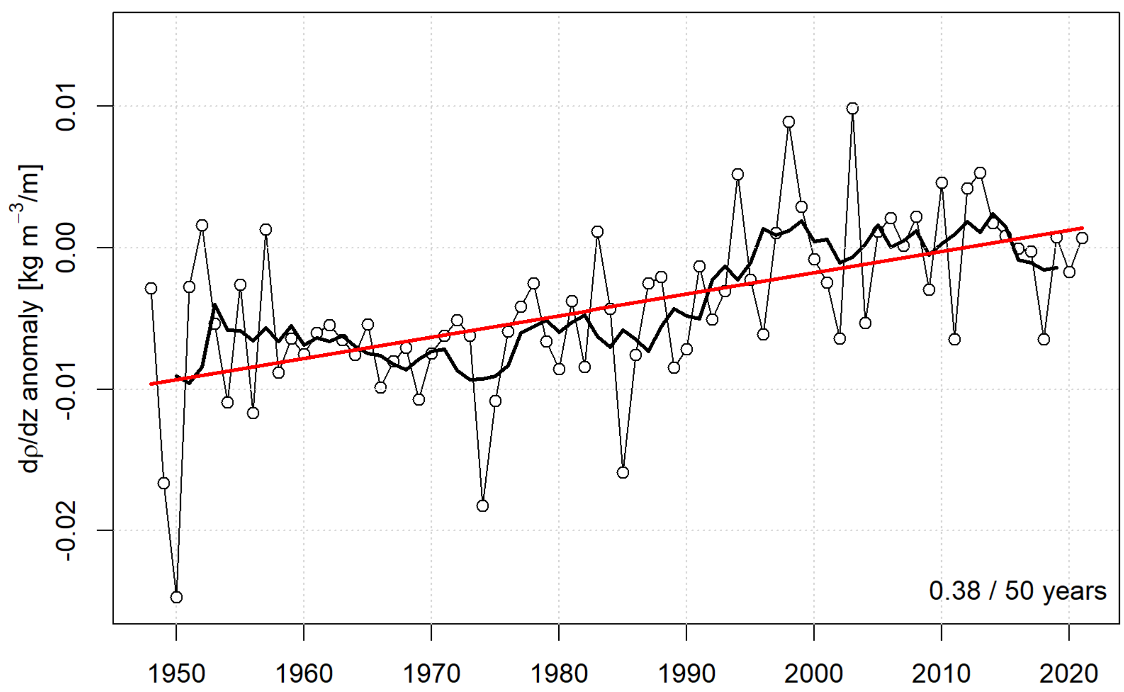

Figure 43. The mean annual anomaly (dashed line with circles) and 5-yr running mean (heavy solid line) of the stratification index (0-50 m density gradient) averaged over the Scotian Shelf. The linear trend (red line) shows a change in the 0-50 m density difference of 0.38 kg m^{-3} over 50 years.

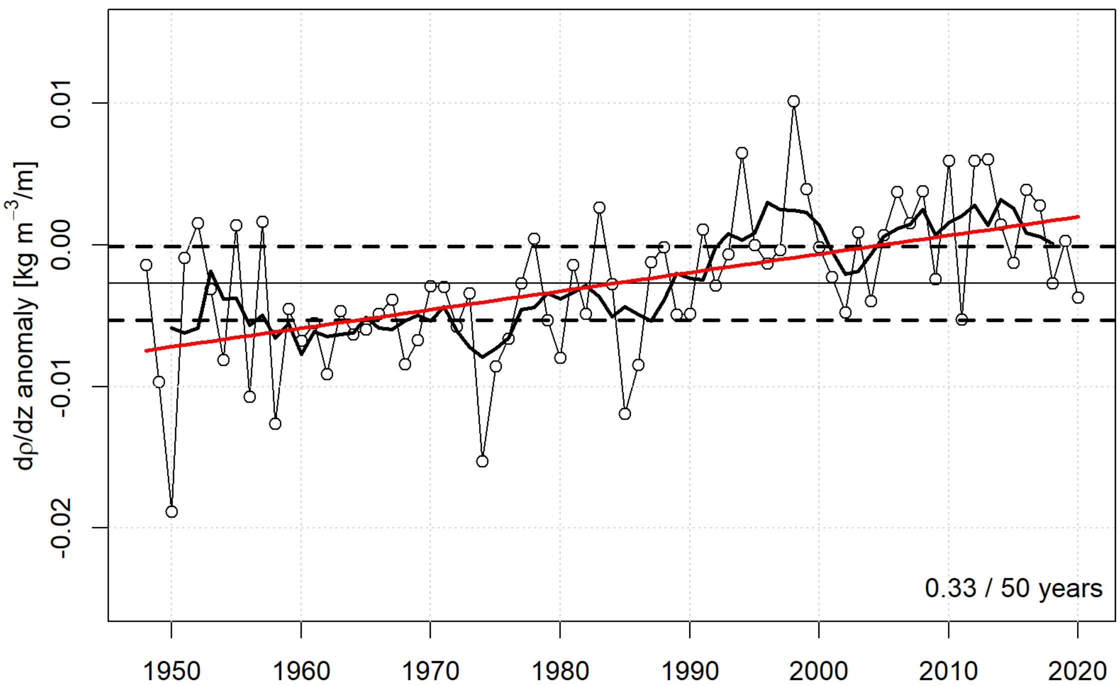

Figure 44. The mean annual anomaly (dashed line with circles) and 5-yr running mean (heavy solid line) of the stratification index (0-50 m density gradient) averaged over the Scotian Shelf. The solid horizontal line is the 1991-2020 mean stratification and dashed lines represent ±0.5 SD. The linear trend (red line) shows a change in the 0-50 m density difference of 0.33 kg m^{-3} over 50 years.

Labrador Current Variability in NAFO Sub-area 2,3 and 4

The circulation in NL region is dominated by the south-eastward flowing Labrador Current system, which floods the eastern shelf areas with cold and relatively fresh subpolar waters (Figure 45). This flow can significantly affect physical and biological environments off Atlantic Canada on seasonal and interannual time scales. The Labrador coastal current originates near the northern tip of Labrador where outflow through Hudson Strait combines with the eastern Baffin Island Current and flows southeastward along the Labrador coast where it is strongly influenced by the seabed topography, following the various cross shelf saddles and inshore troughs. A separate offshore branch flows southeastward along the western boundary of the Labrador Sea. This current is part of the large-scale Northwest Atlantic circulation consisting of the West Greenland Current that flows northward along the West Coast of Greenland, a branch of which turns westward and crosses the northern Labrador Sea forming the northwestern section of the Atlantic subpolar gyre.

Further south, near the northern Grand Bank, the inshore branch becomes broader and less defined. In this region, most of the inshore flow combines with the offshore branch and flows eastward, with a portion of the combined flow following the bathymetry southward around the southeast Grand Bank, and the remainder continuing east and southward around the Flemish Cap. A smaller inshore component flows through the Avalon Channel and around the Avalon Peninsula, and then westward along the Newfoundland south coast. Off the southern Grand Bank the offshore branch flows westward along the continental slope, some of which flows into the Laurentian Channel and eventually onto the Scotian Shelf. This extension of the Labrador Current on the Scotian Shelf (SS) slope is referred to as the Shelf Break Current. Additionally, there are strong interactions between the offshore branch of the Labrador Current and large-scale circulation. A significant portion of the offshore branch combines with the North Atlantic Current and forms the southern section of the subpolar gyre. Further east, the Flemish Cap is located in the confluence zone of subpolar and subtropical western boundary currents of the North Atlantic. Labrador Current water flows to the east along the northern slopes of the Cap and south around the eastern slopes of the Cap. In the eastern Flemish Pass, warmer high salinity North Atlantic Current water flows northward contributing to a topographically induced anticyclonic gyre over the central portion of the Cap.

Satellite altimetry data are used over a large spatial area to calculate the annual-mean anomalies of the Labrador Current transport (Han et al. 2014). A total of nine cross-slope satellite altimetry tracks are used to cover the Labrador Current on the NL shelf break from approximately 47°N to 58°N latitude (Figure 45). Similarly, five tracks from approximately 55°W to 65°W longitude are used for the Scotian shelf break current. The nominal cross-slope depth ranges used for calculating the transport are from 200 to 3,000 m isobaths over the NL shelf break and from 200 to 2,000 m isobaths over the Scotian shelf break

An empirical orthogonal function (EOF) analysis of the annual-mean transport anomalies was carried out. An index was developed from the time series of the first EOF mode and normalized by dividing the time series by its SD. The mean transport values are provided based on ocean circulation model output along the NL shelf break (Han et al. 2008) and over the Scotian shelf break (Han et al.1997). The mean transport of the Labrador Current along the NL shelf break is 13 Sv (1 Sv = 10^6 m^3 s^{-1}) with a SD of 1.4 Sv, and the mean transport of the Scotian shelf break current is 0.6 Sv with a SD of 0.3 Sv. The mean transport values will be updated as new model output becomes available. The SD values will be updated as knowledge on nominal depth improves.

The Labrador Current transport along the NL shelf break was out of phase with that of the Scotian shelf break current for most of the years over 1993–2021 (Figure 46). The transport over the NL shelf break was strong in the early- and mid-1990s, weak in the mid-2000s and early-2010s, and became strong again in late 2010s. In contrast, the transport over the Scotian shelf break fluctuated in a nearly opposite way. The Labrador Current transport index was positively and negatively correlated with the winter NAO index over the NL and Scotian shelves breaks, respectively.

In 2021 the annual-mean transport of the Labrador Current over the NL shelf break continued the weakening trend that began in 2019 and became normal. The transport on the Scotian shelf break in 2021 remained below normal for eight consecutive years at -1.4 SD.

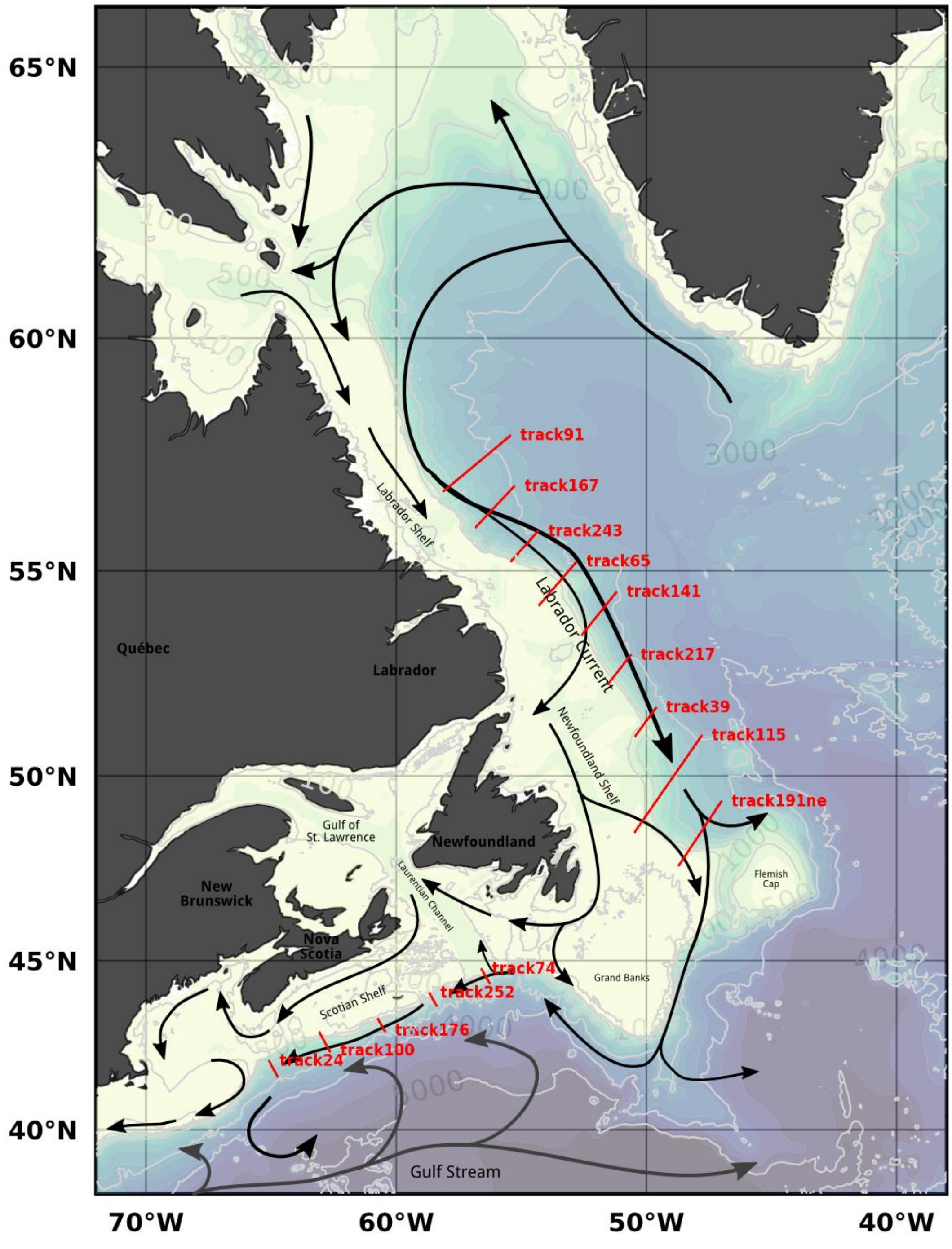

Figure 45. Map showing the Northwest Atlantic bottom topography (depth contour values in light gray) and schematic flow patterns (arrows). The transport is calculated across the cross-slope sections (red lines) identified by their satellite ground tracks numbers. The series of northern tracks are used for the Labrador Current calculation on the Newfoundland and Labrador slope, while the series of tracks in the south are used for the Shelf Break Current transport on the Scotian Shelf slope.

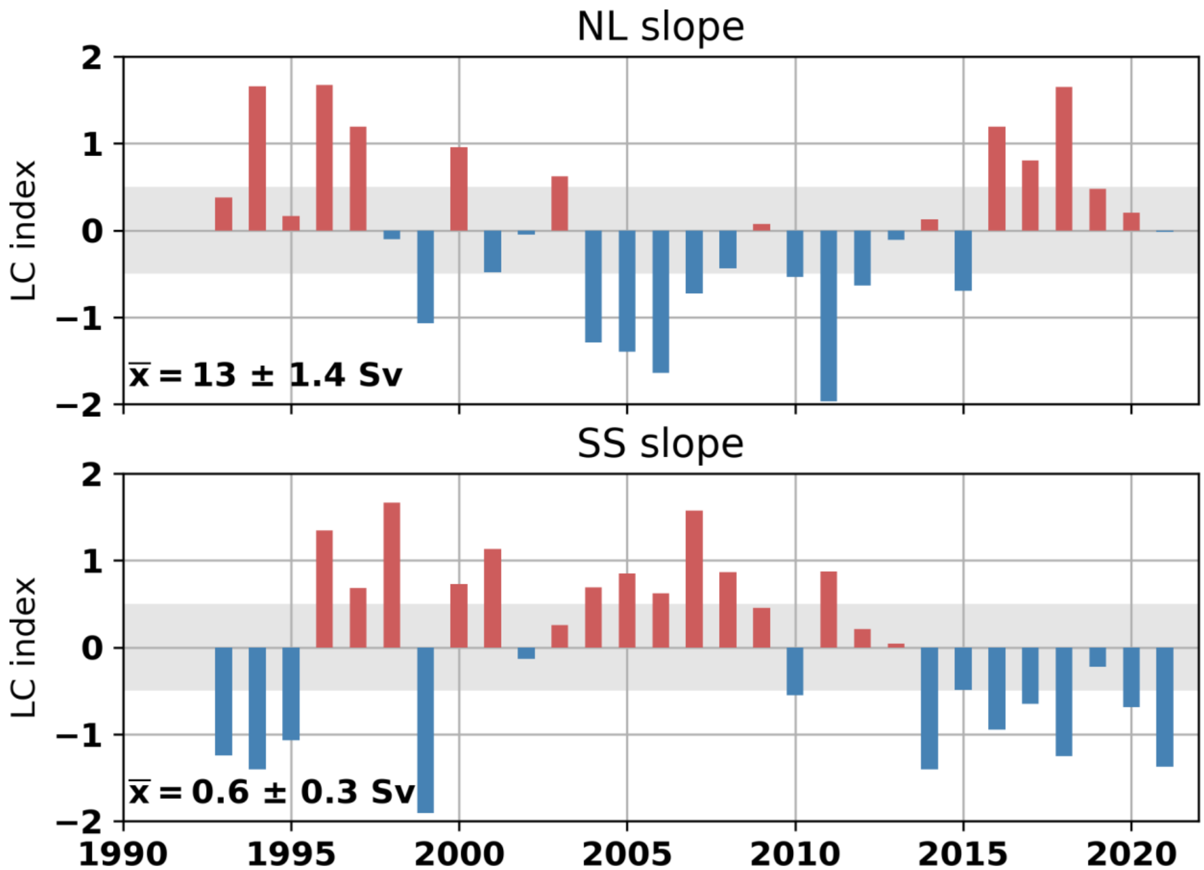

Figure 46. Normalized index of the annual-mean transport of the Labrador Current on the NL shelf break (top) and Scotian shelf break (bottom). Long-term averages over 1993–2021 (with standard deviation) are 13 ±1.4 Sv for the Labrador Current and 0.6 ±0.32 Sv for the Scotian shelf break current. Shaded gray areas represent the ±0.5 SD range considered "normal".

Summary

An overview of physical environmental conditions for NAFO Divisions 2, 3 & 4 were presented. The highlights of 2021 can be summarized as follows:

- The winter North Atlantic Oscillation (NAO) index, a key indicator of the direction and intensity of the winter wind field patterns over the Northwest Atlantic was negative for the first time in 8 years.
- The annual air temperature was above normal across the zone.
- Sea ice conditions (season duration and maximum cover) were at their third lowest level of the time series (started in 1969), after 2010 and 2011.
- Sea surface temperatures averaged over the ice-free months were above-normal on average across the zone for the second consecutive year.
- Observations from the summer AZMP oceanographic survey indicate that the CIL area along Seal Island, Bonavista Bay and Flemish Cap section was at its third lowest since 1950 (after 1965 and 1966).
- Spatially-averaged bottom temperatures in NAFO divisions 3Ps (spring) and 2J3K (fall) were at their second warmest since 1980, including a record in 3Ps.
- The transport on the Scotian Slope remained below normal for an eighth consecutive year.

A series of physical and biogeochemical indices in NAFO subareas 0-4 in support of the Standing Committee on Fisheries Science (STACFIS) that uses some information from this report is presented in Bélanger and Cyr (2022).

Acknowledgments

We thank the many scientists and technicians at the Northwest Atlantic Fisheries Centre, Bedford Institute of Oceanography and St. Andrews Biological Station for collecting and providing much of the data contained in this analysis and to the Ocean Science Branch of Fisheries and Oceans in Ottawa for providing most of the historical data. Environment Canada provided the meteorological data. We also thank the captain and crew of the CCGS Teleost, CCGS Amundsen and CCGS Hudson for successful oceanographic survey during 2021. Finally, we thank the numerous technicians and scientists that contributed to the Atlantic Zone Monitoring Program for making this important work possible. The authors thank the Working Group on Oceanic Hydrography (WGOH) of the International Council for the Exploration of the Sea (ICES) for facilitating this research.

References

Bélanger and Cyr (2022). Environmental indices for NAFO subareas 0 to 4 in support of the Standing Committee on Fisheries Science (STACFIS). NAFO SCR Doc. 22/021. Serial No. N7294.

Colbourne, E. B., S. Narayanan and S. Prinsenberg. 1994. Climatic change and environmental conditions in the Northwest Atlantic during the period 1970-1993. ICES Mar. Sci. Symp., 198:311-322.

Colbourne, E. B., J. Holden, D. Senciall, W. Bailey, J. Craig and S. Snook. 2015. Physical Oceanographic Environment on the Newfoundland and Labrador Shelf in NAFO Subareas 2 and 3 during 2014. NAFO SCR. Doc. 2015/011. Serial No. N6431.

Cyr, F., P. S. Galbraith, C. Layton and D. Hebert. 2021. Environmental and Physical Oceanographic Conditions on the Eastern Canadian shelves (NAFO Sub-areas 2, 3 and 4) during 2020. NAFO SCR Doc. 21/009.

Cyr, F., Colbourne, E., Holden, J., Snook, S., Han, G., Chen, N., Bailey, W., Higdon, J., Lewis, S., Pye, B. and Senciall, D. 2019. Physical oceanographic conditions on the Newfoundland and Labrador Shelf during 2017. DFO Can. Sci. Advis. Sec. Res. Doc. 2019/051.

Cyr, F., Snook, S., Bishop, C., Galbraith, P.S., Pye, B., Chen, N., and, Han, G. 2021. Physical Oceanographic Conditions on the Newfoundland and Labrador Shelf during 2019, DFO Can. Sci. Advis. Sec. Res. Doc. 2021/017. iv + 52 p.

Cyr, F. and P. Galbraith. 2020. Newfoundland-Labrador Shelf. Ch. 4.3 in: ICES report on ocean climate 2019 [González-Pola, C., Larsen, K. M. H., Fratantoni, P., and Beszczynska-Möller, A. (Eds.).] ICES Cooperative Research Reports No. 350. 136 pp. https://doi.org/10.17895/ices.pub.7537

Cyr, F. and P.S. Galbraith. 2021. A climate index for the Newfoundland and Labrador shelf. Earth System Science Data, 13, 1807–1828, DOI: 10.5194/essd-13-1807-2021.

Dever, M., Hebert, D., Greenan, B.J.W, Sheng, J. and Smith, P.C. (2016) Hydrography and Coastal Circulation along the Halifax Line and the Connections with the Gulf of St. Lawrence, Atmosphere-Ocean, 54:3, 199-217, DOI: 10.1080/07055900.2016.1189397

Dickson, R. R., J. Meincke, S. A. Malmberg and A. J. Lee. 1988. The “great salinity anomaly” in the northern North Atlantic 1968–1982. Progress in Oceanography, 20(2), 103-151.

Doubleday, W. G., Editor. 1981. Manual on groundfish surveys in the Northwest Atlantic. NAFC. Sco. Coun. Studies, 2: 56p.

Drinkwater, K.F. and R.W. Trites, 1987: Monthly means of temperature and salinity in the Scotian Shelf region, Can. Tech. Rep. Fish. Aquat. Sci., 1539, 101 p.

Drinkwater, K. F. 1996. Climate and oceanographic variability in the Northwest Atlantic during the 1980s and early-1990s. J. Northw. Atl. Fish. Sci., 18: 77-97.

Galbraith, P.S., Larouche, P., Caverhill, C. 2021. A sea-surface temperature homogenization blend for the Northwest Atlantic. Canadian Journal of Remote Sensing. doi: 10.1080/07038992.2021.1924645

Gilbert, D., B. Sundby, C. Gobriel, A. Mucci and G.-H. Tremblay, 2005: A seventy-two-year record of diminishing deep-water oxygen in the St. Lawrence estuary: The northwest Atlantic connection, Limnol. Oceanogr., 50, 1654-1666.

Han, G., Chen, N., and Z. Ma. 2014. Is there a north-south phase shift in the surface Labrador Current transport on the interannual-to-decadal scale? Geophys. Res. 119: 276-287.

Han, G., Lu, Z., Wang, Z., Helbig, J., Chen, N., and B. deYoung. 2008. Seasonal variability of the Labrador Current and shelf circulation off Newfoundland. Geophys. Res. 113.

Han, G., Hannah, C.G., Smith, P.C., and J.W. Loder. 1997. Seasonal variation of the three-dimensional circulation over the Scotian Shelf. Geophys. Res. 102:1011-1025.

ICNAF. 1978. List of ICNAF standard oceanographic sections and stations. ICNAF selected papers #3.

Petrie, B., S. Akenhead, J. Lazier and J. Loder. 1988. The cold intermediate layer on the Labrador and Northeast Newfoundland Shelves, 1978-1986. NAFO Sci. Coun. Studies 12: 57-69.

Petrie, B., K. Drinkwater, D. Gregory, R. Pettipas, and A. Sandström, 1996: Temperature and salinity atlas for the Scotian Shelf and the Gulf of Maine, Can. Data Rep Hydrog. Ocean Sci. 171, 398 p.

Petrie, B., 2007: Does the North Atlantic Oscillation affect hydrographic properties on the Canadian Atlantic Continental Shelf?, Atmos.-Ocean, 45, 141-151.

Petrie, B., R. G. Pettipas and W. M. Petrie. 2007. An overview of meteorological, sea ice and sea surface temperature conditions off eastern Canada during 2006. DFO Can. Sci. Advis. Sec. Res. Doc. 2007/022.

Therriault, J.-C., Petrie, B., Pepin, P., Gagnon, J., Gregory, D., Helbig, J., Herman, A., Lefaivre, D., Mitchell, M., Pelchat, B., Runge, J., and Sameoto, D. 1998. Proposal for a northwest Atlantic zonal monitoring program. Can. Tech. Rep. Hydrogr. Ocean Sci. 194: vii+57 pp.

Thyng, K. M., Greene, C. A., Hetland, R. D., Zimmerle, H. M., & DiMarco, S. F. 2016. True colors of oceanography. Oceanography, 29(3), 10.

Vincent, L. A., X. L. Wang, E. J. Milewska, H. Wan, F. Yang, and V. Swail. 2012. A second generation of homogenized Canadian monthly surface air temperature for climate trend analysis. J. Geophys. Res. 117, D18110, doi:10.1029/2012JD017859.

Vinther, B. M., Andersen, K. K., Jones, P. D., Briffa, K. R., and Cappelen, J. 2006. Extending Greenland temperature records into the late eighteenth century, J. Geophys. Res., 111, D11105, https://doi.org/10.1029/2005JD006810.

World Meteorological Organization. 2017. WMO guidelines on the calculation of climate normals, Tech. rep., Geneva, Switzerland.